NTNU

Norwegian University of
Science and Technology

Towards minimizing variations in the comet assay: The electric potential during electrophoresis and implications of circulating the electrophoresis solution

Linn Rolstadaas

Master of Science in Physics and Mathematics
Submission date: June 2016
Supervisor: Catharina de Lange Davies, IFY
Co-supervisor: Gunnar Brunborg, Norwegian Institute of Public Health
Kristine Bjerve Gutzkow, Norwegian Institute of Public Health

Norwegian University of Science and Technology
Department of Physics

Preface

This thesis is part of my MSc degree in Biophysics and Medical Technology at the Norwegian University of Science and Technology (NTNU). The presented work was carried out at the Department of Chemicals and Radiation (Department of Molecular Biology from the 1st of April, 2016) at Norwegian Institute of Public Health in Oslo during the spring semester of 2016, under supervision of the former department director and chief scientist Gunnar Brunborg, senior scientist Kristine Bjerve Gutzkow and professor Catharina de Lange Davies at the Department of Physics at NTNU.

I would like to thank my supervisors at Norwegian Institute of Public Health, Gunnar Brunborg and Kristine Bjerve Gutzkow, for the guidance and their continuos motivation and support during this thesis. A special thank to both of them for being a great source of inspiration and always providing help when needed and being available for discussion. I am so grateful for this opportunity to be involved in the great research environment at Norwegian Institute of Public Health. Thanks to all of the employees at the Department of Chemicals and Radiation for taking such good care of me this semester and for showing interest and being involved in this thesis.

Thanks to the two professors at the Department of Material Science and Engineering, NTNU, Svein Sunde and Kemal Nisancioglu, for providing help regarding an electrochemical perspective in this thesis. I would also like to thank the supervisor at the Department of Physics at NTNU, Catharina de Lange Davies, for her feedback on the thesis draft.

Linn Rolstadaas

Trondheim, 10.06.2016

Abstract

The comet assay (single cell gel electrophoresis) is a sensitive and versatile technique for measuring DNA damage and repair at the single cell level. Östling and Johanson were the first to introduce the comet assay in 1984, and the method has been continuously improved thereafter. However, considerable variations in results obtained between different laboratories as well as within the same laboratory are still being observed. Even neighboring cell/agarose samples can give highly different levels of DNA damage.

Minimizing the variability of the comet assay is highly desirable in order to achieve consistent results in different experiments as well as in collaborative studies involving different laboratories. The assay protocol consists of several steps, one of which involves electrophoretic separation of the negatively charged DNA molecules in an electric field. Variations in the electrophoresis condition, have shown to be a major source of error in the comet assay. Potential difference (V/cm) is the driving force in electrophoresis and control of the local voltages during electrophoresis is thus particularly important in order to reduce variability of the comet assay.

The ultimate aim of this thesis was to reduce variation in the comet assay results within and between laboratories, by developing a more stable and robust comet assay protocol. This thesis was chosen to examine systematically the effect of circulating the electrophoresis solution during electrophoresis. Two main experimental works were carried out. The first involved measurements of electric potentials in agarose at defined positions across the platform as a function of electrophoresis time under different experimental conditions. The second included the complete comet assay procedure on human peripheral blood lymphocytes irradiated with X-rays using a high-throughput format with 96 minigels on a plastic support film. No previous studies have investigated in such detail as was done in this thesis regarding the implication of adding circulation of the electrophoresis solution during electrophoresis in the comet assay.

This study showed that the variations in the electric potential across the platform were considerably reduced by circulating the electrophoresis solution. It was then anticipated that these variations would be reflected in parallel variations in DNA damage. However, the variations in voltages observed from the electric potential measurements during electrophoresis without circulation, were only partly paralleled with the variations in tail DNA intensities from the comet assay performed with or without circulation of different flow rates during electrophoresis. A decrease of approximately 1-2 % in the CV in the per cent tail DNA intensity using the high-throughput format was obtained by circulating the electrophoresis solution at flow rates above 109 ml/min compared to without circulation in this study. In addition, a less variable per cent tail DNA intensity was obtained by circulating the electrophoresis solution. The circulation also contributed to a better temperature stability. Based on these observations, circulation of the electrophoresis solution during electrophoresis in the comet assay is thus recommended.

A closer examination of the electrochemical processes occurring at the electrodes was conducted. It was concluded that the electrode system initially constructed for local measurements of potential, were insufficient due to the lack of a reference electrode suitable for the system. A reference electrode must be used in order to determine if the observed variations in electric potentials could have occurred due to minute concentration gradients between the electrodes. Due to limited time available in the thesis this was not accomplished/completed.

Sammendrag

Komet-metoden (enkeltcelle gelelektroforese) er en allsidig og sensitiv metode for å måle DNA-skader og reparasjon i enkeltceller. Analysen ble først utviklet i 1984 av de svenske forskerne Östling og Johanson, og metoden har videre blitt kontinuerlig forbedret. Likevel er det fortsatt observert vesentlige forskjeller i resultatene både mellom ulike laboratorier, samt innen det samme laboratorium. Selv naboceller/agaroseprøver kan gi svært forskjellig nivå på DNA-skade.

Det er sterkt ønskelig å minimere variasjonene i komet-metoden for å oppnå konsistente resultater ved gjentatte forsøk og i samarbeidsstudier med ulike laboratorier. Komet-analysen består av flere trinn, hvorav det ene innebærer elektroforetisk separasjon av de negative ladede DNA-molekyler i et elektrisk felt. Ulike eksperimentelle forhold under elektroforesen har vist å gi store variasjoner i resultatene. Selve drivkraften i elektroforesen er potensialforskjeller (V/cm). Det er derfor svært viktig å oppnå stabile elektriske potensialer under elektroforesen for å redusere variasjoner i komet-metoden.

Formålet med denne masteroppgaven var å redusere variasjoner i komet-metoden innen og mellom ulike laboratorier, ved å utforme en mer stabil og robust protokoll for komet-metoden. Hensikten med masteroppgaven var å systematisk studere effekten av å sirkulere elektroforeseløsningen under elektroforesen. To hovedeksperimentelle arbeid ble utført. Det første eksperimentet involverte målinger av elektriske potensialer i agarose på definerte posisjoner på tvers av plattformen som funksjon av elektroforesetid under ulike eksperimentelle forhold. Den andre eksperimentelle delen inkluderte hele prosedyren i komet-metoden ved bruk av human perifere blodlymfocytter bestrålt med røntgenstråler. Ingen tidligere studier har utforsket implikasjonen av å sirkulere elektroforeseløsningen i slik detalj som utført i denne masteroppgaven.

Det ble vist at variasjonene i elektrisk potensial på tvers av plattformen ble betydelig redusert ved å sirkulere elektroforeseløsningen. Det ble antatt at disse variasjonene ville gjenspeiles i samsvarende DNA-skader. Disse observerte spenningsvariasjonen under elektroforesen uten sirkulasjon samsvarte kun delvis med de observerte variasjonene i DNA-intensitet fra komet-metoden utført både med og uten sirkulasjon under elektroforesen. CV-en i DNA-haleintensiteten ble redusert med 1-2% ved å sirkulere elektroforeseløsningen ved strømningshastigheter høyere enn 109 ml/min sammenlignet med uten sirkulasjon. I tillegg ble det oppnådd mindre varierende DNA-haleintensitet ved å sirkulere elektroforeseløsningen. Sirkulasjonen bidro også til en bedre temperaturstabilitet. Basert på disse observasjonen, anbefales det å sirkulere elektroforeseløsningen under elektroforesen i komet-metoden.

De elektrokjemiske prosessene ved elektrodene under elektroforesen ble nærmere evaluert. Det ble konkludert at elektrodesystemet brukt under måling av elektriske potensialer var utilstrekkelig på bakgrunn av manglende referanseelektrode. En referanseelektrode må brukes for å kunne stadfeste om de observerte variasjonene i elektriske potensialer oppsto som en følge

av små konsentrasjonsgradienter mellom elektrodene. Det var ikke mulig å angi årsaken til de elektriske potensialforskjellene observert i denne studien som følge av begrenset tid tilgjengelig i masteroppgaven.

Contents

Acronyms/Abbreviation

AC Alternating current

ALS Alkali-labile sites

ANOVA Analysis of variance

AP Apurinic/apyrimidinic

APE1 Apurinic endonuclease 1

BER Base excision repair

CV Coefficient of variation

DC Direct current

DNA Deoxyribonucleic acid

DS Double-stranded

DSB Double-strand break

emf Electromotive force

EEO Electroendo-osmosis

FPG Formamidopyrimidine DNA glycosylase

GGR Global genome repair

HMP High-melting-temperature

HPBL Human peripheral blood lymphocytes

HRR Homologous recombination repair

LET Linear energy transfer

LMP Low-melting-temperature

NER Nucleotide excision repair

NHEJ Non-homologous end-joining

NK Natural killer

OECD The Organisation for Economic Co-operation and Development

OGG1 8-oxoguanine DNA glycosylase

PBS Phosphate buffered saline

PCR Polymerase chain reaction

PFGE Pulsed-field gel electrophoresis

Redox Oxidation-reduction

SS Single-stranded

SSB Single-strand break

TCR Transcription coupled repair

UV Ultraviolet

1. Introduction

The comet assay (single cell gel electrophoresis) is a sensitive and versatile technique for measuring DNA damage and repair at the single cell level. Lesions such as single- and double-stranded DNA breaks, as well as alkali-labile sites can be detected using this method. The comet assay is widely used in biomedical research, in genotoxicity testing of chemicals and radiation and in human biomonitoring. A protocol for the in vivo mammalian alkaline comet assay was approved by OECD in 2014 (OECD 2014). The comet assay is one of few techniques available for detection of genotoxicity in specific organs in vivo. The technique is also used in ecotoxicology and to study industrial chemicals, pharmaceuticals and food chemicals. (Azqueta et al. 2015, Dahl et al. 2016)

The procedure of the comet assay begins with mixing a number of sample cells with a volume of agarose, and then embedding a gel on a glass or polyester film. The glass/film with gel samples are then immersed in a lysis solution to disrupt the cells membrane and remove most of their lipids and proteins, leaving supercoiled nuclear DNA in the gel. This is followed by an alkaline treatment, during which the samples are immersed in an electrophoresis solution with high pH to break the hydrogen bond between the opposite DNA bases, resulting in single-stranded (SS) DNA. Electrophoresis of the samples is then carried out, so that the negatively charged DNA of the cell moves inside the gel matrix towards the positive electrode. (Dahl et al. 2016)

If the cell contains DNA damage the structures resemble comets during electrophoresis, and thus the name the comet assay. After electrophoresis, the cells are immersed in a neutralization buffer followed by fixation and staining with a fluorescent dye. An epifluorescence microscope can be used to visualize the comets, and the relative intensity of DNA in the tail reflects the level of DNA damage. The resulting image combined with a dose-response with an agent known to induce a certain number of lesions per cell, can be used to quantify the number of DNA lesions per cell. Calibration by ionizing radiation can be used since X-rays and other low linear energy transfer (LET) radiation produce a known number of lesions per cell per dose of radiation in DNA of a particular genome size. (Dahl et al. 2016, Hall & Giaccia 2012)

*Ö*stling and Johanson were the first to introduce the comet assay in 1984 (Ostling & Johanson 1984), and the method has been continuously improved thereafter. Researchers at the Department of Chemicals and Radiation at Norwegian Institute of Public Health have developed a high-throughput version to increase the capacity and reduce manual operations and costs (Azqueta et al. 2013, Gutzkow et al. 2013), in addition to being active in establishing comet assay revisions (Dahl et al. 2016). However, considerable variations in results obtained between different laboratories as well as within the same laboratory are still being observed (Collins et al. 2014). Even neighboring cell/agarose samples can give highly different comet tail sizes (Gutzkow et al. 2013). These variations seem to occur due to the lack of a standardized protocol with optimized

experimental conditions (Collins et al. 2014).

Parts of the comet assay protocol have been studied in order to identify sources of variability. Variations in the electrophoresis conditions, such as time, temperature and voltage gradient, have shown to be a major source of error in the comet assay, as well as agarose concentration and duration of alkaline incubation (Azqueta et al. 2011). Local variations in voltage during electrophoresis have also been recorded, whereas circulation of the electrophoresis solution reduced these variations (Gutzkow et al. 2013). There have been several attempts of producing standardized comet assay protocols, however, uncertainties regarding the importance of the different components of the protocol makes this difficult. Thus, researchers still seek for a more reliable comet assay. Minimizing the variability of the comet assay is highly desired in order to achieve consistent results in different experiments as well as in collaborative studies involving different laboratories.

The ultimate aim of this thesis was to improve the comet assay stability and performance, and thus reduce variations in comet assay results within and between laboratories. The focus was mainly based on improving the stability during electrophoresis. It was desired to study more systematically variations in the local voltage variations across the platform and the relative tail DNA intensity variations as a function of electrophoresis circulation. The work was carried out at the Department of Chemicals and Radiation (Department of Molecular Biology from the 1st of April, 2016) at Norwegian Institute of Public Health, in Oslo, Norway.

Measurements of electric potentials across the platform during electrophoresis were performed using a measuring gauge with platinum probes at defined height and spacing. The effect of different experimental conditions, including circulation of the electrophoresis solution at different flow rates and with reversed direction, as well as different volumes of the electrophoresis solution, was examined in order to find the most optimal experimental condition. The comet assay was performed using human peripheral blood lymphocytes (HPBL) irradiated with X-rays, in order to detect any variation in percentage tail DNA due to differences in the circulation of the electrophoresis solution. Results from the analysis of irradiated lymphocytes were compared with measurements of electric potentials.

2. Theory

2.1 Ionizing radiation and DNA damage

2.1.1 DNA structure

Deoxyribonucleic acid (DNA) is the molecule carrying the hereditary information of the cell. It consists of two long polynucloeotide chains, called DNA strands. The subunits of DNA are called nucleotides and are composed of a five-carbon sugar (deoxyribose), one phosphate group and one of four nitrogen-containing bases. The nucleotides are linked by covalent bonds through the sugars and phosphates and form the backbone of the DNA.

The four nitrogen-containing bases are adenine (A), cytosine (C), guanine (G) or thymine (T), and the sequence of which specifies the genetic code. Thymine and cytosine are pyrimidines[1], while adenine and guanine are purines[2]. The two DNA strands which are held together by hydrogen bonds between the bases, form a double helical structure as shown in Figure 2.1. The base pairs are packed in the most energetically favorable arrangement by complementary base-pairing, where adenine only pairs with thymine, and cytosine only pairs with guanine.

The double-stranded (DS) DNA molecules are packaged into chromosomes inside the nucleus in eukaryotic cells. The chromosomes consist of a long linear DNA molecule and proteins that fold and pack the DNA into a more compact structure, as well as proteins involved in gene expression, DNA replication and DNA repair. The complex of DNA and proteins is referred to as the chromatin. The proteins can be divided into histones and the non-histone chromosomal proteins, where histones are responsible for the packing of the nucleosome, which is the first level of DNA packing. A nucleosome core particle consists of eight histone proteins and a double-stranded DNA. The histones bind tightly to the negatively charged backbone of the DNA due to the high portion of positively charged amino acids of the histones. (Alberts et al. 2004)

2.1.2 Ionizing radiation and production of X-rays

Ionizing radiation

The absorption of energy from radiation in biologic material can lead to excitation or ionization. Excitation is the process where an electron in an atom or molecule is raised to a higher energy level and does not include ejection of the electron. The process when one or more electrons are ejected from the atom or molecule, is referred to as ionization. The energy dissipated per

[1] Single-ring groups
[2] Double-ring groups

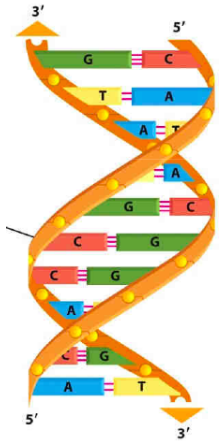

Figure 2.1: A schematic figure illustrating the DNA structure. Each of the two DNA strand is composed of alternating sugars and phosphate groups linked by covalent bonds, forming the backbone with four different nitrogen-containing bases attached. The two DNA strands which are held together by hydrogen bonds between the bases, form a double helical structure. Adenine (A) pairs with thymine (T), while cytosine (C) pairs with guanine (G). From (Alberts et al. 2004).

ionizing event is around 33 eV, and could thus lead to breakage of a strong chemical bond. For example, the energy associated with a C$=$C bond is 4.9 eV.

Ionizing radiation is usually divided into electromagnetic radiation such as X-rays and γ-rays, and particulate radiation such as electrons, protons and neutrons. Further, the radiation could be classified into directly and indirectly ionizing radiation. Charged particulate radiation is direct ionizing radiation, which can disrupt the atomic structure when passing directly through matter and may thus produce chemical and biological changes. Indirectly ionizing radiation, such as X-rays and γ-rays, does not produce chemical or biological damage themselves, but produces secondary fast moving charged particles which can produce damage.

The radiation can interact directly with the critical targets in the cells, which is the dominant process of high linear energy transfer radiation such as neutrons and α-particles. An indirect action of radiation is the process where the radiation interacts with other atoms or molecules in the cell, resulting in production of free radicals that may cause damage in the critical targets. Figure 2.2 illustrates the difference between indirect and direct action of radiation. The critical target for the biologic effects of radiation is the DNA, and includes both cell killing, carcinogenesis and mutation.

A radiation field of photons which passes through a medium will interact with the atoms and be attenuated. The intensity of a thin mono-energetic photon beam passing through a material of thickness x is described by the equation

$$I(x) = I_0 e^{-\mu x}, \tag{2.1}$$

where I_0 denotes the incident intensity without attenuation and μ is the linear attenuation coefficient. The type of interaction process depends on both the energy of the photons and the chemical composition of the absorbing material. The three primary photon interactions are the photoelectric effect, compton scattering and pair production. The photoelectric effect is the

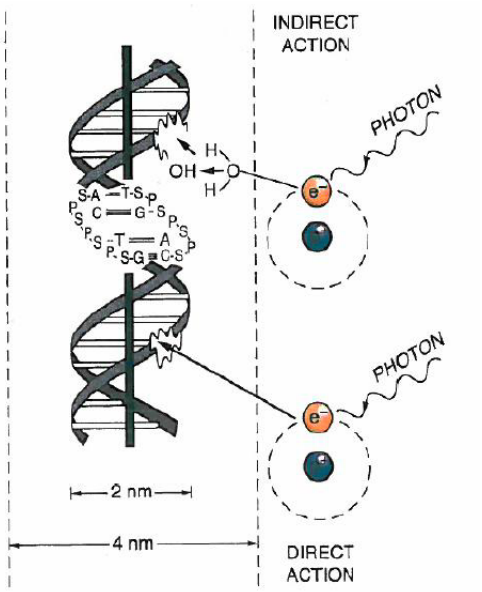

Figure 2.2: A schematic figure illustrating the difference between indirect and direct action of radiation. The direct action of radiation in this figure involves a secondary electron resulting from absorption of an X-ray photon which interacts directly with the DNA. The secondary electron interacts with other molecules than the DNA, such as water molecules, resulting in production of free radicals that may cause lesion in the DNA for the indirect action of radiation. From (Hall & Giaccia 2012).

most likely process when the energy of the photon is close to the binding energy of the atomic electron, which is the case for low energy photons. During this process the entire photon energy is transferred to a bound atomic electron and ejected from the atom. The vacancy left in the atomic shell is filled by an electron from an outer shell leading to a decrease of potential energy which is balanced by an emission of a photon, called characteristic electromagnetic radiation.

Compton scattering involves the process where the photon energy is partly transferred to a secondary electron, resulting in a short range free electron and a scattered lower energy photon. This process occurs most likely at higher photon energies so that the binding energy is negligibly small compared with the photon energy. During the pair production process, the photon interacts with the electromagnetic field of a charged particle creating an electron-positron pair. Further, annihilation takes place where the electron and the positron rest masses are converted into two gamma rays. (Hall & Giaccia 2012, Lilley 2001)

Production of X-rays

X-rays and γ-rays are identical in nature and in property, but are produced differently. X-rays are produced extranucleraly while γ-rays are produced intranuclearly. X-rays are produced in an electrical device which accelerates electrons to high energy and part of this energy is converted to X-rays when the electrons hit a target with high atomic number, such as tungsten.

The X-ray spectrum depends upon the target material, peak voltage, applied voltage waveform and the effect of possible filters used. Two different processes contribute to the X-ray spec-

trum, Bremssthralung and characteristics X-rays. Bremssthralung is referred to the process in which fast incoming electrons loose their kinetic energy through Coulomb interaction with the anode material resulting in energy emitted as photons. Characteristics X-rays are produced only when the energy of the electrons is greater than the binding energy of the atomic electrons from inner shell orbitals.

An illustration of a simplified X-ray tube is shown in Figure 2.3. Electrons are emitted from the cathode and accelerated across the vacuum within the tube by an electric field produced by a high-voltage generator. When the electrons strike the anode/target, Bremssthralung and characteristic X-rays are produced. The X-ray beam passes through collimators when leaving the exit window of the tube.

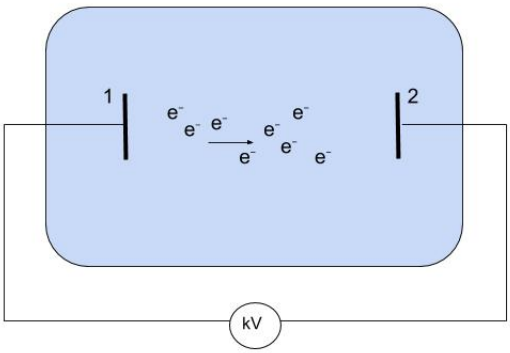

Figure 2.3: An illustration of a simplified X-ray tube. Electrons are emitted from the cathode (1) and accelerated across the vacuum within the tube by an electric field. When the electrons strike the anode/target (2), Bremssthralung and characteristic X-rays are produced. A high-voltage generator produces the high potential difference used to accelerate the electrons.

Filtering of the X-ray spectrum emitted from the anode can be performed both at the soft end and the hard end of the spectrum. Soft-end filtering is obtained by using light element such as Aluminium or Copper. Hard-end filtering is obtained by using an acceleration voltage which is significantly higher than the K-edge and by using the same element in both the anode and the filter. (Flower 2012, Hall & Giaccia 2012)

2.1.3 DNA damage

DNA is constantly exposed to different environmental factors, such as genotoxic chemicals, ultraviolet (UV) radiation and ionizing radiation, which can damage the DNA. Ionization radiation can induce various types of DNA lesions, such as base damage, single-strand breaks (SSBs) and double-strand breaks (DSBs). A single-strand break is referred to as a break in only one strand or breaks in two strands well separated such that they are repaired as independent breaks. Alternatively, breaks that occur at both strands directly opposite or closely separated, i.e. only a few base pairs apart, are defined as DSBs and results in cleavage of chromatin into two pieces. The breaks may be rejoined into their original configuration via complex enzymatic machiner-

ies. However, if they fail to be rejoined correctly, DSBs may result in cell killing (apoptosis or necrosis), mutations, and ultimately the first step in a process of carcinogenesis.

A large number of lesions in DNA is produced by ionizing radiation. For mammalian cells, the number of DNA SSBs per cell detected immediately after a dose of 1 Gy is approximately 1000, while the number of DNA DSBs per cell is only approximately 40. The number of base damages per cell detected after a dose of 1 Gy is larger than 1000. Thousands of single strand breaks also arise spontaneously in cells each day. Mammalian cells are able to repair base damage, SSBs, DSBs, sugar damage and DNA-DNA crosslinks by different repair pathways. SSBs are readily repaired using the opposite strand as template and thus cell killing caused by SSBs occurs rarely. However, if the repair is incorrect, it may result in a mutation.

A base damage in the DNA can be repaired through the base excision repair (BER) pathway. This repair mechanism involves recognition and removal of the wrong or damaged base by DNA glycosylase forming an apurinic/apyrimidinic (AP) site. Further, an apurinic endonuclease 1 (APE1[3]) removes the sugar residue and DNA polymerase replace the correct nucleotide. The repair is completed by DNA ligase which seals the DNA strand.

Nucleotide excision repair (NER) is a complex pathway which removes bulky adducts in the DNA, such as pyrimidine dimers. It includes both global genome repair (GGR) and transcription coupled repair (TCR). The first pathway refers to repair of lesions from DNA both that encode or do not encode for genes, while the latter only removes lesions in the DNA of actively transcribed genes. The difference between these two pathways is the process of detecting the lesion. The main steps in NER are first to recognize the damage, followed by bracket the lesion by DNA incision and removal of the region. Further, the gap is filled by repair synthesis, and the process is completed by DNA ligation. Successful NER involves the action of approximately 30 proteins.

DNA DSBs can be repaired by two different mechanisms, either by homologous recombination repair (HRR) or by non-homologous end-joining (NHEJ). HRR denotes accurate repair without any loss of nucleotides and requires an undamaged DNA strand used as a template for repair. Alternatively, NHEJ involves limited DNA repair synthesis where several nucleotides may not be replaced.

A common technique used to measure DNA strand breaks is the comet assay. It can detect DNA damage and repair at the single-cell level. The assay is cell based, and thus the DNA in these cells are more resistant to damage by radiation than would be expected from studies of free DNA. This is both due to scavengers in the cells that removes some of the free radicals produced by ionizing radiation and the physical protection of the DNA obtained from packaging with proteins. The comet assay is described in more detail in Section 2.6. (Hall & Giaccia 2012)

2.2 Human peripheral blood lymphocytes

Human blood cells consist mainly of erythrocytes[4], leukocytes[5] and platelets. Leukocytes are distinguished from other blood cells by having nuclei. They participate in the human immune response and can be divided into five main types: basophils, eosinophils, lymphocytes, monocytes and neutrophils.

[3] In human cells

[4] Red blood cells

[5] White blood cells

Lymphocytes constitute 99% of the cells in the lymph and 20-40% of the body's white blood cells. They circulate continuously in the blood and the lymph. The lymphocytes can be further divided into three main types, based on function and cell membrane components. These three categories are B cells, T cells and natural killer (NK) cells. B and T lymphocytes participate in the adaptive immunity and NK cells are part of the innate immune system. (Kindt et al. 2007)

2.2.1 Isolation of human peripheral blood lymphocytes by density gradient centrifugation

For research purposes, isolation of blood cells should provide maximum specificity, purity, yield, speed and reproducibility. Density gradient centrifugation is a technique commonly used to isolate blood cells. The sedimentation rate of a particle is proportional to the force applied during centrifugation of a suspension of particles. If the centrifugal force and the liquid viscosity is fixed, the sedimentation rate is proportional to the particle's size and the difference between the particle's density and the surrounding medium's density. Sedimentation of a sphere in a centrifugal field can be given by

$$v = \frac{d^2(\rho_p - \rho_l)}{18\eta} \times g, \tag{2.2}$$

where v and d denote the sedimentation rate and the particle's diameter, respectively. η is the medium's viscosity and g is the centrifugal force. ρ_p and ρ_l are the particle and the liquid density, respectively. (GeneralElectric 2014)

Human peripheral blood lymphocytes can easily be isolated by density centrifugation of peripheral blood. The isolated cells represent recirculating lymphocytes consisting of T lymphocytes (70%), B lymphocytes (20%) and some NK cells and monocytes/macrophages (Gutzkow 2004). NycoPrep^{TM} is a ready-made, sterile and endotoxin solution that can be used for the preparation of pure lymphocyte suspension. The contamination of erythrocytes in the mononuclear cell suspension is approximately 3-10% of the total cell number. The blood sample must be diluted 1:1 with physiological saline before being applied to the gradient in order to obtain the maximum yield. (Axis-Shield 2015)

2.3 Electrical parameters

2.3.1 Electric force and electric field

Electric charge is a physical property of matter and can be referred to as the amount of either positive or negative electric energy. It is a fundamental quantity in electrostatics, the study of forces acting between charges. Conductors permit the easy movement of electric charges through them, while insulators do not. Conductive materials include metals, electrolytes, semiconductors and superconductors, corresponding to different degrees of conductivity. Semiconductors are intermediate in their properties between good conductors and good insulators.

The electric force between two point charges depends on the distance between them as well as the quantity of the charges. According to Coulomb's law, the electric force between two point charges can be given by

$$F = \frac{1}{4\pi\epsilon_0}\frac{|q_1 q_2|}{r^2}, \tag{2.3}$$

where ϵ_0 is the vacuum permittivity, q_1 and q_2 are the two point charges and r is the distance between the charges.

The electric field is defined as the electric force per unit charge and the electric field of a point charge can thus be given by

$$\vec{\mathbf{E}} = \frac{\vec{\mathbf{F_0}}}{q_0} = \frac{1}{4\pi\epsilon_0}\frac{q}{r^2}\hat{\mathbf{r}}. \tag{2.4}$$

(Young et al. 2011)

2.3.2 Electric potential energy and electric potential

When a free charged particle is placed in an electric field, the field exerts a force which cause movement of the particle. This work can be expressed as electric potential energy. The work W done by a force $\vec{\mathbf{F}}$ which acts on a particle that moves from point a to b can be given by

$$W = \int_a^b \vec{\mathbf{F}} \cdot d\vec{\mathbf{l}}, \tag{2.5}$$

where $d\vec{\mathbf{l}}$ is an infinitesimal displacement along the particle's path. If the force is conservative, the work done to move the particle from point a to b can be expressed in terms of potential energy U:

$$W = U_a - U_b = -\Delta U. \tag{2.6}$$

By combining Equation 2.3, Equation 2.5 and Equation 2.6, the electric potential energy of two points charges q and q_0 can be given by

$$U = \frac{1}{4\pi\epsilon_0}\frac{q q_0}{r}. \tag{2.7}$$

The potential energy per unit charge is defined as the potential. The potential V at a point in an electric field can be given by

$$V = \frac{U}{q_0} = \frac{1}{4\pi\epsilon_0}\frac{q}{r}, \tag{2.8}$$

where q_0 is the charge at that point. The relationship between the potential and the electric field can be given by

$$V_a - V_b = \int_a^b \vec{\mathbf{E}} \cdot d\vec{\mathbf{l}}, \tag{2.9}$$

or

$$\vec{\mathbf{E}} = -\vec{\nabla} V. \tag{2.10}$$

In circuits the difference in potential between two points is referred to as the voltage. (Young et al. 2011)

2.3.3 Electric current and Ohm's law

An electric current is a flow of electric charge and can be defined through a cross-sectional area A as

$$I = \frac{dQ}{dt}, \tag{2.11}$$

where dQ and dt is the net charge and time, respectively. An electric current could either be described as direct current (DC) or alternating current (AC). The first refers to a current which always flows in the same direction, while the latter indicates current where the direction periodically changes.

Power generators and batteries can supply energy into a system, referred to as electromotive force (emf). This result is a change in the electric potential at each point in the system. Both the emf and the potential differences in the system produce different voltages throughout the circuit. The voltages at different points are most commonly determined with respect to a single reference point.

Resistance is the ability to oppose the flow of electric current, and components providing this property are referred to as resistors. Ohm's law states that the current I is directly proportional to the voltage V and inversely proportional to the resistance R:

$$I = \frac{V}{R}. \tag{2.12}$$

The power dissipation P of a resistor can be given by

$$P = V \cdot I = I^2 \cdot R. \tag{2.13}$$

The resistance of a component is determined by both its dimensions and the electrical characteristics of the material, referred to as the resistivity, ρ. For a wire, the resistance is related to its length, cross-sectional area and resistivity, and can be given by

$$R = \frac{\rho l}{A}, \tag{2.14}$$

where l and A are the length and the cross-sectional area, respectively. (Storey 2013)

2.3.4 DC power supply

The function of a power supply is to supply electric power to a system. Production of heat will be generated when applying a flow of current through a resistive medium, and the amount of heat can be given by

$$Heat = \varepsilon \cdot I \cdot t, \tag{2.15}$$

where ε, I, and t are the electromotive force, the current and the time, respectively. (Burtis & Ashwood 2001)

DC power supply could be divided into unregulated and regulated. Unregulated DC power supply is most commonly used when a constant output voltage is not required and ripple is

not critically important. On the contrary, the regulated DC power supply produces a more constant output voltage with less ripple, and is most commonly used in applications which requires these situations. AC-DC converter is used to convert AC line voltage to DC voltage used in the DC power supply. Ripple in the voltage can occur by incomplete suppression of alternating waveform within the power supply resulting in a variation of the DC output. When a system is supplied with power from batteries, a DC to DC converter is used in order to maintain a constant voltage. (Storey 2013)

2.4 Electrochemistry

Electrochemistry is concerned with the interchange of chemical and electrical energy, mainly related to processes involving oxidation-reduction reactions. Such processes could either be the generation of an electric current from a chemical reaction or producing a chemical change by the use of a current. The transfer of electrons from the reducing agent to the oxidizing agent is called an oxidation-reduction (redox) reaction. Oxidation involves loss of electrons, while reduction involves gain of electrons.

An electromotive force is required in order to induce movement of electrons through a wire or a medium. The emf is defined as the potential difference between two points in the electric circuit and can be given by

$$emf = \frac{work}{charge}. \tag{2.16}$$

In electrochemistry, the electromotive force is usually referred to as the cell potential ε:

$$\varepsilon = \frac{-w}{q}, \tag{2.17}$$

where w and q are referred to as the work and the charge transferred, respectively. The minus sign indicates that the work is viewed from the point of view of the system. When a current flows through a system, some of the energy is always lost through frictional heating.

The charge in 1 mole of electrons is referred to as the Faraday constant, **F**, and is equal to 96485 C/mol. The charge q transferred, is thus equal to the number of moles of electrons n multiplied with the Faraday constant **F**:

$$q = n\mathbf{F}. \tag{2.18}$$

The work obtained from a process with constant temperature and pressure is equal to the change in Gibbs free energy ΔG:

$$w = \Delta G. \tag{2.19}$$

The Gibbs free energy can be defined as

$$G = H - TS, \tag{2.20}$$

where H, T and S denote the enthalpy, temperature end entropy, respectively. By combining Equation 2.17, Equation 2.18 and Equation 2.19, the change in Gibbs free energy under standard

conditions (denoted with °) is obtained:

$$\Delta G^\circ = -n\mathbf{F}\varepsilon^\circ. \tag{2.21}$$

The cell potential is dependent on the concentration of the solution. An increase in the concentration of a reactant will thus increase the cell potential. This dependency results directly from the dependence of Gibbs free energy on concentration. The change in Gibbs free energy for a chemical reaction can be given by

$$\Delta G = \Delta G^\circ + RTln(Q), \tag{2.22}$$

where ΔG° is Gibbs free energy under standard condition, R is the universal gas constant, T is the temperature and Q is the reaction quotient. By inserting Equation 2.21 into Equation 2.22, the equation becomes

$$-n\mathbf{F}\varepsilon = -n\mathbf{F}\varepsilon^\circ + RTln(Q). \tag{2.23}$$

The Nernst equation which describes the relationship between the cell potential and the concentration of the cell components, is obtained by dividing each side by $-n\mathbf{F}$:

$$\varepsilon = \varepsilon^\circ - \frac{RT}{n\mathbf{F}}ln(Q). \tag{2.24}$$

For a redox reaction given as

$$O + ne^- \rightleftharpoons R, \tag{2.25}$$

the reaction quotient is equal to the ratio of the reduced molecule‘s concentration to the oxidized molecule‘s concentration: $Q = \frac{[R]}{[O]}$. The cell potential is sensitive to the concentrations of the reactants and products involved in the cell reaction occurring at the electrode. Small differences in concentration may cause variation in measured cell potentials. (Zumdahl & DeCoste 2013)

2.4.1 Electrolysis

An electrolytic cell uses electrical energy to produce chemical changes, and a process utilizing this concept is electrolysis. The chemical change for which the cell potential is negative is a nonspontaneous process, and thus a supply of energy in the form of a current through the cell is required to cause this chemical change. In a standard electrolytic cell, the cathode is negatively charged, while the anode is positively charged. The anion[6] and the cation[7] migrate toward the anode and cathode, respectively. Figure 2.4 illustrates the movement of ions in a solution with an applied electric field.

The total coulombs of charge, Q, passing into the solution at the cathode after a time t can be calculated by using the Equation:

$$Q = I \cdot t, \tag{2.26}$$

[6]Negatively charged ion
[7]Positively charged ion

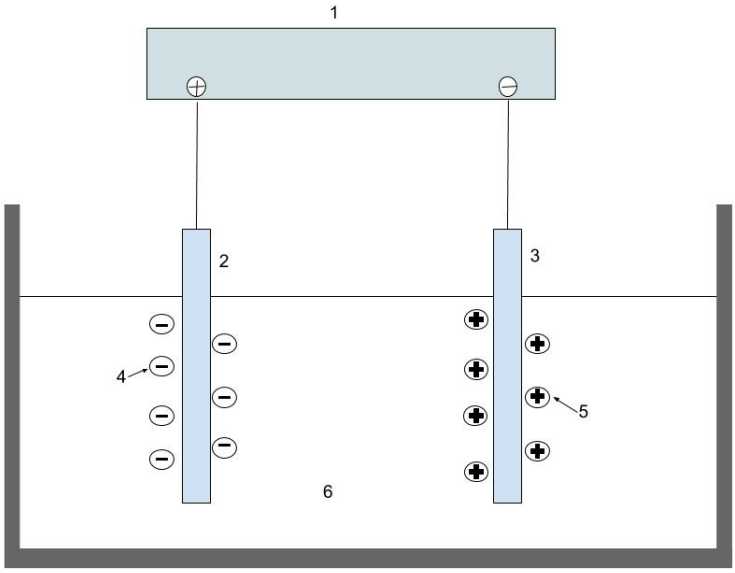

Figure 2.4: A schematic diagram illustrating the movement of ions towards the oppositely charged electrode in a solution with an applied electric field. The figure shows the power supply (1), the anode (2), the cathode (3) and the solution (6). The anions (4) migrate toward the anode, while the cations (5) migrate toward the cathode.

where I and t denote the current and the time, respectively. (Zumdahl & DeCoste 2013)

Electrolysis of water

Pure water conducts electric current poorly, and thus electrolysis of water only occur at a significant rate by adding some salts to the water. The net reaction from electrolysis of water can be given by

$$2H_2O \longrightarrow 2H_2 + O_2, \tag{2.27}$$

where oxidation occurs at the anode:

$$2H_2O \longrightarrow O_2 + 4H^+ + 4e^-, \tag{2.28}$$

and reduction occurs at the cathode:

$$4H_2O + 4e^- \longrightarrow 2H_2 + O_2. \tag{2.29}$$

During electrolysis, hydrogen gas is produced at the cathode while oxygen gas is produced at the anode. (Zumdahl & DeCoste 2013)

2.4.2 Conductivity in a solution

The property of a medium/material allowing an electric current to pass between two electrodes is termed electric conductivity. A solution with ions has a defined conductivity, and the more ions present in the solution, the higher the conductivity.

The conductivity in a solution can be measured by applying a voltage, which generates a current within a conductivity cell. In a 2-pole cell the resulting current, I, is measured after applying a voltage V to two platinum plates immersed in a solution. The resistance R can be calculated by using Ohm's law given in Equation 2.12. Further, the conductance G can be determined by taken the reciprocal of the resistance: $G = \frac{1}{R}$. The conductivity can be calculated by using the obtained conductance G and the expression of the conductivity given as

$$\sigma = G \cdot K, \tag{2.30}$$

where K is the cell constant, which is based on the geometry of the cell.

A 4-pole conductivity cell consists of four rings where the voltage applied generates a current into two outer rings while the potential is measured between the two inner rings. The conductivity will be directly proportional to the applied current. The geometrical configuration of the four-pole conductivity cell requires calibration by using a standard solution with known conductivity.

The temperature affects the conductivity of a solution, resulting in higher conductivity with increasing temperature due to increased mobility of ions. For high precession measurements, the conductivity can be corrected by using a temperature coefficient when comparing measurements taken at different temperatures. By measuring the conductivity at temperature T_1 and T_2, the temperature coefficient can be determined by using the following equation:

$$\theta = \frac{(\sigma_{T_1} - \sigma_{T_2}) \cdot 100}{(T_2 - T_1) \cdot \sigma_{T_1}}, \tag{2.31}$$

where σ_{T_1} and σ_{T_2} are the conductivities at T_1 and T_2, respectively. T_2 should be the typical sample temperature and differ more than 10 C $^\circ$ from T_1. (RadiometerAnalytical 2005)

2.5 Electrophoresis

Electrophoresis is a phenomenon in which charged particles or molecules move under the influence of an electric field. The term also includes techniques utilizing this migration of charged particles or molecules. Biological and biochemical research, molecular biology, pharmacology and protein chemistry are among the main fields of application. (Westermeier 2005)

The electrophoresis system consists of two electrodes, one negatively and one positively charged, referred to as the cathode and the anode, respectively. The electrodes are attached along the sides of an electrophoresis tank, which is filled with electrophoresis solution during the electrophoresis. Usually the tank consists of two wells on the sides with a platform in the middle of these two. The electrodes are connected to a power supply with either a constant current, a constant voltage or a constant power applied. The sample may be placed on the platform in the electrophoresis tank during electrophoresis. A schematic diagram of an electrophoresis system is shown in Figure 2.5. (Burtis & Ashwood 2001)

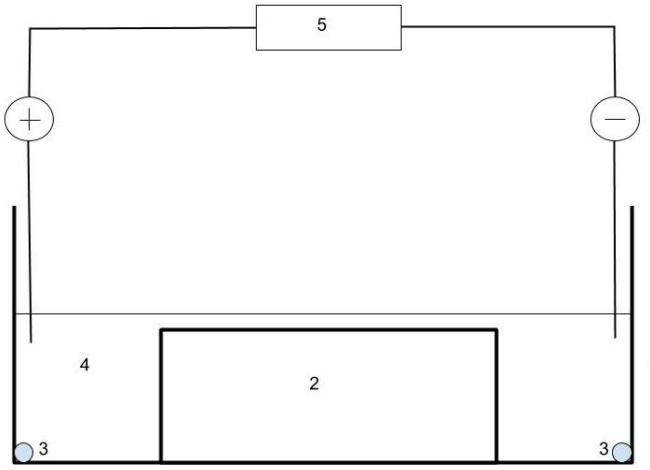

Figure 2.5: A schematic diagram of an electrophoresis system showing the electrophoresis tank (1), the platform (2), the two electrodes (3), the electrophoresis solution (4) and the power supply (5). The cathode is located to the right, while the anode is located to the left. With this design, the sample is placed on the platform during electrophoresis.

Electrophoresis can be used to separate biological molecules, such as proteins or DNA. The sample to be processed is placed in a viscous medium in a conductive solution with an applied external electric field. The following equations in this section are simplified versions of the forces involved during electrophoresis. The charged molecules are driven towards the oppositely charged electrode by the electric force, F_E, given by

$$F_E = Eq, \tag{2.32}$$

where E is the electric field strength and q is the charge of the molecule. (Young et al. 2011)

The electric force is opposed by a hydrodynamic frictional force, F_D, caused by the viscous medium, and can be given by

$$F_D = f v, \tag{2.33}$$

where v is the velocity of the molecule and f is the frictional coefficient depending on both the viscosity of the medium and the size of the migrating molecule (Stryer 1988).

According to Stokes' law, the frictional coefficient for a spherical particle with radius r can be expressed by

$$f = 6\pi\eta r, \tag{2.34}$$

where η denotes the solution's viscosity. Stokes law for a spherical particle assumes no interparticle interactions and is only valid at very dilute solutions. The coefficient 6π depends on the boundary conditions where it is assumed that the first solvent layer adsorbs to the particle surface. Since most of the biological macromolecules are not spherical, an ellipsoidal shape can be a more realistic model. (Næss et al. 2014).

By using Newton's second law, the net force acting on the molecule assuming one-dimensional motion, can be given by

$$\sum F = F_E - F_D = ma, \tag{2.35}$$

where m and a is the mass and the acceleration of the molecule, respectively. At thermal speed the acceleration is zero (Giordano 2013). During electrophoresis the electric force and the hydrodynamic frictional force are thus in equilibrium. By combining the expression for the electric force and the hydrodynamic frictional force given by Equation 2.32 and 2.33, respectively, the velocity of migration v of a charged molecule in an electric field is obtained:

$$v = \frac{Eq}{f}. \tag{2.36}$$

The electrophoretic mobility μ is a more commonly used quantity regarding electrophoresis and is defined as the velocity of migration v divided by the electric field strength E (Stryer 1988). By using Equation 2.36, the electrophoretic mobility can be given by

$$\mu = \frac{v}{E} = \frac{q}{f}. \tag{2.37}$$

The distance x that the molecule moves during the electrophoresis can be obtained by multiplying the velocity of migration given in Equation 2.36 with the electrophoresis time t:

$$x = \frac{Eqt}{f}. \tag{2.38}$$

The electric field E can be determined by dividing the applied voltage V with the distance d between the electrodes. (Young et al. 2011)

The electrophoretic mobility of a particle is affected by its Brownian motion. However, by averaging over a number of particles, the Brownian motion can generally be neglected in practical cases. In addition to the electric force and the hydrodynamic frictional force, an additional force opposing the electric force acts on the sample molecule. This force is due to counterions which tend to surround the molecule and flow in the opposite direction of the molecule migration. (Hunter 1988)

2.5.1 The zeta potential

In this section, the zeta potential will be defined, by first describing the Stern layer, the diffuse electric layer and the Boltzmann distribution of counterions surrounding a particle in solution. The distribution of ions surrounding a particle in solution is affected by the surface charge of the particle. Oppositely charged counterions balance the final surface charge, and could either be bound to the surface within the inner region, called the Stern layer, or be loosely associated within the outer layer, called the diffuse electric double layer, as shown in Figure 2.6. The thickness of the diffuse electric double layer is known as the Debye length.

If only counterions are present without any added electrolyte in the solution, the chemical potential ψ of an ion can be given by

$$\psi = ze\phi + k_B T ln(\rho), \tag{2.39}$$

where ϕ, ρ, z and e denote the electrostatic potential, the number density of ions, the valency,

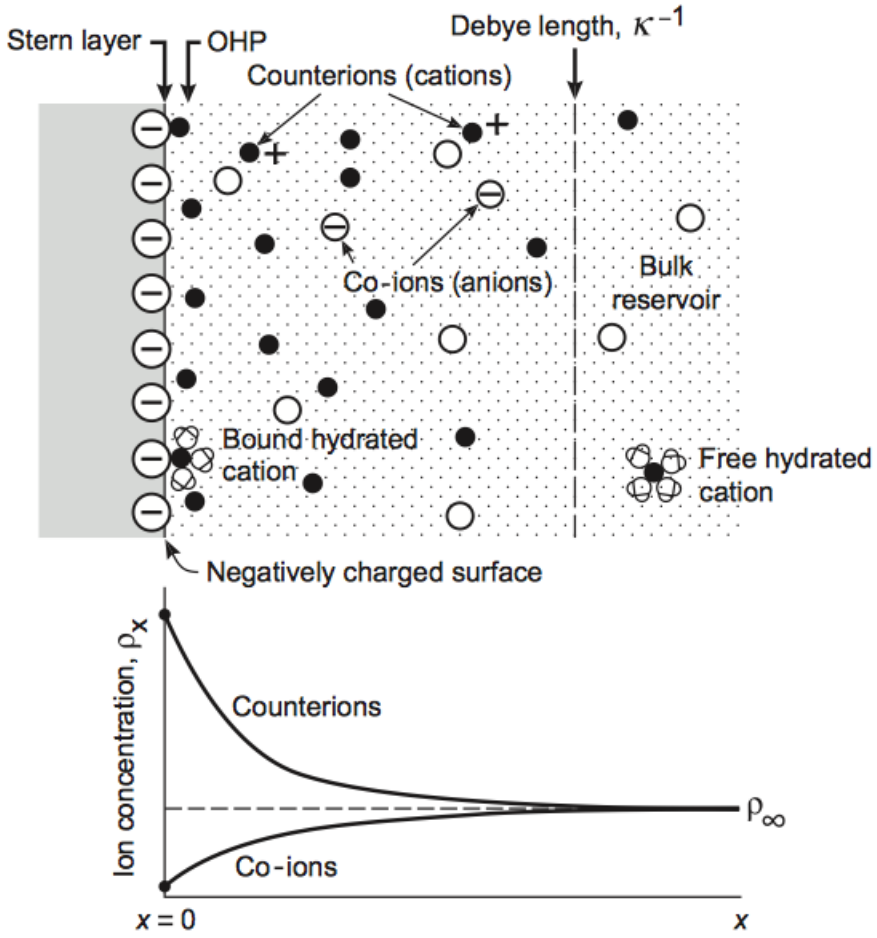

Figure 2.6: A schematic figure illustrating the Stern layer, the diffuse electric double layer and the ion concentration as a function of distance x. Counterions surrounding the negatively charged surface with depletion of coions. p_∞ is the electrolyte concentration at $x = \infty$. The length of the diffuse electric double layer is known as the Debye length. From (Israelchvili 2011).

and the elementary charge of an electron, respectively. k_B is the Boltzmann constant, and T the temperature. The Boltzmann distribution of counterions is obtained by requiring equilibrium so that the chemical potential is the same for all values of x:

$$\rho = \rho_0 e^{\frac{-ze\phi}{k_B T}}. \tag{2.40}$$

However, it is more common that solutions contain electrolyte ions which have a large effect on the electrostatic potential and the forces between charged surfaces. The Boltzmann distribution of ions i at x becomes:

$$\rho_{xi} = \rho_{\infty i} e^{\frac{-z_i e\phi_x}{k_B T}}, \tag{2.41}$$

where $\rho_{\infty i}$ is the ionic concentration.

As the particles migrate through the solution due to the applied voltage during electrophore-

sis, the counterions move with it. Beyond a surface within the diffuse layer, the ions do not move with the particle causing a reduction in the velocity and is thus called electrophoretic retardation. The electric potential existing in this surface is called the *zeta potential*.

The relation between the electrophoretic mobility μ and the zeta potential ζ can be given by

$$\mu = \frac{2\epsilon\zeta F(\kappa a)}{3\eta}, \tag{2.42}$$

where ϵ and η are the permittivity and the viscosity of the medium, respectively. $F(\kappa a)$ is Henry's Function where $1/\kappa$ is the Debye length, and a is the radius of the particle. For small particles, the retardation force acts across the whole double layer, however, the main retardation force acting on the particle is the hydrodynamic frictional force. (Hunter 1988, Israelchvili 2011, Næss et al. 2014)

2.5.2 Electrophoresis solution

One of the main purposes of the electrophoresis solution is to provide ions that can carry a current during electrophoresis. In addition the solution is required in order to maintain a constant pH during the electrophoresis, which is essential since a change in pH alters the net charge and thus the mobility. The pH is a measure of the solution's concentration of H^+, $[H^+]$, and is defined as

$$pH = -log_{10}[H^+]. \tag{2.43}$$

The ionization equilibrium of a weak acid can be given by

$$HA \rightleftharpoons H^+ + A^-, \tag{2.44}$$

where HA and A^- is the weak acid and its conjugate base, respectively.

The equilibrium constant K for the ionization of a weak acid can be defined as

$$K = \frac{[H^+][A^-]}{[HA]}. \tag{2.45}$$

where $[HA]$ is the molar concentration of the undissociated weak acid and $[A^-]$ is the molar concentration of the acid's conjugate base. The relationship between pH and the ratio of acid to base can be described with the Henderson-Hasselbalch equation:

$$pH = pK + log\frac{[A^-]}{[HA]}. \tag{2.46}$$

The pK of an acid is defined as: $pK = -logK$, where K is the equilibrium constant for the ionization. (Stryer 1988)

The ionic strength of the electrophoresis solution influences the ionic cloud surrounding a charged particle and thus affects the rate of migration of the sample molecules. By increasing the ionic strength, the size of the ionic cloud increases resulting in a reduction in the electrophoretic mobility of the sample molecule. (Burtis & Ashwood 2001)

2.5.3 Gel electrophoresis

The viscous medium used in electrophoresis is often in the form of a gel and thus the name gel electrophoresis. There are two main reasons for carrying out the molecule separation in a gel. First, the gel enhances the separation between molecules with different sizes as it serves as a molecular sieve. Larger molecules will not move as easy through the gel as the small molecules, resulting in a difference in the migration between the molecules. Further, the convective currents produced by small temperature gradients are suppressed by the gel, which is important in order to obtain an effective separation. (Stryer 1988)

The choice of gel type relies on being easy to prepare and modify, cheap to produce as well as the requirement that it should be chemically inert[8] during electrophoresis. One suitable matrix which satisfies these requirements is the agarose gel. (Westermeier 2005)

Agarose

Agarose is a linear polysaccharide polymer which consists of alternating residues of D- and L-galactose joined by α and β glycosidic linkage. Agarose chains form helical fibers that further aggregate into supercoiled structures. A three-dimensional mesh of channels is obtained by performing gelation of agarose. (Sambrook & Russel 2001)

The two main types of agarose gel are the high-melting-temperature (HMP) agarose and the low-melting-temperature (LMP) agarose. HMP is referred to as a product manufactured from two species of seaweed, Gelidium and Gracilaria, while the LMP agarose has been modified by hydroxyethylation and thus melt at lower temperatures. An advantage of LMP agarose is that cells can be embedded without damage since it's a liquid at temperature as low as 30-35 °C. (Sambrook & Russel 2001)

2.5.4 DNA gel electrophoresis

A method to resolve and separate DNA molecules based on their length or conformation is DNA gel electrophoresis. This technique is essential in molecular biology and is regularly used in biological, medical and forensic laboratories. Both genomic DNA, plasmid DNA, DNA from mitochondria and polymerase chain reaction (PCR) products can be analyzed. (Walker 2013)

Electrophoresis of DNA molecules are most commonly carried out in agarose gel. For small nucleic acids, polyacrylamid gels are more commonly used. Due to the negative charge on the sugar-phosphate backbone of the DNA molecule, the DNA migrates towards the positively charged anode. The rate of migration of DNA through agarose gel is determined by several factors, including the DNA molecule itself, the agarose gel and the electrophoresis conditions, such as voltage gradient, time, and electrophoresis solution. (Sambrook & Russel 2001, Walker 2013)

The rate of migration is inversely proportional to the logarithm of the number of base pairs for molecules of double-stranded DNA. As the molecule becomes larger, the rate of migration decreases due to greater frictional drag in the gel. The conformation of the DNA also impact the rate of migration. Superhelical circular, nicked circular and linear DNAs move through the gel at different rates, depending on the concentration and type of agarose gel, as well as the ionic strength of the buffer and the applied voltage. (Sambrook & Russel 2001)

[8] Not chemically reactive

The logarithm of the electrophoretic mobility of the DNA is linearly related to the gel concentration ι, which can be given by

$$log(\mu) = log(\mu_0) - K_r \iota, \tag{2.47}$$

where μ_0 is the free electrophoretic mobility and K_r is the retardation coefficient which is determined by the properties of the gel and the size and shape of the molecule. In addition to the gel concentration, the gel type will also influence the rate of migration. (Sambrook & Russel 2001)

Further, the composition and ionic strength of the electrophoresis solution will affect the electrophoretic mobility of DNA. The conductivity is minimal with an electrophoresis solution without ions, while at very high ionic strength the electrical conductance could generate large amounts of heat, which could melt the gel and/or denature the DNA. The applied voltage determines the electric field and thus directly affects the migration of the sample molecules. The rate of migration of linear DNA is proportional to the applied voltage at low voltages. (Sambrook & Russel 2001)

Electroendo-osmosis

Electroendo-osmosis (EEO) denotes the motion of the liquid caused by the applied voltage and thus affects the migration of samples during electrophoresis. This phenomenon occurs due to ionized acidic groups which are attached to the agarose gel inducing positively charged counterions in the buffer. These counterions migrate through the gel in the direction opposite of that of the DNA, thus decreasing the rate of migration of the DNA.

In order to minimize electroendo-osmosis, agarose gels with low levels of EEO can be used, which is achieved by low density of negative charge groups in the agarose, such as sulfate. However, agarose with zero EEO is undesirable since these are chemically modified by adding positively charged groups, which neutralize the sulfated polysaccharides in the agarose gel but may inhibit subsequent enzyme reactions. In addition, these agarose gels have been added locust bean gum which retards expulsion of water from the gel. (Sambrook & Russel 2001)

2.5.5 Ionic migration and potential gradient - a macroscopic description

Electrophoresis could be considered as an electrochemical system where migration of ions occur mainly due to the applied electric field. By applying Ohm‘s law, the current density can be given by

$$J = \sigma E = -\sigma \nabla \phi, \tag{2.48}$$

where σ is the conductivity, E is the electric field and $\nabla\phi$ is the potential gradient.

Both diffusion, migration and convection may contribute to the flux of mobile ions in a dilute electrolyte. The total flux of an ion, N_i, can be given by

$$N_i = -D_i \nabla c_i - z_i \mu_i \mathbf{F} c_i \nabla \phi + c_i \upsilon, \tag{2.49}$$

where D_i, c_i, z_i, μ_i denote the diffusion coefficient, the concentration, the valence, and the mobility of ion i, respectively. υ is the velocity of the electrolyte in dilute solutions and $z_i\mathbf{F}$ is the charge per mole on a species. Diffusion occurs if there exist a concentration gradient ∇c. This

mass transfer phenomenon causes a more uniform ion distribution. Convection is mass transfer due to the bulk motion of a fluid, and is thus a cause of the average velocity of all molecules in the solution.

Under an applied electric field, the ion migration is driven towards the oppositely charged electrode by the electric force, $F_E = qE$, with $q = ze$ where z and e are the valence of the ion and the elementary charge of an electron, respectively. The migration flux of an ion i, is obtained by multiplying the drift velocity with the ion's concentration c_i giving the second term on the right side in Equation 2.49.

The Nernst-Einstein relation gives the relation between the electrochemical mobility μ_i and the diffusion coefficient D_i:

$$\mu_i = D_i \frac{\mathbf{F}}{RT}, \tag{2.50}$$

where $\mathbf{F}$ is Faraday constant, R is the gas constant and T is the temperature.

The current density in an electrolytic solution can be obtained by summing the fluxes of charged ions in the electrolyte:

$$J = \mathbf{F} \sum_i z_i N_i. \tag{2.51}$$

Substituting Equation 2.49 into Equation 2.51 gives:

$$J = -\mathbf{F} \sum_i z_i D_i \nabla c_i - \mathbf{F}^2 \nabla \phi \sum_i z_i^2 \mu_i c_i + \mathbf{F} v \sum_i z_i c_i. \tag{2.52}$$

By assuming electroneutrality in the electrolyte without any concentration gradient, the equation reduces to

$$J = -\kappa \nabla \phi, \tag{2.53}$$

where

$$\kappa = \mathbf{F}^2 \sum_i z_i^2 \mu_i c_i, \tag{2.54}$$

is the conductivity of the solution. Electronutrality is observed in all solutions expect in a thin double charge layer near electrodes. In conductivity measurements, an alternating current is used to avoid build up of concentrations differences.

The current carried by species n can be given by

$$t_n J = -\mathbf{F}^2 z_n^2 \mu_n c_n \nabla \phi = J \frac{z_n^2 \mu_n c_n}{\sum_i z_i^2 \mu_i c_i}, \tag{2.55}$$

where

$$t_n = \frac{z_n^2 \mu_n c_n}{\sum_i z_i^2 \mu_i c_i}, \tag{2.56}$$

is the fraction of the current by species n and denotes the transference number. The migration flux density of species i can thus be given by

$$N_i^{migr} = J \frac{t_i}{z_i \mathbf{F}}. \tag{2.57}$$

By stating a material balance of species gives the equation

$$\frac{\partial c_i}{\partial t} = -\nabla N_i + R_i, \tag{2.58}$$

where the first term denotes the accumulation which is equal to the net input (second term) plus production (third term). R_i is the production per unit volume in homogenous chemical reactions in the bulk of the solution, not including electrode reactions. By multiplying Equation 2.58 with $z_i\mathbf{F}$ and performing addition over species gives

$$\frac{\partial}{\partial t}\mathbf{F}\sum_i z_i c_i = -\nabla \cdot \mathbf{F}\sum_i z_i N_i + \mathbf{F}\sum_i z_i R_i. \tag{2.59}$$

If all the homogeneous reactions are electrically balanced, the last term will be zero. By again assuming, electroneutrailty, the equation reduces to

$$\nabla J = 0, \tag{2.60}$$

which implies conservation of charge. By inserting Equation 2.60 into Equation 2.53 yields

$$\nabla^2 \phi = 0. \tag{2.61}$$

Thus, the potential satisfies Laplace's equation in a region of uniform composition. (Newman & Thomas-Alyea 2004)

2.6 The comet assay

The comet assay (single cell gel electrophoresis) is a sensitive and versatile technique for measuring DNA damage and repair at the single cell level. The comet assay is widely used in biomedical research, in genotoxicity testing of chemicals and radiation and in human biomonitoring. In human peripheral blood mononuclear cells, the number of lesions which can be detected by using the comet assay is as low as a few hundred lesions per cell. (Azqueta et al. 2015, Keohavong & Grant 2005, Walker 2013)

Lesions such as single- and double-stranded DNA breaks, as well as alkali-labile sites (ALS) can be detected with this method. The alkaline comet assay detects mainly SSBs and alkali-labile sites, since there are normally relatively few DSBs. In addition to detecting strand breaks and AP sites, the assay may also detect specific DNA lesions by including DNA repair enzymes which recognize base oxidations. For example formamidopyrimidine DNA glycosylase (FPG) or 8-oxoguanine DNA glycosylase (OGG1) can be used to measure 8-oxoguanine. (Azqueta et al. 2015, Collins et al. 2008*b*, Walker 2013)

The procedure of the comet assay begins with mixing a number of sample cells with a volume of agarose, and then embedding a gel on a glass or polyester film. The glass/film with gel samples are then immersed in a lysis solution to disrupt the cell's membrane and remove most of their lipids and proteins, leaving supercoiled nuclear DNA (nucleoids) in the gel. This is followed by an alkaline treatment, during which the samples are immersed in an electrophoresis solution with high pH to break the hydrogen bond between the opposite DNA bases, resulting in single-stranded DNA. Electrophoresis of the samples is then carried out, so that the neg-

atively charged DNA of the cell moves inside the gel matrix towards the positive anode. The rate of movement and the total movement during a defined time period depend on their three-dimensional packaging and their size. (Dahl et al. 2016)

If the cell contains DNA damage the structures resembles comets during electrophoresis, and thus the name the comet assay. Photomicrographs of undamaged (unirradiated) and damaged (irradiated, 8 Gy) cells detected by the comet assay are shown in Figure 2.7a and Figure 2.7b, respectively. Comets are formed as a result of SSBs which cause relaxation of supercoils and thus extension of DNA loops toward the anode forming a tail of the comet. After alkaline electrophoresis the linear DNA forms a granular form. The unbroken DNA remains supercoiled and thus represent the head of the comet. The percentage of DNA in the tail is increased with increasing frequency of breaks. The tail length is little affected by the frequency of breaks, indicating that the comet tail consists of DNA loops and not fragments. (Collins et al. 2008*b*, Shaposhnikov et al. 2008)

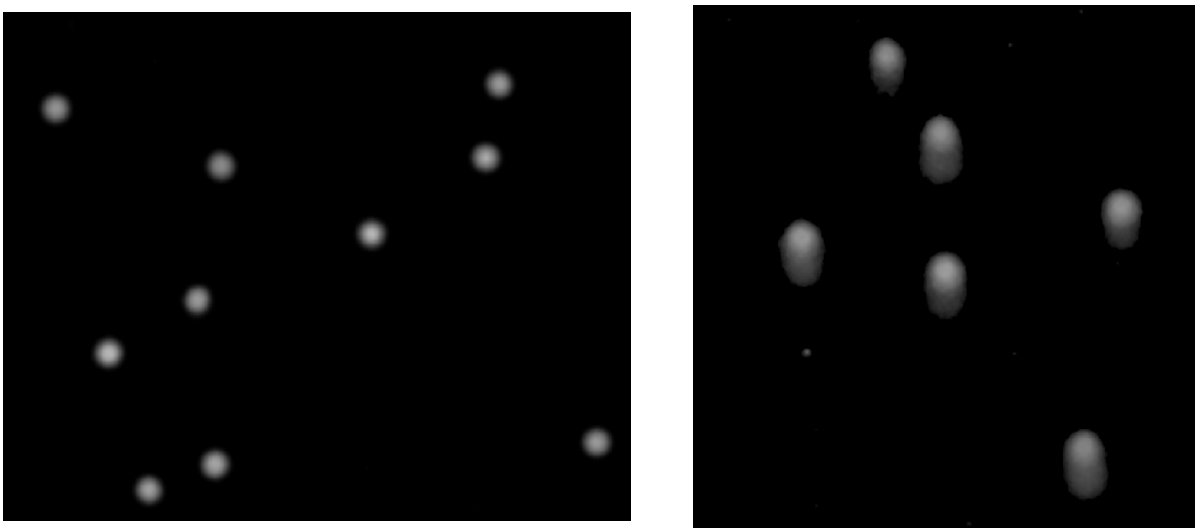

(a) (b)

Figure 2.7: Photomicrographs of unirradiated (2.7a) and irradiated (8 Gy) (2.7b) cells detected by the comet assay using the automated scoring system, IMSTAR Pathfinder^{TM} Auto Comet software. Irradiated cells contain damaged DNA and thus give the appearance of a comet while unirradiated cells without any DNA damage possess a spherical appearance. The photomicrographs were obtained in this study from the comet assay on human peripheral blood lymphocytes.

After electrophoresis, the cells are immersed in a neutralization buffer followed by fixation and staining with a fluorescent dye. An epifluorescence microscope can be used for visualization of the comets, and the relative intensity of DNA in the tail reflects the level of DNA damage since it is linear related to frequency of DNA breaks. The resulting image combined with a calibration where the treatment is done with an agent known to induce a certain number of lesions per cell, can be used to quantify the number of DNA lesions per cell. Calibration by ionizing radiation can be used since X-rays and other low LET radiation produce a known number of lesions per cell per dose of radiation in DNA of a particular genome size. 1 Gy of X-rays will induce approximately 1000 SSBs in a human cell. (Dahl et al. 2016)

Common measures of DNA migration used are the tail length, per cent DNA in tail and tail moment. The tail moment is the product of the tail length and the per cent tail DNA. At very low level of damage, tail length may be most informative. However, the tail length only increases at relatively low levels of damage, and thus at higher levels of damage, tail length is considered unsatisfactory as a measure. A disadvantage of tail moment is that it does not have any standard units and thus the values of the tail moment would be difficult to interpret and to provide an indication of the degree of damage. The relative intensity of DNA in the tail reflects a wide range of DNA damage and it is linear related to the frequency of DNA breaks. Per cent tail DNA is thus recommended to illustrate the level of DNA damage. (Azqueta et al. 2015, Collins et al. 2008*b*, Lovell & Omori 2008)

The magnitude of the comet tail can be estimated using various methods including visual inspection, semi-automated and automated scoring. The tail length can be directly estimated in the microscope, but gives limited information. Visual inspection involves classifying the comets into five categories from 0 to 4. The first category (0) represents undamaged cells, while category 1-4 represent comets with increasing tail intensities. For both semi-automated and automated scoring, the comets are identified and focused using software combined with an epi-fluoresecence microscope and the comet tail parameters are determined. However, semi-automated scoring is highly more time-consuming and requires much more operator interaction than automated scoring. (Azqueta et al. 2015, Collins et al. 2008*b*)

The traditional comet assay format was a glass slide with one or two agarose cell samples, spread out to a certain thickness by putting a glass coverslip on the agarose sample before solidification. More recently, other versions have been developed implying that higher numbers of samples can be processed per experiment. One such refinement uses small droplets of cell/agarose which are applied to a polyester film. An example of such a polyester film used for the comet assay is the GelBond® film. The film has one hydrophobic side and one hydrophilic side where the cell/agarose mixture remains attached through the electrophoresis and all subsequent fixing, staining, and drying procedures. A previous study (Gutzkow et al. 2013) has verified that the gel format accommodating up to 96 cell samples has the same sensitivity and dynamic range for detecting DNA damage as the standard assay based on glass slides. (Azqueta et al. 2015, Collins et al. 2008*b*, Dahl et al. 2016, Keohavong & Grant 2005)

2.6.1 Automated comet scoring using IMSTAR Pathfinder^{TM} Auto Comet software

An automated scoring system is much more efficient compared to visual inspection and semi-automated scoring. IMSTAR Pathfinder^{TM} Auto Comet software can accurately detect and analyze the 96 minigel format used in this thesis. The automated system first identifies and focuses the comets, followed by performing image analysis to determine the comet tail parameters of one image. The following description gives an indication on how the procedure, including identification and the analysis of comets, is performed in IMSTAR Pathfinder^{TM} Auto Comet software. The description is based on a document provided by the producer (IMSTAR SA, Paris, France) to the Norwegian Institute of Public Health from IMSTAR.

The comet detection involves a procedure which determines contours of whole comets and heads. The algorithm used to detect comets includes a high pass filter, threshold detection, the watershed method, sharpening filter, head filtering and comet filtering. The high-pass filter is

used to remove the low-frequency background variations in the image. To detect the comets, an absolute threshold detection of the filtered image is performed, where the threshold value is set according to the fluorescence intensity distribution. The watershed method separates the comets resolved as one object. Head filtering is performed based on the size, shape and symmetry of the comet's head. Comet filtering is performed based on the shape and symmetry of the comet, the angle of the principal axis fluorescence intensity of the head relative to that of the body and the number of heads. Objects without head or with more than one head are rejected.

Parameters to be evaluated are the area of the whole comet and the head (CA and HA), the length of the comet and the head (CL and HL), the coordinate of the gravity center of the comet and the head (CG and HG), the mean fluorescence intensity inside the comet and the head (CI and HI), the area and mean fluorescence in the comet and in the head above the origin (UCA, UHA, UCI and UHI), the 1st order fluorescence intensity and binary moments for the comet (MG and MB) and the background intensity (FB).

The parameters are used to calculate the following quantities:

1. Migration distance: $MD = CL - HL$
2. Total fluorescence in the comet: $CT = (CI - FB) \cdot CA$
3. Total fluorescence in the head: $HT = (HI - FB) \cdot HA$
4. Comet moment: $CM = (MG - FB \cdot MB)/CT$
5. Fraction of the DNA in the tail: $FT = 1 - HT/CT$
6. Corrected DNA % in the comet tail: $FC = 1 - (HT - 2 \cdot ((UCI - FB) \cdot UCA - (UHI - FB) \cdot UHA)/CT)$
7. Tail moment: $TM = ((CA \cdot CG - HA \cdot HG)/(CA - HA) - HG) \cdot FT$

A fluorescence halo around an intact cell nucleoid is observed in the comet assay analysis. This halo should be attributed to the comet's head, so that for an intact cell nucleus the tail intensity should be approximately 0%. A correction of the comet tail is thus performed in order to determine the tail intensity without including this fluorescence halo. An illustration of the an intact and a damaged cell nucleus with their respective fluorescence halos surrounding the nucleoids is shown in Figure 2.8.

2.6.2 Epi-fluorescence microscopy

Fluorescence is the phenomenon in which a substance emits light after absorbing light or electromagnetic radiation. The emitted light has usually longer wavelength and thus lower energy than the absorbed light or radiation. The absorbed photon energy must be of sufficient magnitude in order to excite the molecule, so that the electrons will be excited to a higher energy state. Excitation is followed by de-excitation, where the electrons return to their ground state and the excess energy can result in either fluorescence, phosphorescence or heat.

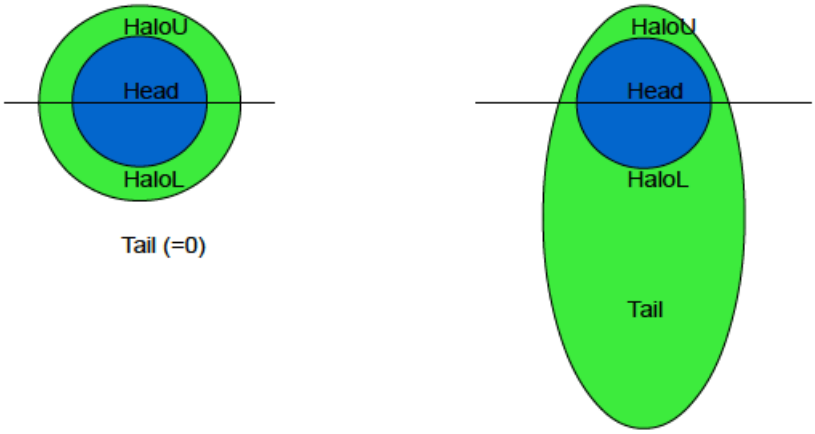

Figure 2.8: Illustration of an intact (left) and a damaged (right) cell nucleus. The fluorescence halo around the nucleus shown in green and the comet head is shown in blue. For the damaged cell nucleus the lower part of the halo (HaloL) is mixed with the tail and thus a correction must be performed in order to determine the tail intensity without including the halo. Figure from IMSTAR SA, Paris, France.

Fluorescent dyes which are used to stain biological material before inspection in a microscope are referred to as fluorochromes. The difference in wavelength or energy between the excitation and the emitted fluorescent photons is called the Stokes shift. A large Stokes shift makes it easier to separate the emitted light from the excited light and is thus of great advantage.

A fluorescence microscope is an essential tool in biology and in biomedical sciences. Epi-fluorescence microscopy is referred to as fluorescence microscopy where both the illuminated and the emitted light travel through the same objective lens. The basic principles of an epi-fluorescence microscope begin with emission of light from a light source, followed by reflection of the incoming light through the objective lens into the sample by a dichromatic mirror. The light is absorbed by the substance resulting in emission of fluorescence light which returns through the objective lens and the dichromatic mirror forming a final image on a detector. Filters for the incoming light as well as for the emitted light to transfer only the desired wavelengths are also among the essential components of an epi-fluorescence microscope. (Chiarini-Garcia & Melo 2011)

2.7 Statistics and statistical tests

Statistical hypothesis testing is commonly performed when comparing a set of data or comparing two or more populations of data against each other. These statistical tests are useful in order to determine if two or more sets of data are significantly different from each other, or if the mean or median of one population is significant larger or smaller than the mean or median of the other populations. (Walpole et al. 2011)

A two-tailed two-sample test is a statistical hypothesis where the alternative is two sided,

such as

$$\begin{aligned} H_0 &: \theta_1 = \theta_2 \\ H_1 &: \theta_1 \neq \theta_2 \end{aligned} \tag{2.62}$$

where θ_1 and θ_2 could be either the mean or the median of population 1 and 2, respectively, depending on the statistical test. The p-value of a statistical test is the probability of observing a test statistic equal or more extreme than the observed value under the null hypothesis. The significance level α is the probability of committing a type I error, which is rejecting the null hypothesis when it is true. (Walpole et al. 2011)

One-way analysis of variance (ANOVA) is a statistical test for differences among group means, which is appropriate when the groups are defined by just one exposure. A standard ANOVA table includes the sum of squares $SS = \sum(x - \bar{x})^2$ due to differences between both the group means and within each group, the total degrees of freedom df which is the total number of observations minus one, the mean squared error $MS = SS/df$, the F-statistic and the p-value. The F-statistic is obtained from the variance-ratio test:

$$F = \frac{MS_{bg}}{MS_{wg}}, \tag{2.63}$$

where MS_{bg} and MS_{wg} denote the mean squared error between groups and within groups, respectively. (Kirkwood & Sterne 2003)

The null hypothesis in a one-way ANOVA states that the means of several populations are equal, while the alternative hypothesis states that at least one mean differs from the others. The one-way ANOVA is thus a two-tailed test. Rejection of the null hypothesis does not provide further information on which group means are different. A multiple comparison test performs multiple pairwise comparison of the group means and can be used when the one-way ANOVA reject the null hypothesis. It can provide different procedures, where in Matlab R2014b (MathWorks, US) the multiple comparison test uses the Turkey's Honestly Significant Difference Procedure as a default setting. (*One-Way ANOVA* 2016, Walpole et al. 2011)

The Lilliefors test is used to test if a set of data is normally distributed. It is based on the Kolmogorov-Smirnov test, but does not require that the parameters of the distribution are known and specified (Lilliefors 1967).

A weighted arithmetic mean is a mean where some data points contribute more than others and can be given by

$$\bar{x} = \frac{\sum(w_i x_i}{\sum w_i}, \tag{2.64}$$

where w_i and x_i are the weighting factor and the data for element i, respectively. The larger the weight of a data point, the more it influences the weighted mean. The weights can be normalized such that $\sum w_i = 1$, giving $\bar{x} = \sum w_i x_i$. (Kirkwood & Sterne 2003)

3. Materials and methods

In this thesis, the experimental work was divided into two main parts:

1. Measurement of electric potentials during electrophoresis.

2. The alkaline comet assay using human peripheral blood lymphocytes.

Electric potentials were measured in agarose at defined positions across the platform as a function of electrophoresis time under different experimental conditions. This included circulation of the electrophoresis solution at different flow rates and with reversed circulation direction, as well as different volumes of the electrophoresis solution. A multi-electrode connected to a multiplexing digital voltmeter was used for the measurements of the electric potentials.

The comet assay was performed using human peripheral blood lymphocytes irradiated with X-rays, in order to detect any variation in percentage tail DNA due to differences in the circulation of the electrophoresis solution, as well as to obtain a dose-response curve. Results from the analysis of irradiated lymphocytes were compared with the measurement of electric potentials.

The products and the recipes for all the stock solutions/buffers used in this study are given in Appendix A and B, respectively.

3.1 Measurement of electric potentials

Materials

The materials used in order to calibrate the circulation pump, to perform measurement of electric potentials during electrophoresis and to perform conductivity measurements are listed in Table A.1 in Appendix A. A schematic diagram of the setup during electrophoresis is shown in Figure 3.1 and the physical dimensions of the electrophoresis tank and the electrode plate are given in Table 3.1. The electrode gauge used to measure the electric potentials during the electrophoreses is shown in Figure 3.2. The electrophoresis tank was placed in a refrigerator and the electrophoresis solution passed through heat exchanger in ice/water during the electrophoreses. The setup is shown in Figure 3.3.

3.1.1 Calibration of the circulation pump

Calibration of the circulation pump was performed in order to specify the flow rate of each nominal circulation speed of the circulation pump used to circulate the electrophoresis solution during electrophoresis. The tube to the entrance of the electrophoresis tank was removed

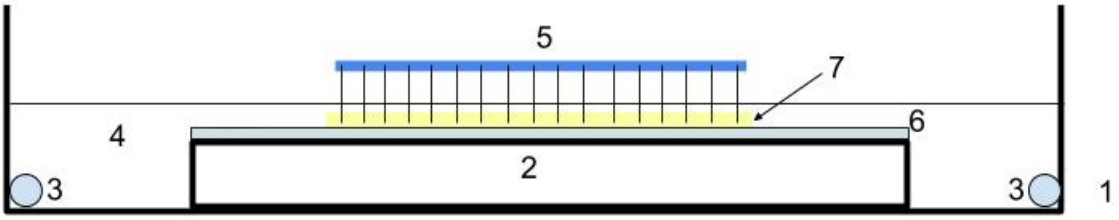

Figure 3.1: A schematic diagram illustrating the electrophoresis tank (1) with the platform (2) and the electrodes (3). During electrophoresis the tank was filled with electrophoresis solution (4) and an electrode gauge (5) was connected to an electrode plate (6) and placed across the centre of the platform with its electrodes covered in agarose (7) when performing the measurements of the electric potentials.

Table 3.1: Physical dimensions of the electrophoresis tank and the electrode plate.

Description	Length [cm]	Width [cm]	Height [cm]
Tank	29	26.2	7
Platform	18	26.2	2.6
Chambers x2	11	26.2	2.6
Electrode plate	18	26.2	0.9

and placed into a graduated cylinder in order to measure the flow rate. Electrophoresis solution (2 L, pH>13.2) was prepared with 200 ml electrophoresis stock solution (3 M NaOH, 0.01 M Na_2EDTA) and 1800 ml distilled water. The electrophoresis tank was filled with 1400 ml of the electrophoresis solution and the graduated cylinder was placed below (60 cm) the electrophoresis tank. The flow rate [ml/min] was measured at different circulation speeds using the external pump to circulate the electrophoresis solution.

The flow rate was measured twice at 19 different nominal speeds, varying the settings from 10 to 100 with steps of 5. The electrophoresis solution in the graduated cylinder was returned to the electrophoresis tank after each measurement. In addition, a graduated cylinder was placed closer to the electrophoresis tank (still 20 cm below the electrophoresis tank) in order to measure if the flow rate [ml/min] for the nominal speeds from 10 to 30, varied due to the position of the cylinder.

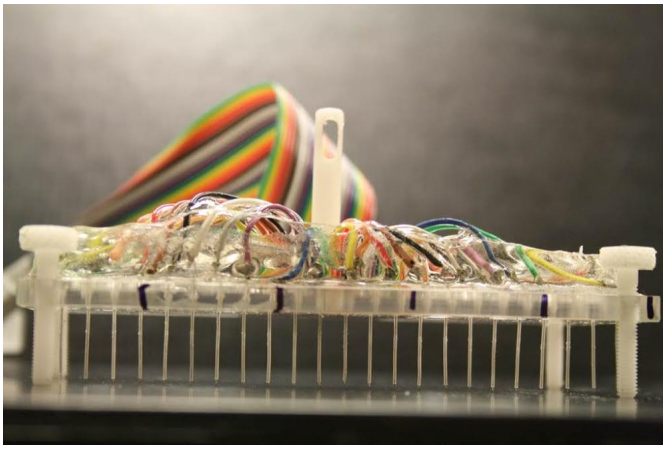

Figure 3.2: The electrode gauge produced at Norwegian Institute of Public Health in Oslo was used to perform measurement of electric potentials during electrophoresis. It contains 22 thin platinum electrodes covered in plastic. Only 1 mm of the lower part of the electrodes is exposed to the solution. The distance from the electrodes to the platform surface may be adjusted. Photo taken from the Department of Chemicals and Radiation at Norwegian Institute of Public Health, in Oslo, Norway.

Figure 3.3: The setup during electrophoresis. The electrophoresis tank (on the top) was placed in a refrigerator and the electrophoresis solution passed through heat exchanger (60 cm below the electrophoresis tank) in ice/water during electrophoresis. Photo taken from the Department of Chemicals and Radiation at Norwegian Institute of Public Health, in Oslo, Norway.

3.1.2 Electrophoresis

The measurements of electric potentials were performed under approximately equal electrophoresis conditions as used in a standard comet assay, in order to compare the results from the analysis of irradiated lymphocytes with the measurement of electric potentials. The electric potentials were thus chosen to be measured in a thin layer of agarose across the platform since this is where the DNA migration occur in the comet assay, with a final agarose concentration of 0.675%. This is the same concentration as achieved in the comet assay after mixing the agarose with the cell suspension.

Standard procedure

The LMP agarose was made by adding phosphate buffered saline (PBS) to pre-weighted LMP agarose. The final concentration of 0.675% was obtained by using the equation:

$$\frac{X[mg]}{C[\%] \cdot 10} = Y[ml], \tag{3.1}$$

where X is the weight in mg of the pre-weighted LMP agarose and Y is the volume in ml of PBS needed in order to obtain the final agarose concentration, C, in percentage. The agarose solution was dissolved in a closed glass by microwave heating, followed by cooling it to 37 °C in a heating block.

Electrophoresis solution (2 L, pH>13.2) was prepared with 200 ml electrophoresis stock solution (3 M NaOH, 0.01 M Na_2EDTA) and 1800 ml distilled water. The solution was stored in a cold room (4 °C) until 1640 ml of the electrophoresis solution was poured into the electrophoresis tank. Normally, a volume of 1400 ml is used during electrophoresis in the comet assay procedure, but due to the electrode plate placed on the platform, the volume was increased to 1640 ml in order to obtain approximately the same depth (8.5 mm) of liquid on the platform. A GelBond® film was cut to proper size (35 mm x 125 mm) by using a cutting device made from paper cutter. The film was glued to the electrode plate, followed by attaching the electrode gauge to the plate. By using a plastic pasteur pipette, 1.5 ml agarose was added to the film to form an even layer of approximately 1 mm thickness so that all the electrodes were covered in agarose.

To make the system less sensitive to varying depth of the solution on the platform, the electrophoresis tank was accurately levelled before performing the electrophoresis for all measurements. The plate with the electrode gauge was then immersed in the cold electrophoresis solution (9-10 °C) in the electrophoresis tank, and connected to a multiplexing digital voltmeter. The DC power supply was connected to the electrodes in the electrophoresis tank, and the voltage was set to 25 V. The depth of the liquid on the platform was approximately 8.5 mm and the current around 700-800 mA. The voltage potential was 0.8-0.9 V/cm on the platform where the electrode gauge was placed. The electrophoresis time was 25 minutes for each measurement. An external pump was used to circulate the electrophoresis solution for the measurements with circulation.

Recordings of electric potentials at electrode positions as a function of time

Measurements were performed by recording the specific voltage at each electrode, i.e its potential relative to the first electrode set as the reference, with time. A multiplexing digital voltmeter

(Agilent 34972A with Multiplexer 34901A) was used to scan all electrodes during one second, every ten seconds, resulting in obtained time-dependent local voltages collected by the software Agilent BenchLink Data Logger 3. One of the channels was connected to a thermistor placed in the tank to record the time-dependent temperature in the electrophoresis solution. The multiplexing digital voltmeter was placed at a distance away from the power supply and an aluminum foil was used around the wire in order to reduce ripple in the voltage output.

Electric potentials at electrode positions as a function of circulation speed

Measurements without circulation and with nominal circulation speeds of 10 to 70 at steps of 20 were performed. First, the circulation speed was increased for each measurement, followed by measurements of decreasing circulation speed from 70 down to 0, and then measurements by increasing circulation speed again. Three measurements for each nominal circulation speed were thus completed. 14 additional measurements without circulation were performed, as well as four additional measurements with nominal circulation speed of 30 and three measurements with nominal circulation speed of 20.

Electric potentials at electrode positions as a function of circulation speed with reversed circulation

Measurements of the electric potentials during electrophoresis with reversed circulation direction were performed, by changing the direction of the electric field (reversing the power supply connector wiring). Three measurements for each nominal circulation speed of 10, 20, 30 and 50 were performed. The measurements were first performed by increasing the circulation speed, followed by decreasing the circulation speed and then with increased circulation speed.

Electric potentials at electrode positions as a function of electrophoresis solution volume

Measurements of the electric potentials during electrophoresis with reduced electrophoresis solution volume from 1640 to 1340 ml were performed. The depth of the liquid on the platform was thus reduced to approximately 4.5 mm. The first measurement was performed without any circulation, followed by measurements with nominal circulation speeds of 10 to 30 at steps of 10, and then down again from 30 to 0. Two measurements for each nominal circulation speed were performed.

3.1.3 Calculations of the measured electric potentials

The relative voltage at each electrode for each scan time was obtained from the electrophoresis measurements. The voltage gradient between each electrode for all the scans was calculated from the obtained data, followed by calculating the voltage gradient per cm. A correction factor was used in order to calculate more accurately the voltage gradients, due to uncertainties regarding accurate spacing between the electrodes. The relative correction factor was obtained by dividing the mean of the voltage gradients per cm in the readings between seven and fourteen minutes of the electrophoresis, with the mean voltage gradients per cm of all the electrodes.

3.1.4 Conductivity measurements

Conductivity measurements of the electrophoresis solution were performed both before and after electrophoresis without circulation and with nominal circulation speed of 30 in order to detect any changes in conductivity. The conductivity meter was calibrated by the following procedure:

The 4-pole conductivity cell was placed in distilled water for two hours before the cell was rinsed with a standard conductivity solution, followed by immersing the conductivity cell in a beaker with the standard conductivity solution. The immersion depth was four cm. The cell constant was then determined by adjusting the conductivity value until it matched the actual value of the standard conductivity solution.

After calibrating the conductivity meter, measurements of the electrophoresis solution were performed. The electrophoresis solution (50 ml) on the platform was collected into a beaker by using a pipette. The conductivity cell was first rinsed with distilled water before immersing the cell in the sample beaker. The conductivity of the electrophoresis solution was measured for a fresh solution, and after two hours with electrophoresis without circulation, as well as after two additional hours with a nominal circulation speed of 30. Three measurements were performed for each electrophoresis solution.

The conductivity meter was set for automatic temperature correction to 25 °C. Since the temperature of the electrophoresis solution differs between with and without circulation, the measured conductivities were re-corrected back to correspond to the original temperature. A linear increase of conductivity with temperature of 2.20% per degree was used for the automatic temperature correction. The actual conductivity at the given temperature of the electrophoresis solution was obtained by using the equation:

$$\sigma_T + \sigma_T \cdot (25 - T) \cdot \theta = \sigma_{25}, \tag{3.2}$$

where θ is the correction factor and σ_T and σ_{25} are the conducitivities at the measured temperature, T, and at 25 °C, respectively. (RadiometerAnalytical 2005)

3.1.5 Voltage drop across the electrodes in the electrophoresis tank

Calculation of the voltage drop across the electrodes in the electrophoresis tank was performed in order to evaluate the effect of the voltage gradient on the platform as a function of position. The expressions for voltage and resistance of a wire given in Equation 2.12 and Equation 2.14, respectively, in Section 2.3.3 in Chapter 2, with the parameters of the electrodes given in Table 3.2 were used for the calculations.

Table 3.2: Parameters of one platinum electrode in the electrophoresis tank.

Description	Value
Diameter	0.35 mm
Length	26.2 cm
Resistivity	$10.5 \cdot 10^{-8}\Omega$m

3.2 The comet assay

The procedure of performing the comet assay on the human peripheral blood lymphocytes, including isolation, exposure to ionizing radiation, making the high-throughput gel format, unwinding and electrophoresis and staining took about 3-4 days. Scoring analysis of the comets required 3-4 additional days. Four independent experiments were performed including the complete comet assay procedure. Each experiment including scoring analysis took approximately two weeks work.

The materials used to isolate HPBLs from fresh blood, to expose the cells to ionizing radiation, to make the high-throughput gel format, to perform unwinding, electrophoresis, staining and scoring of comets, are listed in Table A.1 in Appendix A.

3.2.1 Isolation of human peripheral blood lymphocytes

Human peripheral blood lymphocytes were isolated from fresh blood obtained from one healthy volunteer. The blood (40 ml) was drawn in EDTA-supplemented vacutainers to prevent blood from clotting/coagulation. The blood was mixed 1:1 with PBS divided in two 50 ml tubes stored on ice. Two additional 50 ml tubes were filled with 15 ml NycoPrep. 30 ml of the blood/PBS mixture was added carefully on top of the NycoPrep in each tube.

The tubes with blood/NycoPrep mixtures were centrifuged at 800 x g for 20 minutes without brake at 20 °C. To avoid disturbing the cell layers, the centrifugation was performed without brake, indicating that the centrifuge speed was gradually decreased before ending the centrifugation. Lymphocytes were collected from the interface between plasma and NycoPrep/red blood cells (RBC) as shown in Figure 3.4, with a plastic pasteur pipette and transferred to a new 50 ml tube stored on ice. The tube was filled with PBS up to 50 ml to rinse cells. The lymphocytes were handled carefully to avoid damaging the cells when working with them.

Cell samples were then pelleted by centrifugation at 350 x g for 10 minutes with brake at 4 °C. The supernatant was discarded and the pellet was gently suspended in PBS, before finally being resuspended at a concentration of 1 million cells per ml. The cells were counted in a haemocytometer with 10 μl cell suspension per chamber using a compound light microscope.

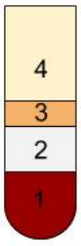

Figure 3.4: Illustration showing the resulting separation between the different blood cells in the sucrose gradient after centrifugation, where the lymphocytes (3) forms a cloudy band in the interface between the plasma (4) and the NycoPrep (2) and red blood cells (1). The lymphocytes can be collected from this band using a plastic pasteur pipette.

Cell samples were further pelleted for 10 minutes at 400 x g at 4 °C, and resuspended in freezing medium (RPMI 1640 with 20% fetal calf serum and 10% DMSO) to a concentration of 2×10^6 cells/ml. The cell suspension (1ml) was distributed in eppendorf tubes. The samples were placed in a freezer at -80°C inside an isopropanol-filled insulated box (Mr. Frosty from Nalgene) to achieve slow freezing, in order to prevent physical damage to the DNA due to ice crystal formation.

3.2.2 Ionization radiation exposure

Frozen HPBLs from the large batch produced were thawed and exposed to ionizing radiation for each experiment. The HPBLs from the freezer were quickly thawed by adding cold PBS/EDTA. Cells were then pelleted by centrifugation at 350 x g for 6 minutes with brake at 4 °C, followed by discarding the supernatant and gently resuspending the pellet in PBS at an optimal concentration of approximately 1 million cells per ml for comet assay. The cells were counted in a haemocytometer with 10 μl cell suspension per chamber using a compound light microscope.

Experiment 1

Eppendorf tubes on ice were filled with the HPBL/PBS mixture, and the tubes were marked according to which dose of radiation (1-15 Gy) the cells would be exposed to. The tubes planned for unirradiated cells and cells irradiated with 8 Gy were filled with 400 μl HPBL/PBS mixture, while the rest of the tubes were filled up to 100 μl for the X-ray dose-response curve. To induce DNA strand breaks, HPBLs were irradiated with X-rays (1-15Gy) in the eppendorf tubes placed in a Petri dish filled with ice/water. The X-rays were delivered by a PXI XRAD 225 X-ray Unit operated at 225 kV and 13 mA, with a dose rate of 3.47 Gy/min, and filtered through 0.5 mm copper. Both controls and irradiated HPBLs were kept on ice during the whole procedure.

Experiment 2, 3 and 4

The eppendorf tubes planned for control cells (0 Gy) and irradiated cells (8 Gy) were filled with 500 μl and 1.5 ml HPBL/PBS mixture, respectively. To induce DNA strand breaks, HPBLs were irradiated with X-rays (8 Gy) in the eppendorf tube placed in a Petri dish filled with ice/water. The X-rays were delivered as above, but with a dose rate of 3.82 Gy/min calibrated by the Norwegian Radiation Protection Authority in 2014 (Hansen 2014).

3.2.3 Protocols for analysis of cellular DNA damage using the comet assay high-throughput gel format (96 minigels)

Experiment 1, 2 and 3

The lysis solution was prepared with 300 ml lysis stock solution (2.5 M NaCL, 100 mM Na_2EDTA x $2H_2O$, 10 mM Tris-base, 10 mM NaOH, 34mM N-Laurosylsarcosine), 33.3 ml DMSO and 3.3 ml TritonX. The lysis solution was stirred with a magnet and stored at 4 °C until used. The LMP agarose was made by adding PBS/EDTA to weighted LMP agarose. A concentration of 0.75% was obtained by using the equation:

$$\frac{X[mg]}{7.5} = Y[ml], \tag{3.3}$$

where X is the weight in mg of the weighted LMP agarose and Y is the volume in ml of PBS/EDTA. The agarose solution was dissolved by heating in the microwave, followed by cooling it to 37 °C in the heating block. After mixing the agarose with the cell suspension, a final concentration of 0.675% was obtained.

Six GelBond® films were produced with proper size (85 x 125 mm) using a cutting device made from paper cutter with guides attached. Two modified office paper punches were used to make holes in each corner. Films were then hooked onto plastic frames with stainless-steel metal feet in order to stretch the films flat as well as to protect the gels from mechanical damage.

Immediately after irradiation, the HPBL cell suspension was mixed carefully 1:10 with LMP agarose (37 °C) using a 8-channel pipette. The polyester films with the plastic frames were placed on a cold plate and 96 samples (12 x 8) of 5 μl cell/agarose mixture each were then added to each of the six films using an 8-channel pipette. A master plastic plate with conical holes for the pipette tips was used to ensure exact positioning and even spacing. Figure 3.5 and Figure 3.6 show the 96 minigel format used for the comet assay and the GelBond® film with 96 minigels applied, respectively. The films were immersed in cold lysis solution (50 ml lysis solution per film) overnight at 4°C.

Figure 3.5: The 96 minigel format used for the comet assay. The GelBond® film was attached to the plastic frame with a master plastic plate with 96 conical holes and placed on a cold plate. 96 samples of 5 μl cell/agarose mixture was added to the film using an 8-channel pipette. Photo taken from the Department of Chemicals and Radiation at Norwegian Institute of Public Health, in Oslo, Norway.

In the first experiment, one of the films contained both unirradiated HPBLs and irradiated HPBLs in the range from 1 to 15 Gy, whereas the other five films contained only HPBLs irradiated with 8 Gy in addition to unirradiated HPBLs. For the second and the third experiment, all six films contained only HPBLs irradiated with 8 Gy in addition to unirradiated HPBLs. Figure 3.4 illustrates the distribution of non-irradiated and irradiated lymphocytes on the 96-gel format for the first three experiments. Each film consist of 96 samples corresponding to positions along

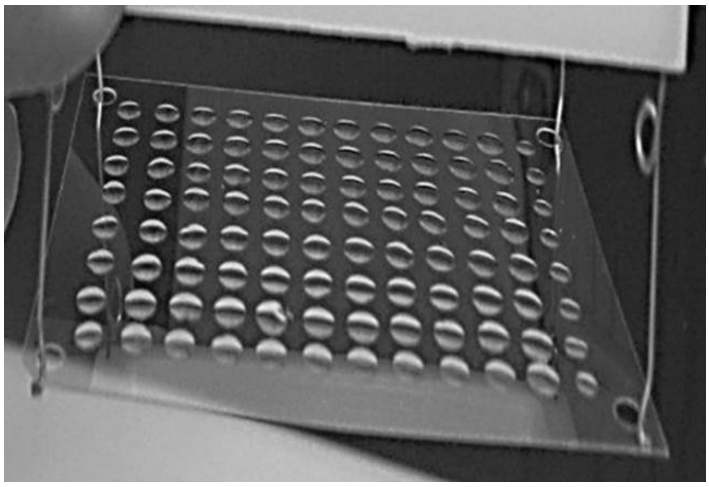

Figure 3.6: GelBond® film with 96 minigels applied. The film was hooked onto a plastic frame with stainless-steel metal feet in order to stretch the film flat and to protect the gels from mechanical damage. Photo taken from the Department of Chemicals and Radiation at Norwegian Institute of Public Health, in Oslo, Norway (Gutzkow et al. 2013).

12 rows and 8 columns.

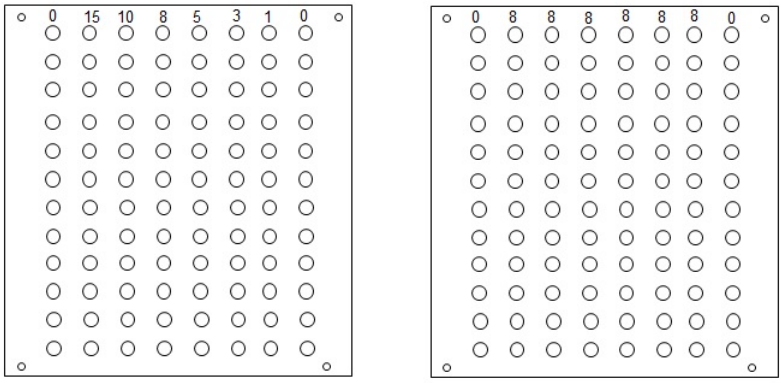

Figure 3.7: Schematic figure illustrating the distribution of non-irradiated and irradiated (1-15 Gy) lymphocytes on the 96 minigel format, where the numbers on the top of the film indicate the doses in Gy. The film format to the left was used to obtain dose-response curve, while the format to the right was used for the other films in Experiment 1, 2 and 3 of the comet assay.

Experiment 4

Almost identical procedure of making the high-throughput gel format was applied in the fourth experiment. The only difference was that eight GelBond® films were produced, where six of the films contained only HPBLs irradiated with 8 Gy, while the two other films contained controls in the first row and irradiated HPBLs (8 Gy) in the remaining rows.

3.2.4 Unwinding and electrophoresis

Electrophoresis solution (4 L, pH>13.2) was prepared with 400 ml electrophoresis stock solution (3 M NaOH, 0.01 M Na_2EDTA) and 3600 ml distilled water. The solution was stored in a cold room (4 °C). The electrophoresis tank was accurately levelled before performing the electrophoresis. The films with the cell samples were immersed in cold electrophoresis solution for 5 minutes and then for another 35 minutes for the unwinding process. The electrophoresis tank was then filled with 1400 ml of the electrophoresis solution, giving a depth of approximately 8.5 mm of liquid on the platform.

The electrophoreses of films were carried out for 25 minutes, with a nominal electrophoresis voltage of 25 V. The voltage potential was approximately 0.8-0.9 V/cm on the platform, on which films were placed. In Experiment 1, 2 and 3, the film was placed in the centre of the platform, while in Experiment 4, four films were placed covering the whole platform as shown in Figure 3.8. Position 1 and Position 2 corresponded to the two films in the top of the platform to the left and right, respectively, while Position 3 and Position 4 corresponded to the two films in the bottom of the platform to the left and right, respectively. Immediately after electrophoresis, each film was rinsed in distilled water, immersed in PBS for 2x5 minutes for neutralization, rinsed again in distilled water, followed by fixation in 96% ethanol for 5 + 105 minutes. Films were then dried overnight.

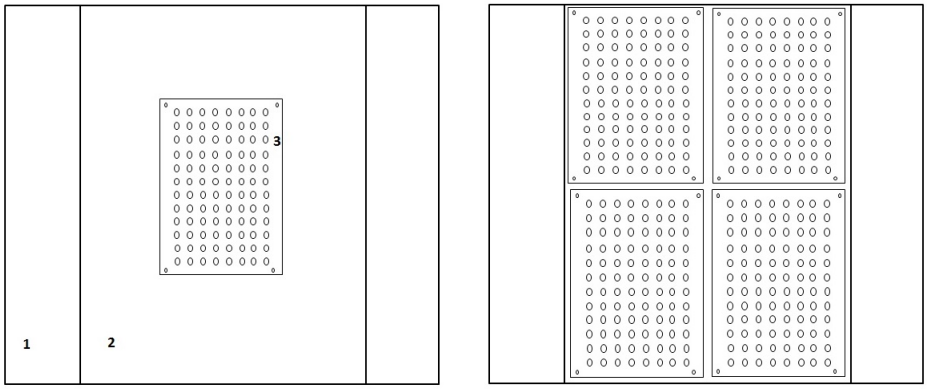

Figure 3.8: Schematic figure illustrating the position of the film (3) on the platform (2) in the electrophoresis tank (1). For experiment 1, 2 and 3, one film was placed in the centre of the platform for each electrophoresis (left figure). For experiment 4, four films were placed on the platform for each electrophoresis (right figure). Position 1 and Position 2 correspond to the two films in the top of the platform to the left and right, respectively, while Position 3 and Position 4 correspond to the two films in the bottom of the platform to the left and right, respectively.

In the first experiment (Experiment 1), the electrophoresis was carried out without any circulation of the electrophoresis solution for one of the films, while for the other four films, the electrophoresis was carried out with nominal circulation speed of 10, 20, 30 and 40, respectively. For the film providing the dose-response curve, the electrophoresis was carried out with a nominal circulation speed of 30. For the second and third experiment (Experiment 2 and 3), the electrophoresis was carried out without any circulation for two of the films, while for the four other films, the electrophoresis was carried out with nominal circulation speed of 10, 20, 30 and

40, respectively. For the last experiment (Experiment 4), the electrophoresis was carried out first without circulation and then with a nominal circulation speed of 30.

3.2.5 Staining and scoring of comets

For staining, the SYBR® Gold was diluted 1:1000 in TE-buffer (1mM Na_2EDTA, 10 mM Tris-HCL). Films were immersed in this solution for rehydration and staining for 20 minutes at room temperature with mild shaking. The films were then rinsed in distilled water for one minute and stored on wet paper in a closed box at 4 °C in a humidified atmosphere until scoring the next day. For one of the films, both semi-automated and automated scoring were performed. For the other films, only automated scoring was performed due to limited time. Three films were re-stained and re-scored due to insufficient staining and background noise in the acquired image resulting in incorrectly determined per cent tail DNA intensity.

Semi-automated scoring

The software Comet assay IV by Perceptive Instruments was used for semi-automated scoring with an epifluorescence microscope using the lens giving 20 x magnification. The comets were identified manually, followed by measurement analysis performed by the software including background correction, determination of head and tail regions and computation of all parameters. Field of view within a gel was chosen by manually controlling the microscope stage. Thirty comets were scored per gel, where overlapping comets were excluded.

Automated scoring

For the automated scoring, IMSTAR Pathfinder^{TM} Auto Comet software was used with an epifluorescence microscope. The automated system identified and focused the comets followed by manually refocusing if needed. The image was then stored and the automated system performed image analysis to determine comet tail parameters. A detailed description of the IMSTAR Pathfinder^{TM} Auto Comet software was given in Section 2.6.1 in Chapter 2.

3.2.6 Processing the raw data of tail DNA intensities

Comet assay IV, Perceptives Instruments

The Comet Assay Spreadsheet Generator Version 1.4.1 by Perceptives Instruments, was used to generate tables in Excel from the raw data produced by the software Comet Assay IV. The different data files for the same radiation dose were first merged into one common data file, before tables of both mean and median tail DNA intensities were generated. The provided data in the Excel files was further imported into MATLAB R2014b to generate dose-response curves together with the data scored with IMSTAR.

IMSTAR Pathfinder^{TM} Auto Comet

Raw data of the corrected median tail DNA intensities for each gel produced by the software IMSTAR Pathfinder Auto Comet was processed in MATLAB R2014b. By using loop control state-

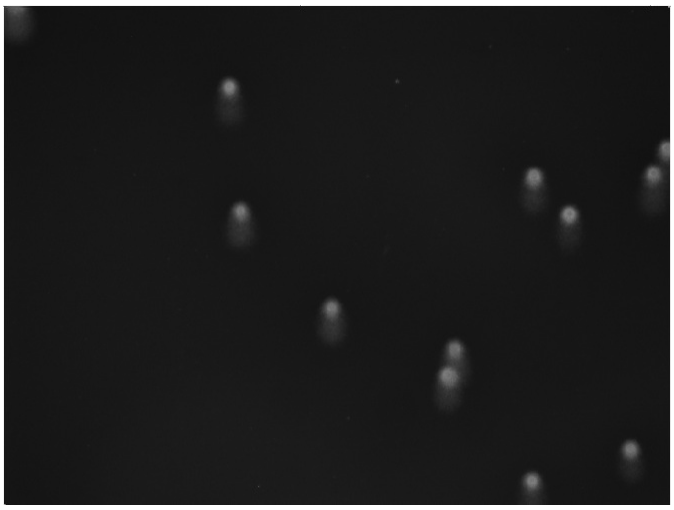

Figure 3.9: Stored image of the comets after being identified and focused in the automated scoring system IMSTAR Pathfinder^{TM}. Lymphocytes were irradiated with X-rays (8 Gy).

ments and execute statements, the median tail DNA intensities and the number of comets scored for each gel were placed in the row and column of a matrix corresponding to its position on the film. Gels containing less than 20 scored comets were not included in the study.

In addition, a weighted mean per cent tail DNA intensity was calculated based on the number of comets scored. Gels containing a high number of comets had larger contribution to the calculated mean than the gels containing few comets. The weight w_i for each gel i was obtained by dividing the number of comets scored in that particular gel with the sum of all comets scored in the 96 minigel format film. The weights were thus normalized such that $\sum_{i=1}^{n} w_i = 1$, where n was the total number of gels. The mean $\bar{x}$ was calculated by using the equation: $\bar{x} = \sum_{i=1}^{n} w_i x_i$, where x_i was the per cent tail DNA intensity of gel i.

In Experiment 4, four 96 minigel films were positioned over the whole platform. In order to analyze the time-dependent variations in the tail DNA intensities across the platform, systematic variations due to the positions of the films were corrected for. A relative correction factor was obtained both for the rows and the columns along the film by dividing the mean tail DNA for each row and column with the mean tail DNA for all the rows and columns in one film, respectively. The obtained per cent tail DNA intensity for each gel along a given row and column was multiplied with the corresponding correction factor, resulting in a corrected per cent tail DNA intensity.

Statistical tests

In order to indicate if the per cent tail DNA intensities (scoring by Perceptives) for each radiation dose were normally distributed, a Lilliefors test was performed in MATLAB R2014b. The significance level was set to 5%. The mean per cent tail DNA intensity and coefficient of variation (CV) were calculated for each film as well as for each row and each column in each film for all the four experiments.

In order to analyze the differences in tail DNA intensities and CVs among the different groups (circulation speeds, rows and columns) an one-way ANOVA test combined with a multiple com-

parison test were performed in Matlab R2014b. A structure of statistics obtained from the one-way ANOVA test was used to perform the multiple comparison test, which determined if any group means were significant different. Two group means were significant different if their intervals were disjoint. A Wilcoxon rank sum test does not require the population to be normally distributed and can thus be used if the per cent tail DNA intensities were shown to not be normally distributed by the Lilliefors test. In order to visualize outliers in addition to the degree of variation in per cent tail DNA intensity, boxplots were mainly used to illustrate the results of relative tail DNA intensity obtained in this study.

4. Results

The presented results are divided into two main parts in accordance with the experimental work performed:

1. Measurement of electric potentials during electrophoresis with and without circulation.

2. The implication of electrophoresis solution circulation in the alkaline comet assay on human peripheral blood lymphocytes.

4.1 Measurement of electric potentials

The purpose of the electric potential measurements was to examine the variations due to different experimental conditions during electrophoresis, in order to establish the most optimal condition. Electric potentials were measured in a thin layer of agarose at defined positions across the platform as a function of electrophoresis time. The focus was to study more systematically the implication of different circulation speeds compared to without circulation of the electrophoresis solution. In addition, the impact of reversed circulation and reduced electrophoresis solution volume were also examined. The circulation pump was first calibrated before performing the electric potential measurements. Conductivity measurements of the electrophoresis solution were also performed.

4.1.1 Calibration of the circulation pump

The circulation pump was calibrated in order to specify the flow rate of each nominal circulation speed of the circulation pump used during electrophoresis. The mean flow rates from two measurements for nominal circulation speeds from 0 to 100 are shown in Figure 4.1, with a fitted linear regression performed in MATLAB R2014b. The linear relation obtained was y=4.03x and the coefficient of determination was determined to be R^2=0.99, which indicated that the data fitted the linear regression line well. Slightly lower flow rates compared to the linear regression line were observed for the nominal circulation speeds of 10 to 30.

The mean flow rates for the nominal circulation speeds used in this study are listed in Table 4.1. For these measurements, the graduated cylinder was placed 60 cm below the electrophoresis tank, referred to as the original position. Additional measurements where the graduated cylinder was placed 20 cm below the electrophoresis tank, referred to as Position 2, were also performed. Figure D.1 in Appendix D shows the mean values of the flow rates for nominal circulation speeds from 0 to 30 for the two different positions of the graduated cylinder.

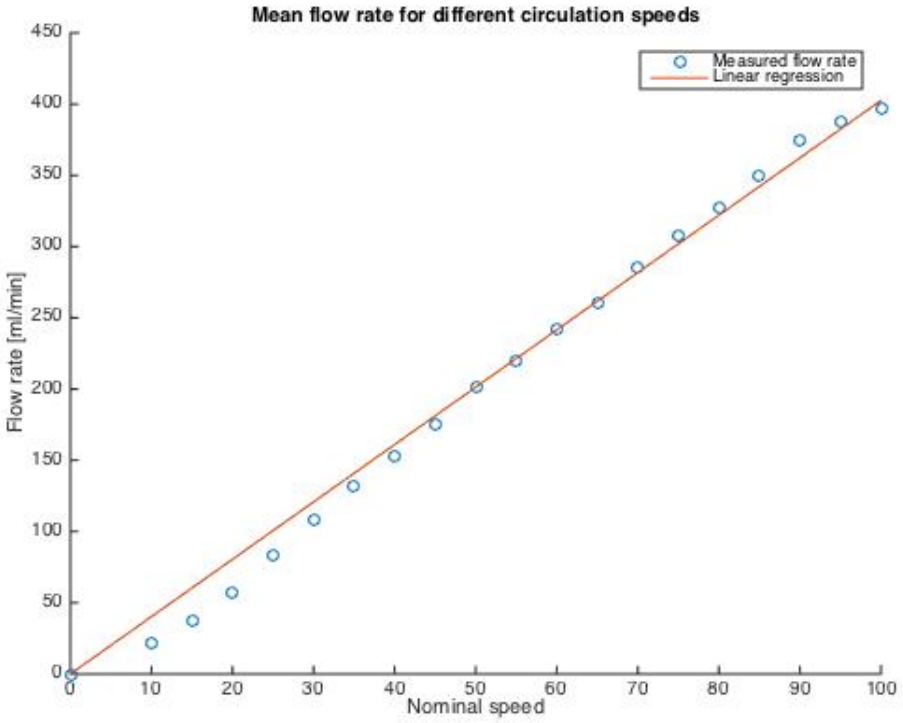

Figure 4.1: Flow rate of electrophoresis solution with different nominal circulation speeds of the circulation pump. Mean flow rate [ml/min] from two measurements for each nominal speed are shown as blue circles. A fitted linear regression line with the linear relation of y=4.03x is shown in red. The coefficient of determination was determined to be R^2=0.99.

Table 4.1: Flow rate of the circulation pump. Mean flow rates from two measurements for the nominal circulation speeds used in this study. The per cent of volume across the platform (404 ml) is also given.

Nominal circulation speed	Flow rate [ml/min]	Per cent of volume over platform [%]
0	0	0
10	21	5
20	58	14
30	109	27
40	153	38
50	201	50
70	285	71

4.1.2 Electric potentials at electrode positions as a function of circulation speed

Electric potentials at the different electrode positions were measured as a function of circulation speed. In total, 36 measurements were conducted which corresponded to three measurements

for each flow rate (0-285 ml/min), 14 additional measurements without circulation and four additional measurements with circulation (109 ml/min). Relative voltage at each electrode and the temperature for each scan time were obtained from measurements during electrophoresis for 25 minutes.

Time-dependent local voltages and temperature from one representative experiment with (109 ml/min) and without circulation of the electrophoresis solution are shown in Figure 4.2. The local voltages at each electrode position across the platform showed a substantial instability during the electrophoresis without any circulation compared to electrophoresis performed with circulation at flow rates above 58 ml/min. Ripple in the voltage output was observed for all electric potential measurements. The temperature was increased with approximately 2-3 °C during the electrophoreses without circulation for 25 minutes. A better temperature stability was achieved by circulating the electrophoresis solution.

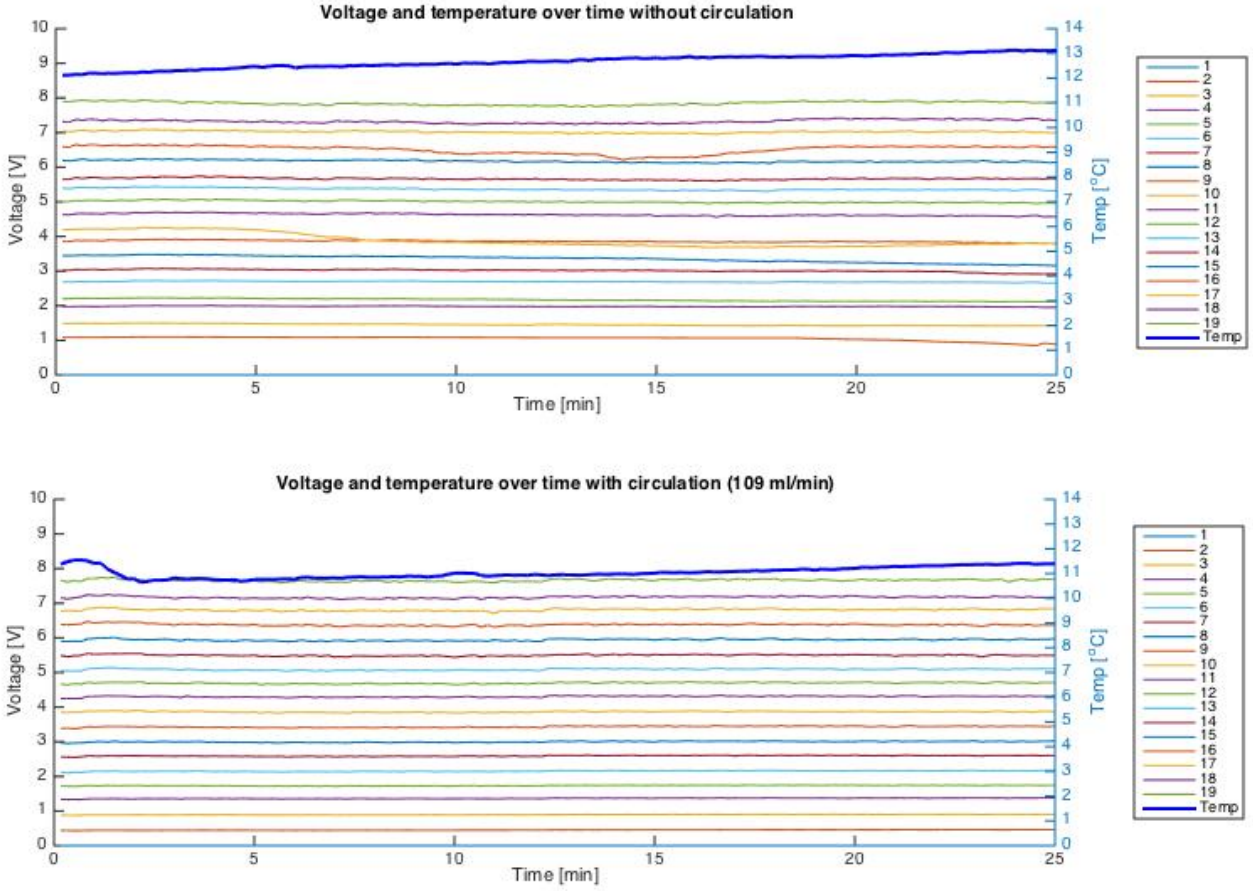

Figure 4.2: Measured voltage across the platform during electrophoresis. Relative voltage at each electrode and temperature over time during an electrophoresis time of 25 minutes from one representative experiment with (109 m/min) and without circulation. The number of each electrode and the temperature are indicated to the right of the plot. The blue thick lines in both plots represent the temperature.

Since the voltage gradient is one of the main contributors to the degree of DNA migration, time-integrated corrected electrode voltage per cm was calculated from the obtained relative voltage at each electrode for each scan time. Corrections due to uncertainties regarding the accurate spacing between the electrodes were included in the calculations. The five first scans of the voltages were excluded in the results, with the purpose of measuring the voltage variations over time after the electrophoresis system was stabilized.

In order to illustrate variations in voltage per cm during the electrophoresis, the obtained corrected voltage per scan per cm was subtracted from the mean corrected voltage per cm for all the scans for each electrode. The result of the voltage variations from the same representative experiment as above is shown in Figure 4.3. The variation in voltage per cm was considerably lower when the electrophoresis solution was circulated (109 ml/min). The voltage variation per cm seemed to occur independently of the time, i.e. variations were not observed to increase with time during the electrophoresis, but seemed to occur randomly throughout the electrophoresis time.

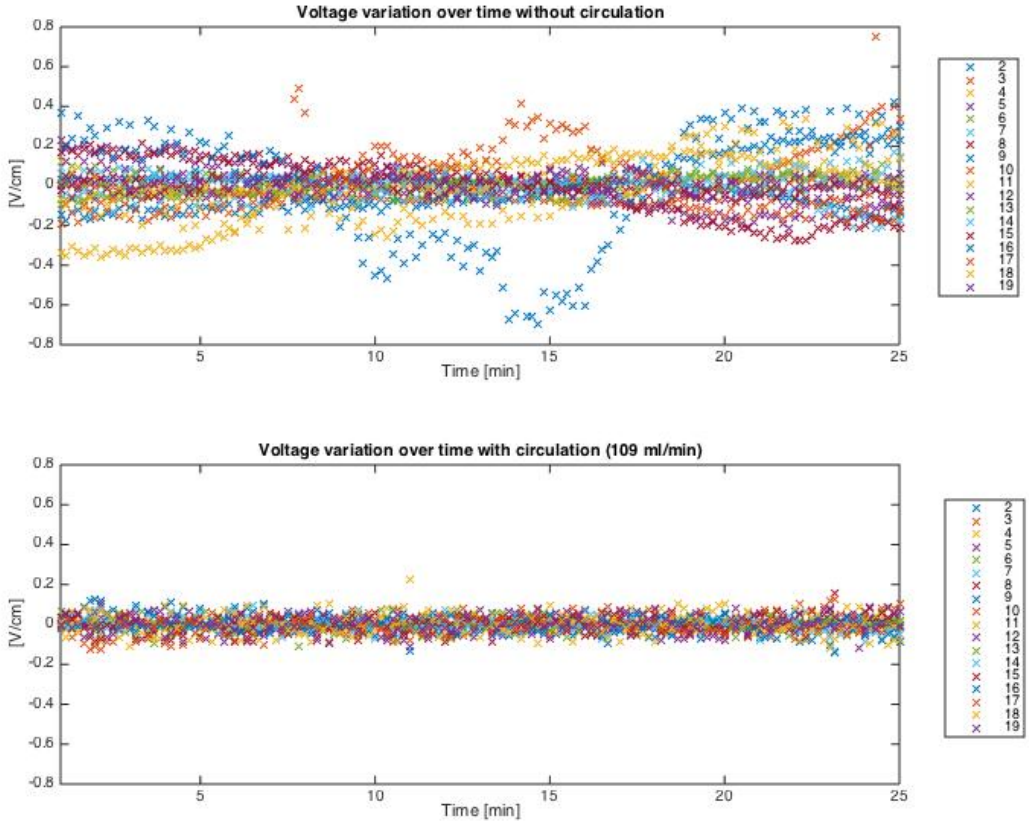

Figure 4.3: Stabilization of the voltage at each electrode with circulation. Corrected voltage variations per cm during the electrophoresis time of 25 minutes for each of the electrodes from one representative experiment with (109 m/min) and without circulation. The number of each electrode is indicated to the right of the plot. In this specific experiment, electrode #16 showed particularly large variations, whereas other electrodes were affected in other experiments.

Figure 4.4 shows the time-integrated corrected electrode voltage per cm as averaged for all electrodes during electrophoreses for 25 minutes. Data are based on three experiments without circulation and with circulation at 21 ml/min, and one representative experiment for each of the four other flow rates. Substantial variations in voltage between each electrode within an experiment and between each experiment were observed during electrophoresis without circulation. These variations were considerable reduced by circulating the electrophoresis solution at flow rates above 58 ml/min.

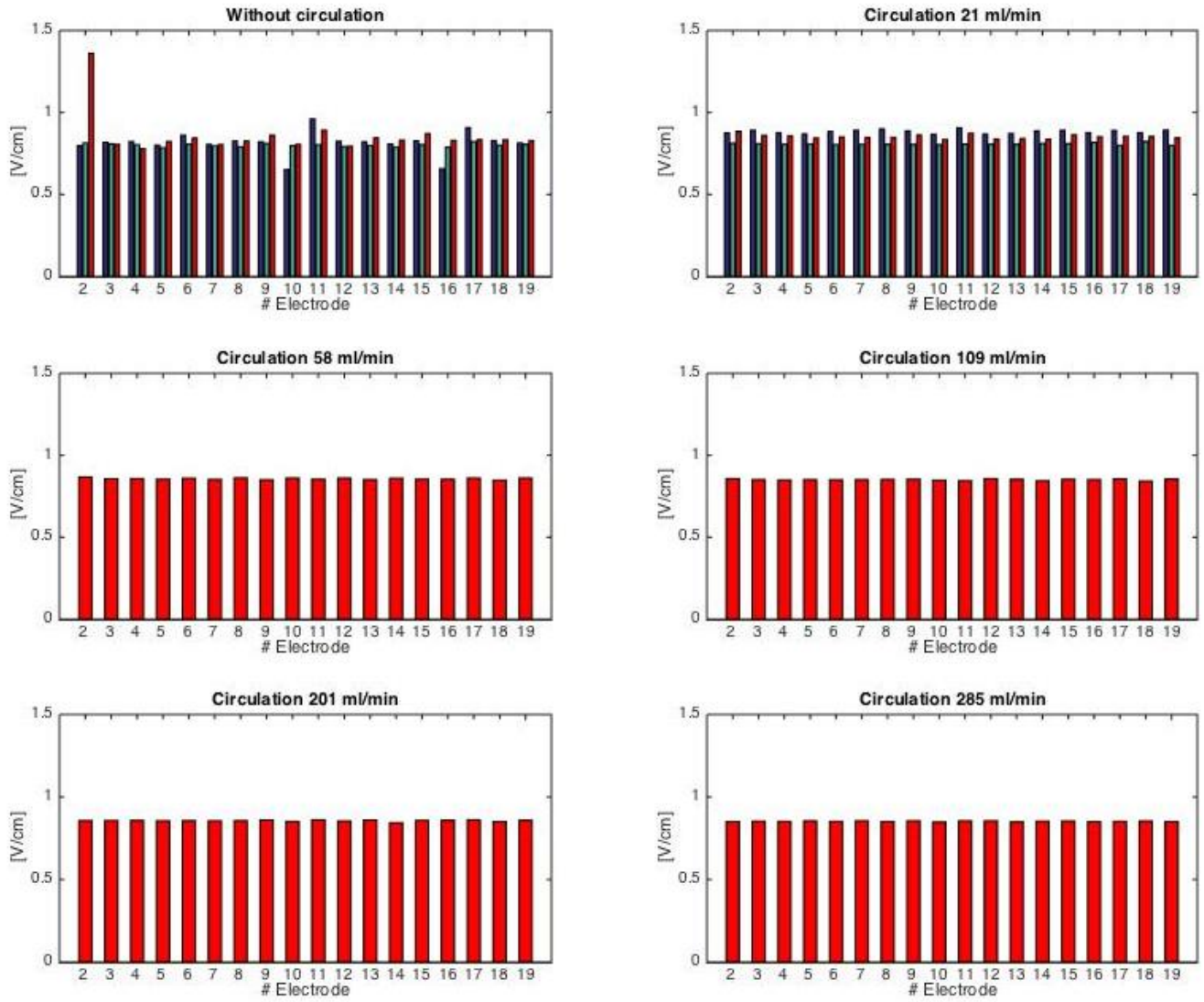

Figure 4.4: Voltage gradient at each electrode during electrophoresis with different circulation speeds. Time-integrated corrected electrode voltage per cm as averaged for all electrodes during an electrophoresis time of 25 minutes. Data are based on three experiments without circulation and with circulation at 21 ml/min, where the blue, green and red bars correspond to each of the three experiments. Data are based on one representative experiment for each of the four other flow rates (58, 109, 201 and 285 ml/min). The time-integrated corrected electrode voltage per cm for all three experiments are given in Table C.1 in Appendix C.

Time-integrated corrected electrode voltage per cm and coefficient of variation averaged for all electrodes during an electrophoresis time of 25 minutes were calculated for each of the 18 measurements. The results are given in Table C.1 in Appendix C. The 18 measurements corresponded to three experiments for each flow rate. Mean corrected electrode voltage and CV for each flow rate from these three experiments were calculated and the results are given in Table 4.2.

The absolute voltage gradient seemed to be approximately equal for different circulations speeds during electrophoresis. However, the mean CV was considerably lower when the electrophoresis solution was circulated at flow rates above 58 ml/min. A reduction from 8.28% to 0.65% in the mean CV was obtained by circulating the electrophoresis solution at a flow rate of 109 ml/min compared to without circulation. In addition, the variation in CVs between the measurements without circulation was considerable larger than with circulation. Voltage variations across the platform during electrophoresis were thus reduced by circulating the electrophoresis solution.

Table 4.2: Electric potentials at electrode positions as a function of circulation speed. The time-integrated corrected electrode voltage per cm and CV averaged for all electrodes during an electrophoresis time of 25 minutes. Data from three experiments with and without circulation at different flow rates. The corresponding standard deviations and ranges in the CVs are also given.

Flow rate $[\frac{ml}{min}]$	Mean corrected electrode voltage $[\frac{V}{cm}]$	Mean CV [%]	Standard deviation CV [%]	Range CV [min,max] [%]
0	0.82	8.28	6.82	[1.27, 14.9]
21	0.85	1.17	0.42	[0.71, 1.53]
58	0.86	0.53	0.23	[0.27, 0.73]
109	0.83	0.65	0.13	[0.52, 0.78]
201	0.84	0.70	0.28	[0.52, 1.02]
285	0.83	0.50	0.32	[0.28, 0.87]

In order to further validate the large voltage variations for electrophoresis without circulation, a total of 17 measurements were performed without circulating the electrophoresis solution. These were compared with seven measurements for electrophoresis with circulation (109 ml/min). Time-integrated corrected voltage per cm averaged for all electrodes during an electrophoresis time of 25 minutes with their corresponding standard deviations were calculated for all the 17 measurements without circulation and for the seven measurements with circulation (109 ml/min). Results are given in Table C.2 in Appendix C and shown in Figure 4.5.

The calculated standard deviations were significantly higher during electrophoresis without circulating the electrophoresis solution compared to with circulation. In addition, larger variations in the average corrected electrode voltage per cm between the measurements were observed without circulation. The mean CVs from the seven (with circulation 109 ml/min) and 17 (without circulation) measurements were calculated to be 0.79% and 16.74%, respectively. The CVs in 7 of the 17 measurements without circulation were relatively low (below 3%).

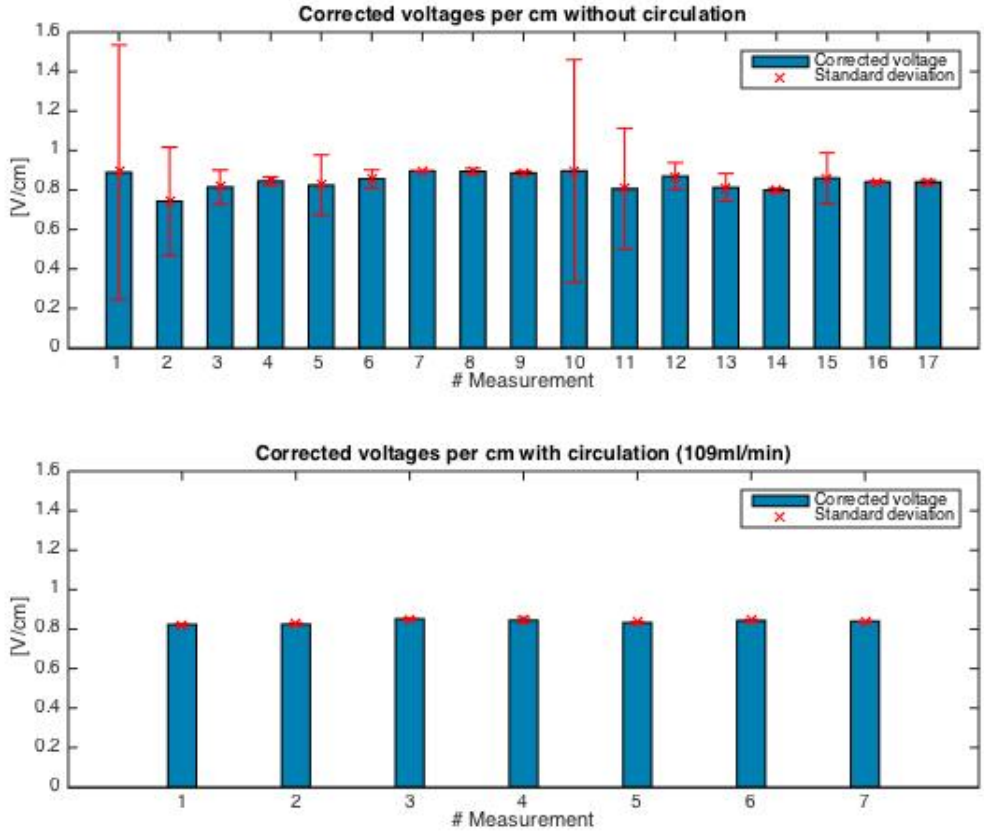

Figure 4.5: Stabilization of the voltage gradient by circulating the electrophoresis solution. Time-integrated corrected voltage per cm averaged for all electrodes during an electrophoresis time of 25 minutes for each measurement with (109 m/min) and without circulation. The standard deviations plotted as red error bars illustrate the degree of variation in voltage per cm for each measurement.

4.1.3 Electric potentials at electrode positions as a function of circulation speed with reversed circulation

The impact of reversed circulation during electrophoresis was analyzed since variations in the obtained electric potentials at electrode positions was considerably reduced by circulating the electrophoresis solution. A total of 12 measurements of the electric potentials with reversed circulation were conducted. Time-integrated corrected electrode voltage per cm and coefficient of variation averaged for all electrodes during an electrophoresis time of 25 minutes were calculated for each of the 12 measurements corresponding to three experiments for each flow rate. The results are given in Table 4.3, including the mean corrected electrode voltage and CV for each flow rate.

The averaged CV of the electric potentials from three measurements for each flow rate with reversed circulation was decreased with increased flow rate, as also observed with the original direction of circulation, i.e., flow rate of liquid positive from the positive to the negative elec-

trode. However, the CV was substantially higher compared to the CV for the corresponding flow rate from the measurements with original direction of circulation.

Table 4.3: Electric potentials at electrode positions as a function of reversed circulation. The table gives the time-integrated corrected electrode voltage per cm and CV averaged for all electrodes during an electrophoresis time of 25 minutes. Data from three experiments with reversed circulation at different flow rates. The mean corrected electrode voltage and CV are also given for each flow rate.

Flow rate $[\frac{ml}{min}]$	Experiment number	Mean corrected electrode voltage $[\frac{V}{cm}]$	CV [%]
21	1	0.92	5.16
	2	3.45	309.57
	3	0.93	23.75
	Mean	**1.76**	**112.83**
58	1	0.93	23.46
	2	0.84	25.89
	3	0.87	5.48
	Mean	**0.88**	**18.28**
109	1	0.88	1.42
	2	0.88	1.51
	3	0.85	13.54
	Mean	**0.87**	**5.49**
201	1	0.87	2.3
	2	0.87	5.32
	3	0.88	1.88
	Mean	**0.87**	**3.17**

4.1.4 Electric potentials at electrode positions as a function of electrophoresis solution volume

In order to evaluate the electric potentials at electrode positions as a function of electrophoresis solution volume, a total of eight measurements were conducted in which the volume was 1340 ml instead of 1640. Time-integrated corrected electrode voltage per cm and coefficient of variation averaged for all electrodes during an electrophoresis time of 25 minutes were calculated for each of the eight measurements corresponding to two experiments for each flow rate. The results are given in Table 4.4, including the mean corrected electrode voltage and CV for each flow rate.

By decreasing the volume, the resistance across the platform will increase and thus result in a larger voltage gradient across the platform, explaining the slightly increased mean corrected electrode voltages obtained from the measurements with reduced electrophoresis solution. The averaged CV of the electric potentials from two measurements for each flow rate with reduced volume was decreased with increased flow rate, as observed with original electrophoresis solution volume of 1640 ml.

Table 4.4: Electric potentials at electrode positions as a function of electrophoresis solution volume. The table gives the time-integrated corrected electrode voltage per cm and CV averaged for all electrodes during an electrophoresis time of 25 minutes. Data from two experiments with reduced electrophoresis volume (1340 ml). The mean corrected electrode voltage and CV are also given for each flow rate.

Flow rate $[\frac{ml}{min}]$	Experiment number	Mean corrected electrode voltage $[\frac{V}{cm}]$	CV [%]
0	1	0.86	3.29
	2	0.91	2.01
	Mean	**0.89**	**2.65**
21	1	0.95	1.42
	2	0.92	2.09
	Mean	**0.93**	**1.76**
58	1	0.92	0.77
	2	0.92	0.43
	Mean	**0.92**	**0.60**
109	1	0.92	0.54
	2	0.92	0.52
	Mean	**0.92**	**0.53**

4.1.5 Conductivity measurements

Conductivity measurements of the electrophoresis solution both before and after electrophoresis with (109 ml/min) and without circulation were performed. The mean conductivity of the electrophoresis solution, both fresh and after a given time of electrophoresis with the corresponding mean temperature of the solution from three measurements were calculated and the results are given in Table 4.5. A slight increase in the conductivity of the electrophoresis solution from fresh to two hours after electrophoresis without circulation was observed. Further, the conductivity of the electrophoresis solution was decreased after two additional hours of electrophoresis with circulation (109 ml/min).

Table 4.5: Mean conductivity of the electrophoresis solution with the corresponding mean temperature of the solution. Data from three measurements.

Electrophoresis solution	Mean conductivity [mS/cm]	Mean temperature [°C]
Fresh	50.3	12.6
After 2 hours electrophoresis without circulation	51.1	16.5
After 2 hours electrophoresis with circulation	45.9	11.2

4.1.6 Voltage drop across the electrodes in the electrophoresis tank

The resistance of each electrode in the electrophoresis tank was calculated to be $R = \rho \frac{l}{A} = 0.29\Omega$. With an applied current of 800 mA through both the two electrodes which was used during electrophoresis, the voltage drop along one electrode (26.2 cm) was calculated to be $V = IR = 0.23V$. The voltage drop along both electrodes was thus 0.46 V corresponding to a decrease of 1.84% of an applied voltage of 25 V.

4.2 The comet assay

The purpose of applying the alkaline comet assay to study DNA damage in irradiated human peripheral blood lymphocytes was to examine the variations in the tail DNA intensity as a function of electrophoresis solution circulation, and ultimately to compare the results with the electric potential measurements. Frozen HPBLs, from a large batch produced in the first phase of this study, were thawed and exposed to a defined dose of ionizing radiation for each comet assay experiment.

4.2.1 Dose-response curve

In order to select an optimal X-ray dose for further experiments a dose-response curve of HPBLs was constructed. Quantification of the number of DNA lesions per cell at the different X-ray doses could also be estimated, since low LET ionizing radiation induces a defined number of DNA SSBs plus alkali-labile sites per Gy, in a genome of known size. HPBLs were irradiated with X-rays (0-15 Gy). Dose-response curve is shown in Figure 4.6 with fitted linear regression lines. Circulation (109 ml/min) of the electrophoresis solution was used during the electrophoresis of the 96 minigel format. DNA damage for each radiation dose measured using both the semi-automated (Perceptives) and the automated (IMSTAR) scoring system are shown in the figure. The per cent tail DNA intensities are given as median values.

The linear relation and coefficient of determination obtained were $y = 3.99 + 4.37x$ and $R^2 = 0.72$ for IMSTAR and $y = 0.10 + 4.30x$ and $R^2 = 0.96$ for Perceptives. This indicated that scoring with Perceptives resulted in a better linear fit for the range of radiation exposures used. For both the semi-automated and the automated scoring system, the per cent tail DNA intensity was considerably lower at the highest dose (15 Gy). The experimental points at dose 15 Gy were omitted from the linear regression, since DNA detection with the comet assay has a limited dynamic range and saturates at high levels of damage (at approximately 8-12000 SSBs + ALS in a human cell). This level seemed to be lower for IMSTAR than for Perceptives.

The number of comets scored for both the semi-automated and the automated scoring system are listed in Table 4.6 with the corresponding median per cent tail DNA intensity for each dose of X-rays. The number of comets scored with Perceptives for each dose varied since gels containing fewer comets than 20 were not included. The per cent tail DNA intensities for each radiation dose (0, 1, 3, 5, 8, 10, 15 Gy) from the scoring in Perceptives were determined to be normally distributed at a significance level of 5% (p= 0.23, 0.5, 0.21, 0.06, 0.26 0.3, 0.08) by the Lilliefors test performed in MATLAB R2014b.

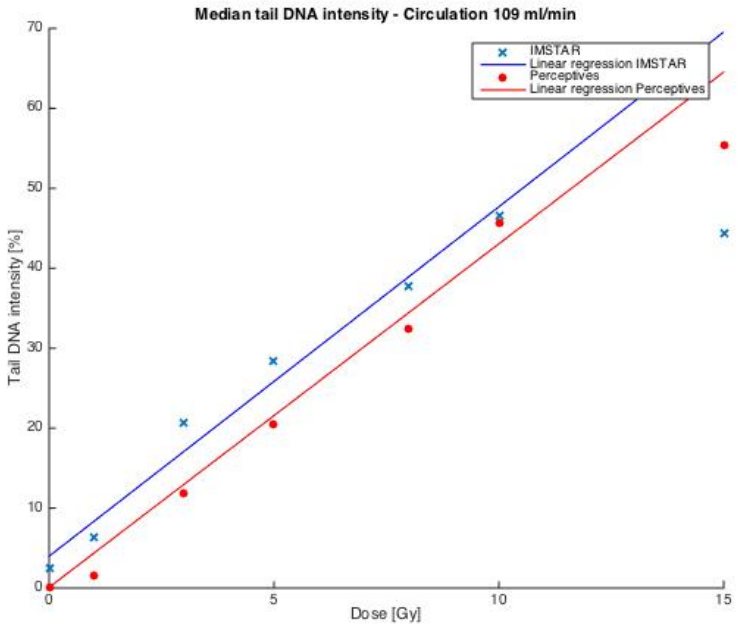

Figure 4.6: X-ray dose-response curve showing DNA damage vs radiation dose from one experiment. The semi-automated (Perceptives) and the automated scoring (IMSTAR) systems were compared. The lymphocytes were irradiated with X-rays (0-15 Gy) and circulation (109ml/min) was used during electrophoresis of 96 minigels. The % tail DNA relative to the head is given as a median value. Fitted linear regression lines are shown with the linear relations $y = 3.99 + 4.37x$ and $y = 0.1 + 4.30x$, and the coefficients of variation $R^2 = 0.72$ and $R^2 = 0.96$, for IMSTAR and Perceptives, respectively. The experimental points at dose 15 Gy were omitted from the linear regression.

Table 4.6: X-ray dose-response analyzed by Perceptives and IMSTAR. Median per cent tail DNA intensity for the dose-responses from one experiment for both the semi-automated (Perceptives) and the automated (IMSTAR) scoring system, with the corresponding number of comets scored. The 96 minigel format was used and the electrophoresis solution was circulated (109ml/min).

Dose [Gy]	Median tail DNA intensity [%]		# Comets scored	
	Perceptives	IMSTAR	Perceptives	IMSTAR
0	0.10	2.40	513	4644
1	1.53	6.74	342	2763
3	11.84	20.40	270	1842
5	20.45	29.41	360	2173
8	32.47	37.08	360	4272
10	45.58	47.26	360	3061
15	55.37	44.20	360	2190

4.2.2 Relative tail DNA intensity as a function of circulation speed

The comet assay was performed with and without circulation at different flow rates during the electrophoresis, in order to detect any variation in per cent tail DNA intensities as a function of circulation speed and to compare the results from the electric potential measurements. An X-ray dose of 8 Gy was selected as the most optimal dose for subsequent experiments. Lymphocytes were thus irradiated with 8 Gy and the 96 minigel format was used. The per cent tail DNA intensity of individual irradiated samples from three experiments (Experiment 1, 2 and 3) with (109 ml/min) and without circulation are shown in Figure 4.7. No differences in the variations of individual samples between electrophoresis performed with (109 ml/min) and without circulation were observed.

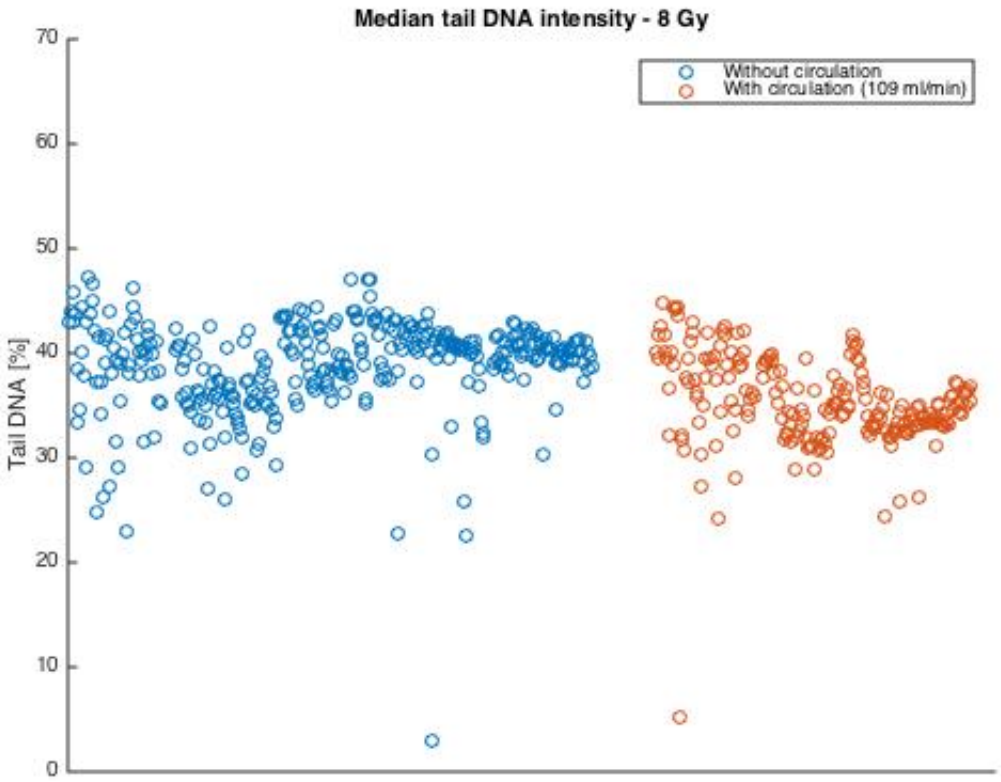

Figure 4.7: Variations in per cent tail DNA intensity of individual samples irradiated with X-rays (8 Gy) from three experiments (Experiment 1, 2 and 3) with (109 ml/min) and without circulation shown as red and blue circles, respectively. The data is distributed along the x-axis for visualization, the x-axis has thus no unit. In Experiment 2 and 3, two films were run without circulation during electrophoresis. The tail DNA intensity is given in percentage relative to the head intensity.

The variabilities of the per cent tail DNA intensities in samples exposed to 8 Gy X-rays were analyzed. The results of the per cent tail DNA intensities from three separate experiments (Experiment 1, 2 and 3) and the three experiments together as a function of circulation speed are

illustrated as box plots in Figure 4.8 and Figure 4.9, respectively. These boxplots also indicated that the variations in relative per cent tail DNA intensities were not larger without than with circulation.

In order to further investigate whether the sample positioning on the films could be significant, variations in the per cent tail DNA intensities along each row and each column were analyzed. Boxplots of the per cent tail DNA intensity along each column and each row of the films in Experiment 1, 2 and 3 with and without circulation at different flow rates during electrophoresis are shown in Figure D.2, D.3 and D.4 in Appendix D, respectively. There was a decrease in the median per cent tail DNA intensity along the rows of the film.

Statistical analyses using the one-way ANOVA test and the multiple comparison test showed that the CVs in per cent tail DNA intensities among the different circulation speeds were not significantly different from the CVs without circulation and also not different from each other (p=0.93). However, some of the data sets for median per cent tail DNA intensities were significantly different (p=0.002). The median per cent tail DNA intensity without circulation was significantly higher than with circulation of 58 ml/min (p=0.049) and the median per cent tail DNA intensity at flow rate of 21 ml/min was significantly higher than with circulation of 58 ml/min (p=0.0026), 109 ml/min (p=0.011) and 153 ml/min (p=0.0076).

The CVs in per cent tail DNA intensities for each row (1-12) among the different circulation speeds were not significantly different (p=0.62, 0.70, 0.50, 0.69, 0.34, 0.70, 0.56, 0.97, 0.62, 0.49, 0.96, 0.76). Neither were the CVs for each circulation speeds (0, 21, 58, 109 and 153 ml/min) among the different rows (p=0.062, 0.39, 0.84, 0.69 and 0.18). The CVs in per cent tail DNA intensities for each column (1-8) among the different circulation speeds were only significantly different for column 1 and 5. In column 1, the CV was significantly higher without circulation than with circulation of 109 ml/min (p=0.0076) and 153 ml/min (p=0.0097). In column 5, the CV was significantly higher without circulation than with circulation of 21 ml/min (p=0.022) and 153 ml/min (p=0.026). The CVs for each circulation speed (0, 21, 58, 109 and 153 ml/min) among the different columns were not significantly different (p=0.73, 0.13, 0.73, 0.073 and 0.54).

Weighted mean per cent tail DNA intensity based on the number of comets scored with its standard deviation and CV from three experiments (Experiment 1, 2 and 3) with and without circulation at different flow rates during electrophoresis are listed in Table 4.7 and shown in Figure 4.10. The weighted mean CV in the per cent tail DNA intensity was reduced from 10.5% to 8.14% when circulating (153 ml/min) the electrophoresis solution compared to without circulation. In addition, a less variable per cent tail DNA intensity was observed with circulation at flow rates between 58 ml/min and 153 ml/min, compared to without any circulation and circulation at flow rate of 21 ml/min.

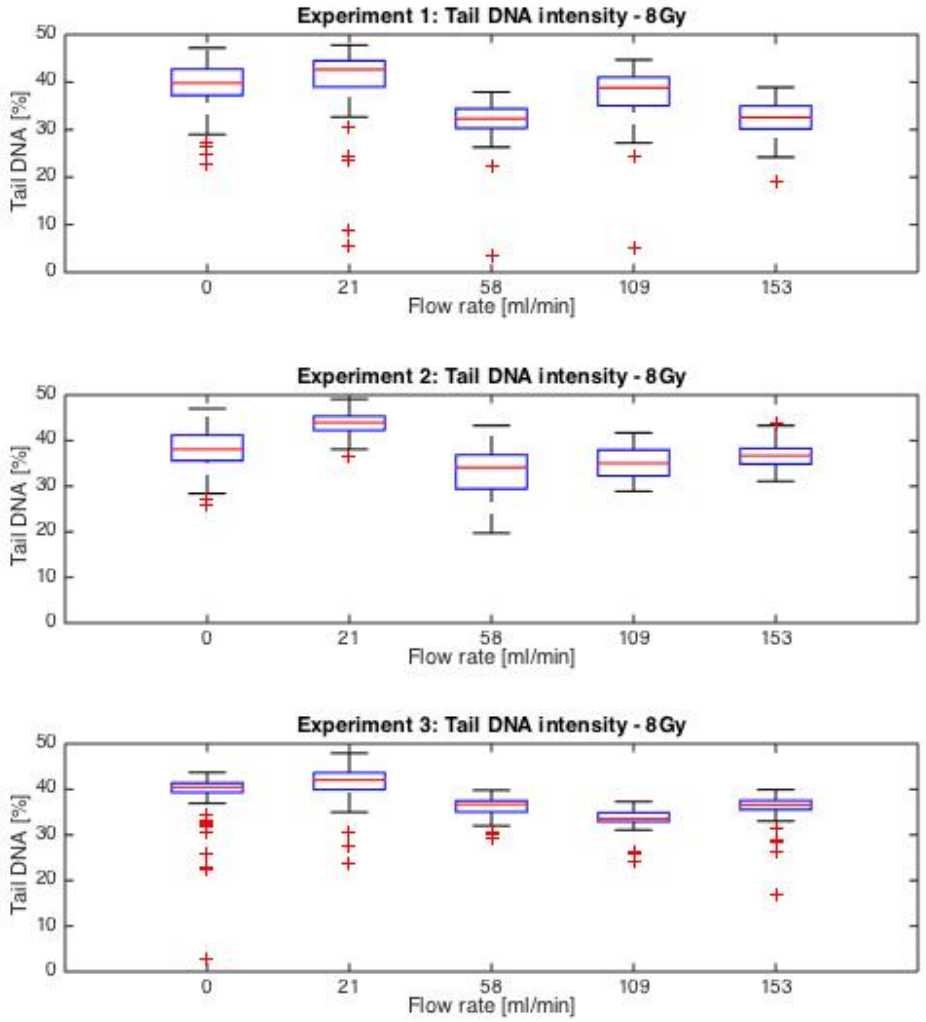

Figure 4.8: Relative tail DNA intensities as a function of circulation speed during electrophoresis. Lymphocytes were irradiated with X-rays (8 Gy) and the 96 minigel format was used for all analyses. Boxplots of the per cent tail DNA intensity relative to the head intensity for each of the three separate experiments (Experiment 1, 2 and 3) with and without circulation at different flow rates during electrophoresis are shown. In Experiment 2 and 3, electrophoresis without circulation was performed twice. For each box, the central mark is the median, the edges of the box correspond to the 25th and 75th percentiles and the whiskers extend to the most extreme data points not considering outliers. The outliers are plotted individually.

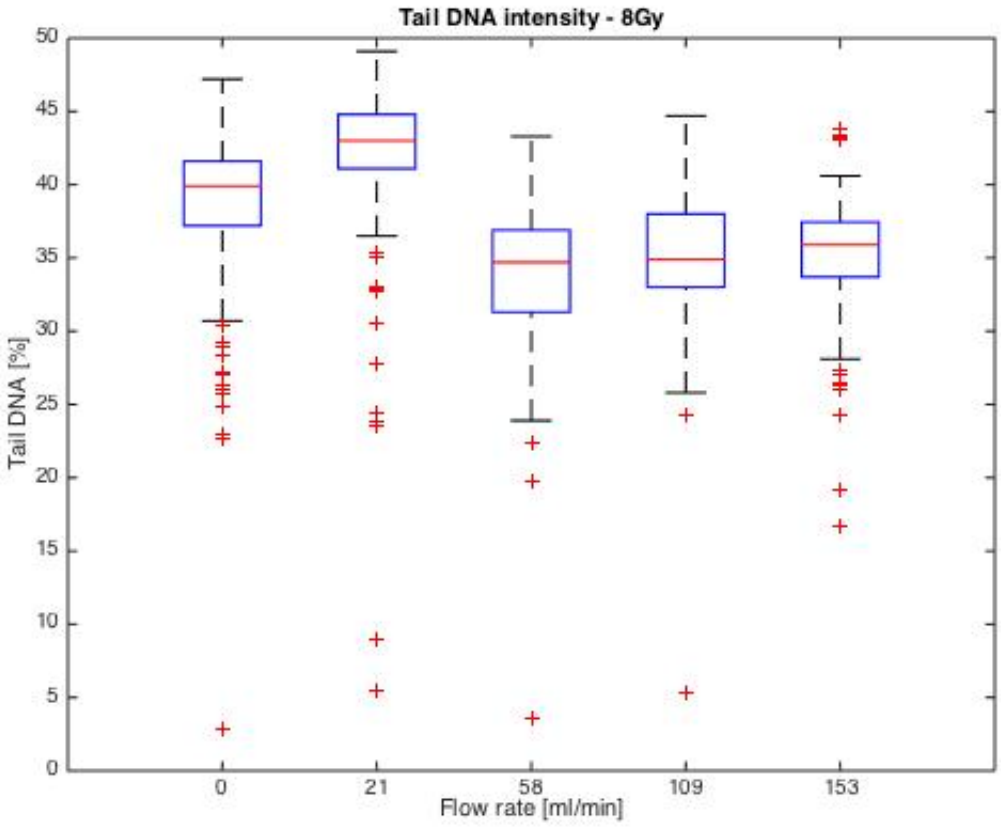

Figure 4.9: Relative tail DNA intensities as a function of circulation speed during electrophoresis. Lymphocytes were irradiated with X-rays (8 Gy) and the 96 minigel format was used for all analyses. Boxplot of the per cent tail DNA intensity relative to the head intensity from three experiments (Experiment 1, 2 and 3) with and without circulation at different flow rates during electrophoresis. For each box, the central mark is the median, the edges of the box correspond to the 25th and 75th percentiles and the whiskers extend to the most extreme data points not considering outliers. The outliers are plotted individually.

Table 4.7: Mean per cent tail DNA intensity weighted on the basis of the number of comets scored. Lymphocytes were irradiated with X-rays (8 Gy) and the 96 minigel format was used for all analyses. The tail DNA intensity is given in percentage relative to the head intensity. Standard deviations and coefficients of variation are also listed. Data from three experiments with and without circulation at different flow rates during electrophoresis.

Flow rate [ml/min]	Mean tail DNA intensity [%]	Mean STD[%]	Mean CV [%]
0	39.53	4.15	10.50
21	42.75	4.31	10.07
58	34.83	3.89	11.18
109	34.75	3.28	9.44
153	36.27	2.28	8.14

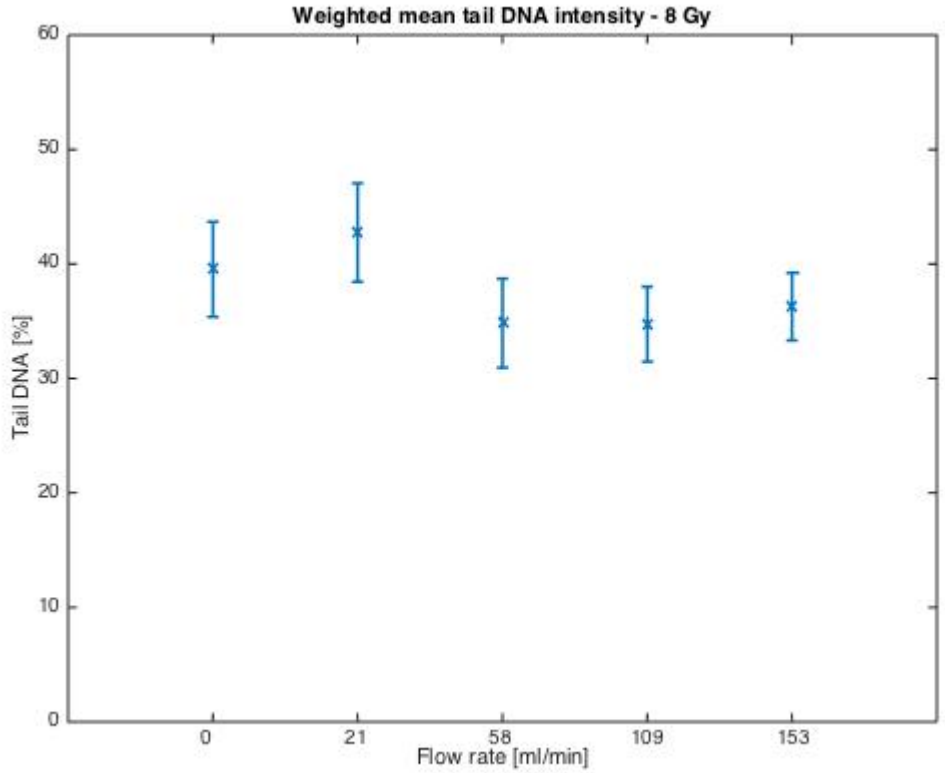

Figure 4.10: Mean per cent tail DNA intensity weighted on the basis of the number of comets scored. Lymphocytes were irradiated with X-rays (8 Gy) and the 96 minigel format was used for all analyses. The tail DNA intensity is given in percentage relative to the head intensity. Graph shows the mean per cent tail DNA intensity with its standard deviation (whiskers). Data from three experiments with and without circulation at different flow rates during electrophoresis.

4.2.3 Relative tail DNA intensity as a function of position on the whole platform and circulation speed

In order to evaluate the importance of the sample position during electrophoresis, four 96 minigel format films, covering the whole platform area of the electrophoresis tank, were filled with gel samples that had been exposed to 8 Gy X-rays. Comet assay electrophoreses were performed with (109 ml/min) and without circulation. The rows and columns corresponding to the four positions of films (Position 1, 2, 3 and 4) on the platform are given in Table 4.8.

Table 4.8: Sample positions across the platform. The number of rows and columns for each position (Position 1, 2, 3 and 4) on the platform in the electrophoresis tank.

	Position 1	Position 2	Position 3	Position 4
Row	1-12	1-12	13-24	13-24
Column	1-8	9-16	1-8	9-16

Median per cent tail DNA intensity for each point on the platform was obtained and is shown in Figure 4.11a for the comet assay performed without circulation during electrophoresis and in Figure 4.11b for the comet assay performed with circulation (109 ml/min) during electrophoresis. Due to technical problems when adding the cell/agarose mixture to the films, results for some of the gels (particularly in the last rows of the films) were excluded. For clarity, data are shown without any bars in the figures.

Boxplots of the per cent tail DNA intensity along each column and each row of the positions on the platform with (109 ml/min) and without circulation during electrophoresis are shown in Figure D.5 and D.6 in Appendix D, respectively. Variations in the per cent tail DNA intensity as a function of position across the film was observed in all experiments, particularly between rows. A decreasing per cent tail DNA intensity along the rows was detected.

Time-dependent variations in per cent tail DNA intensities across the platform were evaluated, disregarding systematic variations due to the positions of the films by using a correction factor. Both uncorrected and corrected per cent tail DNA intensities along each column and each row of the four films covering the platform with (109 ml/min) and without circulation during electrophoresis are shown in Figure 4.12 and in Figure 4.13, respectively. The coefficients of variation for each position and for the whole platform with (109 ml/min) and without circulation were calculated and the results are given in Table 4.9. Both uncorrected CVs and CVs corrected for the row positions are included in the table. The total uncorrected CVs on the whole platform were determined to be 14.32% and 15.47% for electrophoresis without circulation and with circulation, respectively. After corrections due to systematic variations in the rows, the corresponding CVs were decreased to 11.71% and 13.88%, respectively.

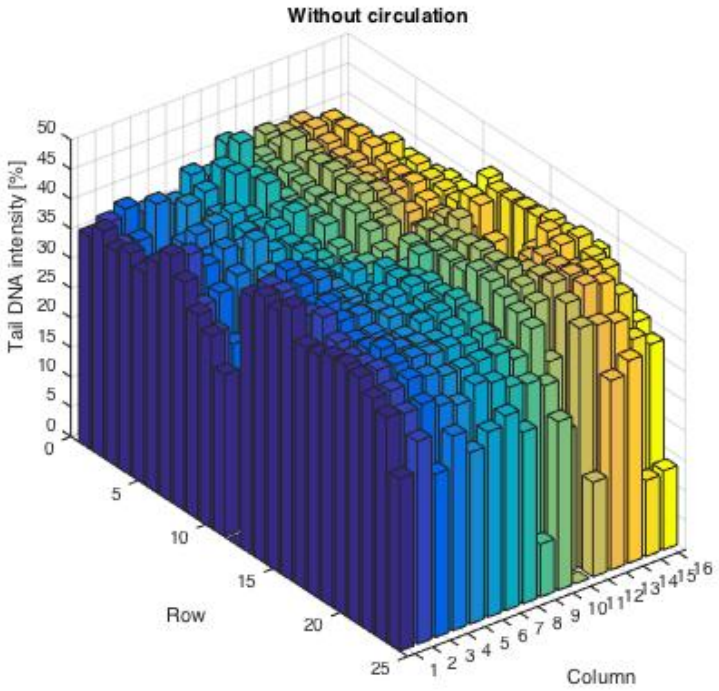

(a)

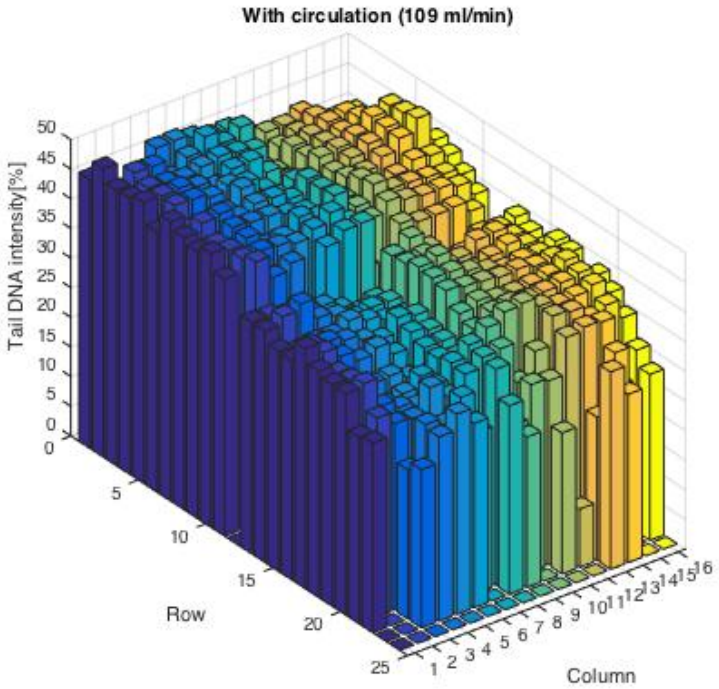

(b)

Figure 4.11: Relative tail DNA intensities as a function of position on the whole platform. The lymphocytes were irradiated with X-rays (8 Gy) and moulded onto four 96 minigel format films placed on the platform and electrophoresed simultaneously. A three-dimensional bar chart of the median per cent tail DNA intensities relative to the head intensities for the comet assay performed without circulation (4.11a) and with circulation of 109 ml/min (4.11b) during electrophoresis. Each bar corresponds to one individual sample on a film located on the platform.

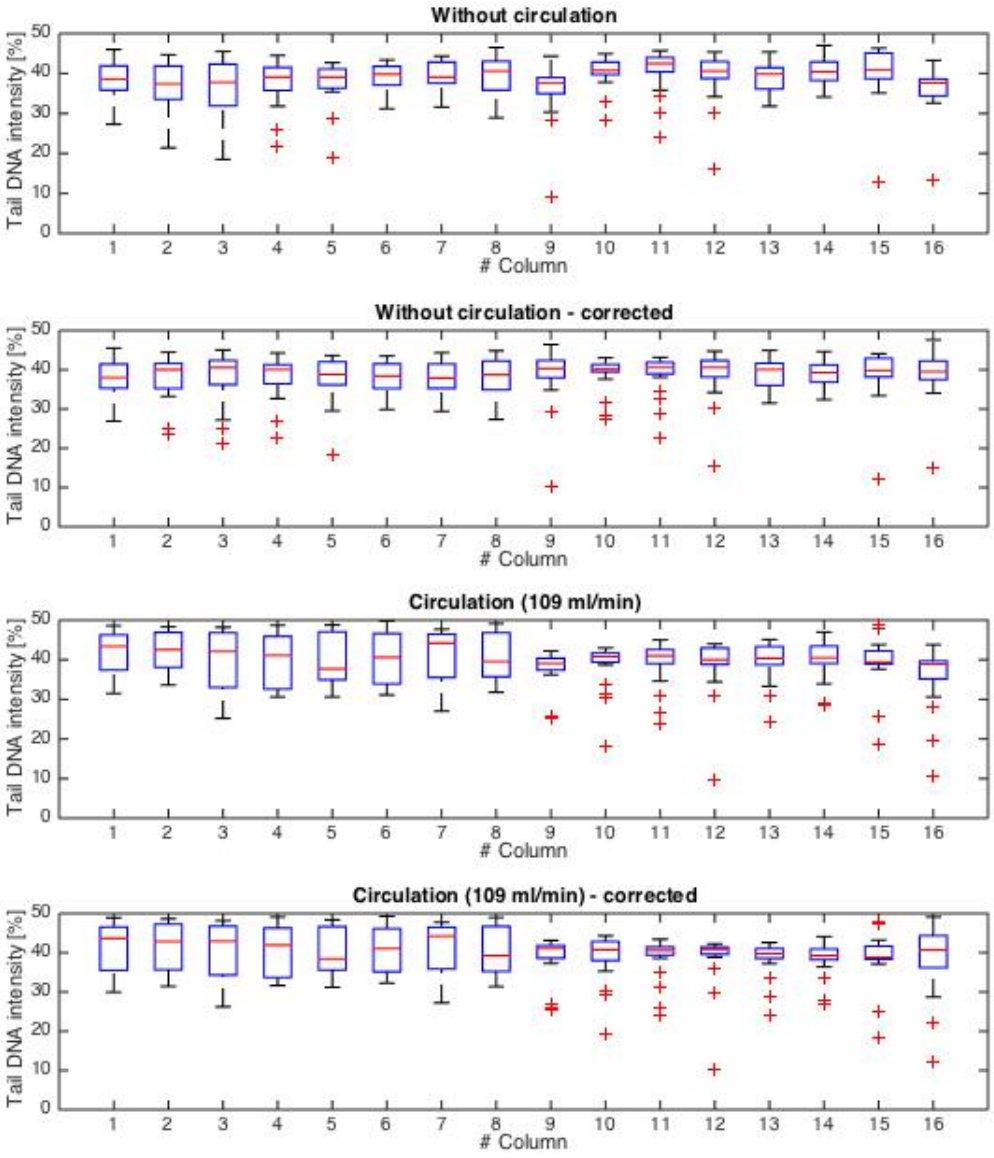

Figure 4.12: Per cent tail DNA intensity as a function of column position along the platform. Lymphocytes were irradiated with X-rays (8 Gy) and four 96 minigel format films were used. Boxplots of the per cent tail DNA intensity relative to the head intensity along each column of the four films together covering the whole platform in Experiment 4 with (109 ml/min) and without circulation during electrophoresis. Both uncorrected and corrected data based on the column positions are shown. For each box, the central mark is the median, the edges of the box correspond to the 25th and 75th percentiles and the whiskers extend to the most extreme data points not considering outliers. The outliers are plotted individually.

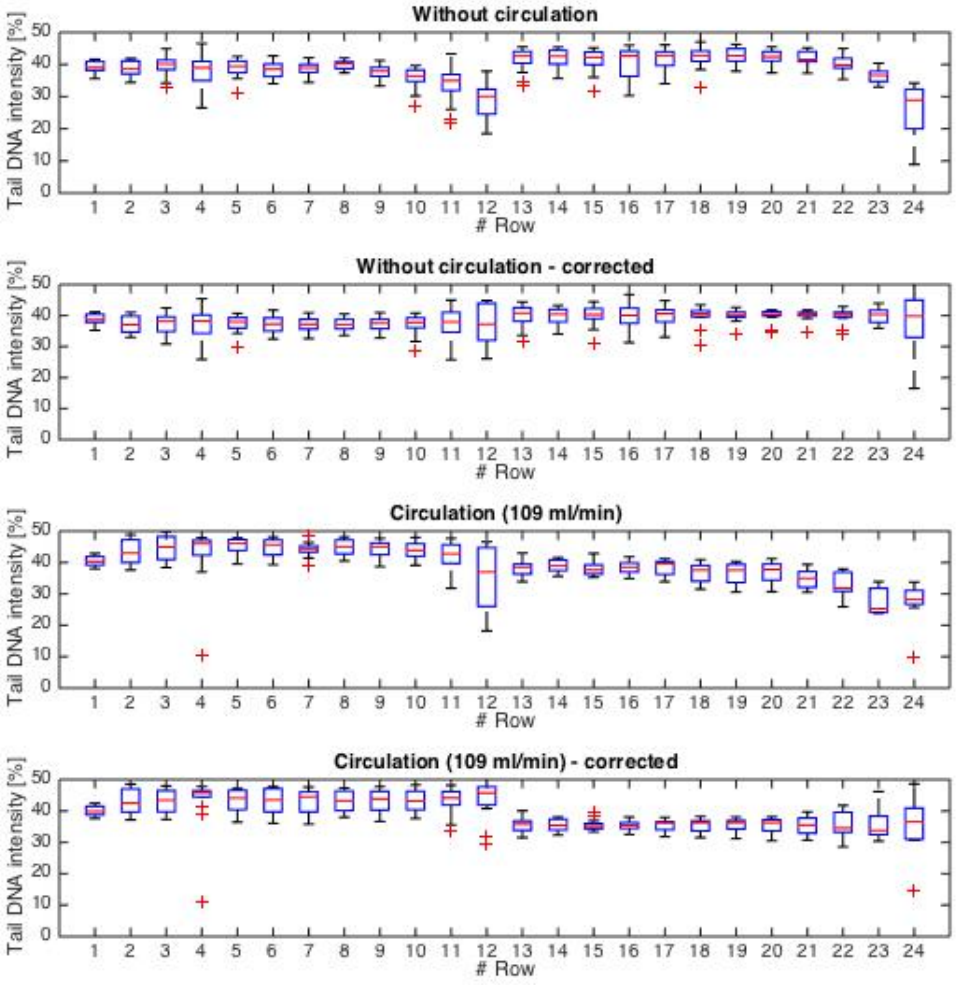

Figure 4.13: Per cent tail DNA intensity as a function of row position along the platform. Lymphocytes were irradiated with X-rays (8 Gy) and four 96 minigel format films were used. Boxplots of the per cent tail DNA intensity relative to the head intensity along each row of the four films together covering the whole platform in Experiment 4 with (109 ml/min) and without circulation during electrophoresis. Both uncorrected and corrected data based on the row positions are shown. For each box, the central mark is the median, the edges of the box correspond to the 25th and 75th percentiles and the whiskers extend to the most extreme data points not considering outliers. The outliers are plotted individually.

Table 4.9: Coefficient of variations as a function of position on the whole platform. Uncorrected CV and CV corrected due to systematic variations along the rows for the different positions on the platform and the whole platform from one experiment with (109 ml/min) and without circulation.

Position	Without circulation		With circulation	
	CV [%]	Corrected CV [%]	CV [%]	Corrected CV [%]
1	15.73	11.58	3.46	2.85
2	7.9	6.15	15.98	11.28
3	9.39	4.09	8.82	6.14
4	18.77	15.22	13.98	9.84
Whole platform	14.32	11.71	15.47	13.88

4.2.4 Variations in automated scoring due to insufficient staining of DNA

Insufficient staining of films was occasionally a problem during scoring. Three films, for which weak and insufficient staining was observed, were re-stained and re-scored. These films corresponded to the films in Experiment 1 with flow rate 153 ml/min, Experiment 4 (Position 1) without circulation and Experiment 4 (Position 3) with circulation (109 ml/min). The results presented for these three films were based on the second scoring. Data from the first and the second IMSTAR scoring of the first film in Experiment 4 (Position 1 - without circulation) is shown in Figure 4.14.

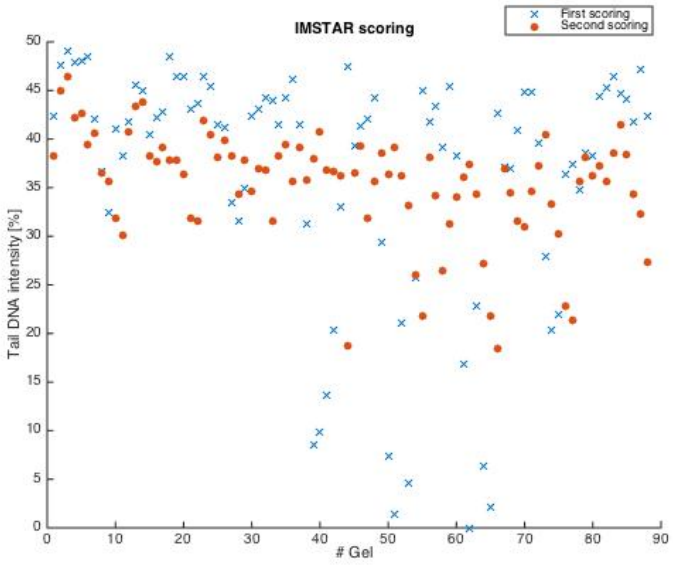

Figure 4.14: Variations in automated scoring due to insufficient staining of DNA. Variations in the median per cent tail DNA intensity relative to the head intensity of individual samples from the first (blue cross) and the second (red circles) scoring of the first film in Experiment 4 (Position 1 - without circulation). Lymphocytes were irradiated with X-rays (8 Gy). The automated scoring system (IMSTAR) with the same settings were used for both scorings.

5. Discussion

The ultimate aim of this thesis was to reduce variation in the comet assay results within and between laboratories, by developing a more stable and robust comet assay protocol. It is highly desirable to establish technical conditions in the comet assay protocol with the aim of minimizing variations in the results. The technical specifications may then be recommended to comet assay users.

This study examined systematically the effect of circulating the electrophoresis solution during electrophoresis, as part of a more detailed analysis and description of the local voltage variations across the platform. The variations in relative tail DNA intensity as a function of circulation speed were analyzed, and compared with the local voltage variations. The hypothesis was that the observed variations in electric potentials across the platform would be reflected in similar variations of the relative tail DNA intensities, when the comet assay was carried out with and without circulation during the electrophoresis. This was based on the fact that the voltage gradient is a major parameter which determines the degree of DNA migration. Prelimenary observations Gutzkow et al. (2013) had suggested that there were indeed less variations in DNA damage of samples, when circulation during electrophoresis was employed.

The implication of circulating the electrophoresis solution during electrophoresis in the comet assay has not previously been investigated in detail as was done in this thesis. The results obtained in this study should be useful for establishing the level of experimental variation which is to be expected in the comet assay. This thesis will hopefully be of value for researchers working with the comet assay.

5.1 Discussion of the materials and methods used

5.1.1 Measurement of electric potentials

The circulation pump was calibrated in order to specify the flow rate of each nominal circulation speed of the circulation pump used during electrophoresis. The position of the graduated cylinder used for calibration relative to the electrophoresis tank was considered to have negligible impact on the measured flow rates from the results for the two different positions of the graduated cylinder, based on the obtained results as shown in Figure D.1 in Appendix D. Insufficient tube pressure in the peristaltic pump affected the flow rate. The major source of uncertainty in the flow rate determination for the nominal circulation was the tightening of the pump head, which, if suboptimal, could have caused small variations in the actual flow rate for the same nominal circulation speed between experiments.

The measurements of electric potentials were performed with an electrode gauge consisting of 22 thin platinum electrodes attached to a plastic plate. The plate was assumed to be of sufficient conductivity to prevent buildup of static charges on the surface of the plate during electrophoresis.

Ripple in the voltage output was initially observed in the test measurements. The ripple could have been caused by incomplete suppression of alternating waveform within the power supply resulting in a variation of the DC output (Storey 2013). The ripple could also have occurred due to interference with electromagnetic (EM) energy from the power supply with the multiplexing digital voltmeter (Storey 2013). In order to reduce this observed ripple, the multiplexing digital voltmeter was placed a distance away from the DC power supply and aluminum foil was used around the wire for EM shielding. This setup was used for all the measurements of electric potentials used in this study, and the design reduced the ripple in the voltage output.

The impact of reversed circulation during electrophoresis was analyzed since variations in the obtained electric potentials at electrode positions were considerably reduced by circulating the electrophoresis solution. The tank design and the external pump configuration made it difficult to reverse the circulation direction. The easiest and most convenient way of performing electrophoresis with reversed circulation without introducing other errors, was by reversing the power supply connector wiring. This resulted in opposite direction of the electric field compared to the circulation of the electrophoresis solution.

5.1.2 The comet assay

HPBL and ionization radiation exposure

The comet assay was performed using human peripheral blood lymphocytes, since these cells are very convenient for experimentation. The lymphocytes are easily obtained in large numbers by centrifugation of blood and isolatation of mononuclear cells (lymphocytes) from the other blood cells by means of centrifugation in a density gradient (NycoPrep). In addition, these cells do not require cell culture facilities and are more robust than many other primary cell types. (Collins et al. 2008*b*)

The genotoxic treatment of the lymphocytes was chosen to be X-rays, since ionizing radiation produces a known number of lesions per cell per dose of radiation in DNA of a particular genome size. In addition, ionizing radiation is a convenient and robust agent which is less affected by physical, chemical or biological conditions compared to treatment with chemicals. (Hall & Giaccia 2012)

In order to select an optimal X-ray dose for the experiments which followed, a dose-response curve of HPBLs was made. The obtained X-ray dose-response curve for the human peripheral blood lymphocytes showed the expected linear relation between the DNA damage and the radiation dose in the comet assay, as shown in Figure 4.6. An X-ray dose of 8 Gy was selected as the most optimal dose, since it is well within the linear part of the dose-response curve; this dose is of sufficient magnitude to induce DNA damage without reaching saturation level in the comet scoring.

In the first experiment using X-rays, the total radiation dose was calculated based on a dose rate of 3.47 Gy/min resulting from calibration documents prepared by the Norwegian Institute of Public Health. However, results from more recent calibrations by the Norwegian Radiation

Protection Authority (Hansen 2014) were found to give a slightly higher dose rate (3.82 Gy/min) after the first experiment were performed. Due to this difference, cells were exposed to a slightly higher dose in the first experiment (Experiment 1): 8.79 Gy, rather than the dose of 8 Gy used in the two later experiments (Experiment 2 and 3). For human cells, the number of DNA SSBs (+ ALS) per cell detected immediately after (i.e. no repair) a dose of 8 Gy and 8.79 Gy is approximately 8000 and 8790, respectively (Hall & Giaccia 2012). This difference is, however, not expected to be of major impact for the results, since the variations in tail DNA intensities were mainly evaluated in this study and not the number of lesions.

However, in retrospect the total time should preferably have been kept unaltered so that all the lymphocytes were irradiated with the same absolute dose. The differences in the dose given between these experiments, resulted in a slightly increased level of the tail DNA intensities which must be taken into consideration. However, it did not impact how the CVs in the tail DNA intensities varied between the circulation speeds, since the amount of variation were equally increased for all the flow rates.

Comet assay protocol

The final agarose concentration of 0.675% after mixing with cell samples was chosen based on a previous study indicating that an agarose concentration between 0.6 and 0.8% is most optimal in practice (Azqueta et al. 2011). Low concentrations can cause the gel to become unstable, while at higher concentrations the DNA migration is slower, resulting in less extensive comet tail formation, and thus requiring longer electrophoresis time (Sambrook & Russel 2001). A fresh agarose solution was prepared for each experiment to avoid evaporation of water during heating of the agarose which could result in an uncontrolled agarose gel concentration.

The high-throughput comet assay using the 96 minigel format was used in order to analyze a large number of samples in each experiment. In addition, this high-throughput format required less time needed for processing, which was a great advantage. The 96 minigel format has been verified to have the same sensitivity and dynamic range for detecting DNA damage as the standard assay based on glass slides (Azqueta et al. 2013), and was thus assumed to be reliable in this study. The edge effect, i.e., anomalous comets seen at the border of the gel due to drying, was prevented by transferring the 96 minigel films to lysis solution immediately after setting the gels (Azqueta et al. 2013). This edge-effect is particularly a problem with small gels because of the large surface area to volume ratio.

The total unwinding time was chosen to be 40 minutes. This is based on a previous study showing that the net per cent tail DNA was constant when using an alkaline incubation time before electrophoresis of between 40 and 60 minutes (Azqueta et al. 2011). In the same study, a voltage gradient of either 1.15 V/cm or 0.83 V/cm across the platform seemed optimal for electrophoresis times of 20 minutes or 30 minutes, respectively. For the comet assay in general, it is particularly important to use the same voltage gradient across the platform in all experiments within a study. Electrophoresis of 25 minutes with a total applied voltage of 25 V was chosen in this study resulting in a voltage gradient of approximately 0.85 V/cm across the platform, with the electrophoresis tank design used in this study.

The electrophoresis was performed with the same electrophoresis solution for the subsequent 6-8 electrophoresis runs for both the electric potential measurements and the comet assay. The conductivity of the electrophoresis solution was found to be approximately constant

during electrophoresis with circulation, since the circulation contributed to better temperature stability of the system, and should thus not affect the DNA migration when circulating the electrophoresis solution. However, if the comet assay is performed with subsequent electrophoresis runs without circulation, the DNA migration could vary due to variations in the conductivity. Calculations to indicate whether the current flowing through the electrophoresis system during a run of 25 minutes could have caused changes in the composition of the solution were also performed. The total charge transported by the current used during electrophoresis for 25 minutes was assumed to be insufficient to cause ionic changes. Subsequent electrophoresis runs were thus considered not to contribute to different DNA migration, compared to using electrophoresis runs with fresh electrophoresis solution in each run.

Staining and scoring of comets

The per cent tail DNA intensity was chosen as the parameter reflecting the level of DNA damage. This parameter covers a wide range of damage and is linearly related to the frequency of DNA breaks (Collins et al. 2008*a*). The gels were post-stained with diluted SYBR Gold overnight before scoring in order to reduce the "doughnut-effect", i.e. poor staining in the middle of the nucleotide (Dahl et al. 2016).

Semi-automated scoring of comets could not have been used in this study, since it is highly time consuming; scoring a 96 minigel film with 30 comets scored per gel requires 1-2 days of work. For convenience and due to the limited time of the thesis, only one film was scored using the semi-automated system, for comparison. All other films were scored using the fully automated scoring system, IMSTAR Pathfinder^{TM} Auto Comet. With the latter system, the time for scoring six to eight films (corresponding to one experiment) was reduced from 8-12 days to 3-4 days.

There are both advantages and disadvantages using either the semi-automated scoring or the automated scoring system. Advantages with the automated scoring system by IMSTAR, are that the comets to be scored are randomly selected. Since both the scoring time and the manpower are considerably reduced compared with the semi-automated system, large numbers of comets can be scored; the size of experiments needed in this study is thus facilitated by the automated scoring system. However, quality check of the automatic focusing and analysis in the automated system needed to be performed, since the system was not always able to find the optimal focus in each sample. Incorrect determination of the head and tail in the comets does occur. Artifacts and overlapping comets may also occur. However, this is considered to be negligible problems due to the large number of comets scored with IMSTAR.

In the semi-automated scoring system the user manually selects and identifies the comets to be scored. Poor staining which may result in incorrect analysis is more easily detected in Perceptives; overlapping comets and comets where parts of the tail are outside the picture can be de-selected by the operator of the semi-automated system due to the manually selection. Disadvantages with the semi-automated scoring system are that it is highly time-consuming, as already mentioned, and there is not a random selection of comets being scored. Manually selection might also give bias towards scoring undamaged cells in a mixed population of cells, since they are less likely than damaged cells to overlap with neighboring cells.

Performance of the comet assay

The performance of the comet assay is sensitive to certain details of the protocol. There is a requirement for considerable experience, particularly with the handling of cells. Critical operations comprise pipetting (avoiding shear forces due to liquid and cells passing through narrow pipettes) and application of gel samples in the 96-minigel format. A certain degree of inexperience with the comet assay was reflected in the outliers shown in the boxplot of the per cent tail DNA intensity in Figure 4.8. However, the variations in tail DNA intensities seemed to decrease for all the circulation speeds in the third experiment, which can be explained by the acquired experience and better skills to perform a comet assay. This is commonly observed for researchers new to the assay. It would thus be highly recommended that researchers working with the comet assay regularly practice the technique in order to maintain their experience and thus avoid variations as a result of poor performance.

5.2 Discussion of the obtained results

5.2.1 Stabilization of the electric potentials by circulating the electrophoresis solution

Local variations in voltage across the platform without circulation during electrophoresis have previously been recorded at the Department of Chemicals and Radiation at Norwegian Institute of Public Health in Oslo (Gutzkow et al. 2013). In these initial observations, the variations appeared to be reduced by mild circulation of the solution via an external pump.

This was thus the motivation behind studying systematically the effect of circulating the electrophoresis solution during electrophoresis in this thesis. In addition, no studies at other laboratories have examined these local voltage variations across the platform during electrophoresis in the comet assay. Since the voltage gradient is a major parameter which determines the degree of DNA migration, examination of electric potentials, as was done in this thesis, was thus considered to be essential for achieving a more stable and robust comet assay protocol.

In this thesis, the local voltage variations across the platform during electrophoresis were shown to be considerably reduced by circulating the electrophoresis solution, as stated in the previous study (Gutzkow et al. 2013). Stabilization of the electric potential by circulating the electrophoresis solution could be related to a better temperature stability and/or avoiding buildup of concentration gradients of the electrophoresis solution across the platform.

A better temperature stability could also contribute to an unaltered conductivity of the electrophoresis solution, since the temperature affects the conductivity of a solution. Higher conductivity occurs with increasing temperature due to increased mobility of ions (RadiometerAnalytical 2005). The conductivity of the electrophoresis solution is among the factors which could affect the local voltage gradient and hence the electrophoretic migration of DNA (Sambrook & Russel 2001).

By performing electrophoresis with circulation, the temperature was kept approximately constant during the whole run. On the contrary, the temperature was increased with approximately 2-3 °C during the electrophoreses without circulation for 25 minutes, as shown in Figure 4.2. Successive electrophoreses without circulation using the same electrophoresis solution are

thus likely to cause further increases in temperature, resulting in a large difference between the temperature in the later runs compared to the first runs, as well as within a run.

A positive feedback loop created by an increase in temperature followed by an increase in conductance could occur during electrophoresis without circulation (Brody & Kern 2004). Variations in temperature within and between electrophoresis measurements would thus also lead to a variation in conductivity. The decrease in conductivity observed for electrophoresis with circulation compared to without circulation, could thus be due to the corresponding decrease in temperature. This indicated that a positive feedback loop during electrophoresis would indeed be prevented by circulation, mainly because the temperature was kept more constant throughout the electrophoresis.

Elchrom^{TM} Scientific has investigated briefly the effect of circulating the electrophoresis solution. They have developed a gel electrophoresis apparatus (not specifically intended for the comet assay) with integrated pump for buffer circulation which achieved a constant temperature and eliminated pH gradient during electrophoresis which could affect the DNA migration (*Elchrom Scientific* 2016). This electrophoresis system also included parallel double-electrodes which they stated could provide a homogeneous and uniform electric field. Further work in the electric potential measurements performed in this study could thus include examination of the effect of a double-electrode design.

It should be noted that some of the electric potential measurements performed without circulation showed standard deviations and coefficients of variation approximately as low as the measurements performed with circulation (109 ml/min), as shown in Figure 4.5. The CVs in seven of the 17 measurements without circulation was lower than 3%. This indicated that differences in the CVs of the electric potentials between electrophoresis without circulation and with circulation may not be a representative measure of the variations if few measurements are performed. However, the possibility of obtaining large voltage variations during the electrophoresis is increased without circulating the electrophoresis solution.

Electric potentials at electrode positions as a function of electrophoresis volume

In order to evaluate the effect of electrophoresis solution volume, measurements of electric potentials were obtained with reduced volume, i.e. from the standard 1640 ml to 1340 ml. The coefficient of variation was approximately equal at a given flow rate for the two different volumes, indicating that a 300 ml reduction of electrophoresis solution was not a critical factor for this electrophoresis tank design. However, this can be a critical factor for a tank system where the depth of liquid on the platform will be less than 3-4 mm when reducing the electrophoresis volume with 300 ml. A depth of 8-9 mm has previously been recommended for the comet assay to make the system less sensitive to variations in the depths on the platform, which has been seen for depths of only 1-3 mm (Gutzkow et al. 2013). Thus reduced depth (3-4 mm) of the electrophoresis solution is not recommended.

For electrophoresis without circulation, the average CV was lower with reduced volume (1340 ml) compared to the original volume (1640 ml). The system could have been more sensitive to vibrations when the depth of liquid on the platform was reduced. A small movement of the refrigerator (the door open etc) could thus have caused a larger portion of the solution on the platform to be blended with the solution in the side wells resulting in the same effect as a mild circulation. However, only two measurements were performed without circulation with reduced

solution volume, and as indicated, the coefficient of variation without circulation can vary between the different measurements of electrophoresis without circulation. Thus, two measurements may not be completely representative for indicating the amount of voltage variation.

Voltage drop along the electrodes in the electrophoresis tank

When electric current passes through a conductor, some of the supplied energy is lost due to the conductor's resistance, resulting in a voltage drop along the conductor (Storey 2013). The voltage drop can be estimated by using Ohm's law given in Equation 2.12. This voltage drop depends on the electrode material (platinum), its cross sectional area and the current passing through the electrodes (Storey 2013). A voltage drop, which is due to ohmic resistance along the electrode, could cause a slight difference in DNA migration for gels positioned at the far end of the platform (relative to the electric connections) compared to the near end of the platform (Sambrook & Russel 2001).

The voltage drop along one electrode across the width of the electrophoresis tank was for both electrodes in sum determined to be 0.46 V. This voltage drop was relatively small and thus considered to not represent a critical factor of the differences in DNA migration, taking other experimental variations into account. However, a more optimal system design would be electrodes with a larger cross section of platinum wire, resulting in decreased voltage drop at a constant current due to decreased resistance of the electrodes. Platinum is chemically persistent against oxidation (NGU 2015), which is a great advantage when running electrophoresis.

5.2.2 The comet assay: dose-response curve

In order to select an optimal X-ray dose for further experiments a dose-response curve of HPBLs was conducted. For both the semi-automated and the automated scoring system, the per cent tail DNA intensity was considerably lower at the highest dose (15 Gy), and even lower than at 10 Gy for the IMSTAR scoring. Dose-response curves have been shown to be highly linear in this dose range of radiation, using the same equipment and experimental setup as in the present study (Gutzkow et al. 2013).

A likely explanation for the deviation from a linear dose-response, as observed for both scoring methods, is that there is a limited sensitivity for quantifying the fluorescence in tails (relative to background fluorescence) of very low intensities, relative to the total fluorescence of the whole comet (Collins et al. 2014). In IMSTAR, which is an unsupervised method of identifying and measuring each comet, there seemed to be a problem of distinguishing the head from the tail at doses of 15 Gy, which resulted in comets being scored as heads-only without any tails. This was associated with poor staining, and re-staining reduced the problem.

5.2.3 The implication of electrophoresis solution circulation in the alkaline comet assay on HPBL

The variabilities of the tail DNA intensities in samples exposed to 8 Gy X-rays as a function of circulation speed were analyzed in this thesis. Only one other study (as this far known) has investigated the implication of electrophoresis solution in the alkaline comet assay (Gutzkow et al. 2013). It should be emphasized that this previous study did not examine the per cent tail

DNA intensity as a function of circulation speed in such detail as was done in this thesis. In this section, the results obtained for per cent tail DNA intensity will be discussed and compared with the results in this previous study.

The CVs in per cent tail DNA intensity among the different circulation speeds were confirmed not to be significantly different from each other. The variations in per cent tail DNA intensity in this study were thus not consistent with the results obtained in the previous study which suggested that these variations were significantly reduced by mild circulation (Gutzkow et al. 2013). It should be noted that in the previous study the lymphocytes were irradiated with 10 Gy X-rays and the circulation speed used was not identical to the ones used in this study. In addition, the comets were scored using the semi-automated scoring system by Perceptives, while in this thesis the automated scoring system by Imstar was used. Differences in the experimental conditions and in the scoring analysis could thus have caused some of the variations in the per cent tail DNA intensity between these two studies.

The results obtained in this thesis could be useful for estimating the level of CV which is expected in the alkaline comet assay. Mean CVs of approximately 8%, 9% and 11% in the per cent tail DNA intensity were obtained by circulating the electrophoresis solution at 153 ml/min, 109 ml/min and without circulation, respectively. In comparison with the only other study which examined the implication of circulation, the mean CVs were shown to be approximately 7 % and 26 % with (84 ml/min) and without circulating the electrophoresis solution, respectively (Gutzkow et al. 2013). This indicates that the CVs were approximately equal between the two studies when circulating was included. However, the CV without circulation was considerably higher in the previous study compared to the CV obtained in this thesis. The reasons for this are still unknown.

However, it should be noted that the experimental data obtained in the present study are much more extensive than in (Gutzkow et al. 2013): A total of 36 replicates were analyzed per experiment with and without circulation in the previous study (Gutzkow et al. 2013), compared to a total of approximately 126 and 360 replicates with and without circulation at each flow rate, respectively, in this study. Considering the number of replicates analyzed in each experiment, the results in this thesis may be more representative and give a better indication of the level of CV in the comet assay, at a moderate level of DNA damage. Both studies showed a decrease in the variations in tail DNA intensities by circulating the electrophoresis solution. However, in this study, the circulation was considered not to represent a critical factor in the assay due to the low decrease of CV obtained by circulation.

There was an observed decrease in the median per cent tail DNA intensity along the rows of the film, as shown in figures in Appendix D. This can not be explained by variations in the potential gradient (V/cm) during electrophoresis due to the voltage drop along the electrodes in the electrophoresis tank, since the voltage drop was considered negligible and in the opposite direction as observed (lowest voltage gradient i the first rows). The decrease in per cent tail DNA intensity observed could thus be a result of DNA repair occurring in the 37°C agarose in the tips of the pipette while adding the gels to the film (Collins & Azqueta 2012). In the last experiment (Experiment 3), the decrease in per cent tail DNA intensity along the rows were less compared to the first two experiment (Experiment 1 and 2). This indicated that a faster performance of making the 96-minigel format was obtained in the last experiment, and thus less DNA repair occurred.

In this study, the DNA lesions were induced by X-rays; these lesions are repaired relatively

fast and readily, compared to DNA lesions produced by various chemicals (Hall & Giaccia 2012). Fast and accurate processing of the 96-minigels was necessary in order to avoid reduction in the apparent level of DNA damage which are caused by repair of DNA damage during the comet procedure - hence representing a possible artifact. For an experienced comet assay user, this is mostly not a problem since application of samples are carried out very quickly. In order to minimize possible DNA repair, it could be advisable to add gels to parts of the film of the whole film at once, with cells being stored on ice prior to moulding. However, usually when conducting the comet assay, testing cells are added in three technical replicates at a time and will thus not be able to repair.

Repair of DNA strand breaks after adding the gels on the film was considered to be negligible since samples were quickly cooled down to few degrees above 0 °C, achieved by using a cold aluminum plate for support during ample application. This stage was followed by immersing films in lysis solution after adding all gel samples. (Azqueta et al. 2014, Collins & Azqueta 2012)

Relative tail DNA intensity as a function of position on the whole platform and of the circulation flow rate

Four 96 minigel format films were placed on the platform during electrophoresis in the comet assay, in order to evaluate the per cent tail DNA intensity across the whole platform. One electrophoresis with circulation (109 ml/min) and without circulation were performed. No other studies (as this far known) have investigated the variations in per cent tail DNA intensity as a function of position across the platform. The results in this thesis could thus provide useful information regarding the implication of sample position across the platform and hence facilitate further work among researchers working with the comet assay.

The three dimensional bar charts in Figure 4.11 illustrated how large the variation in median tail DNA intensities was across the platform both without circulation and with circulation (109 ml/min) during electrophoresis. The hypothesis of decreased variation in tail DNA intensities from circulating the electrophoresis solution could not be validated, since the CV over the whole platform without any correction made for the rows were determined to be 15.47% and 14.32% for the electrophoresis with and without circulation, respectively.

The decreasing tail DNA intensities along the rows in each film was also observed such as in Experiment 1, 2 and 3. It was well visualized for the electrophoresis without circulation, where in Position 1 (row 1-12) the per cent tail DNA intensity decreased, and suddenly at row 13, where a new position (Position 3, row 13-24) began and thus new gels added to the film, the per cent tail DNA intensity was approximately equal to the first rows in Position 1, and then decreased along the rows down to row 24. This further indicated some repair of DNA lesions: the decreased level of DNA damage is likely to reflect repair of DNA damage in cells still at elevated temperature while in the pipettes.

Corrections due to systematic variations in the positions of the films were performed in order to evaluate only the time-dependent variations in tail DNA intensities across the platform. These systematic variations in positions were mainly observed along the rows due to DNA repair, and thus the corrections performed along the rows had largest effect for the variation in tail DNA intensities across the platform. It was no clear relation between the CV and the position on the platform as a function of circulation speed, as shown in Table 4.9. Position 1 showed a larger variation in tail DNA intensities without circulation compared to with circulation, while

Position 2, showed the opposite, i.e. less variation without circulation than with circulation. Further measurements are considered necessary in order to give a representative indication of the implication of sample position across the platform.

Unfortunately, there were technical problems with adding the gels on the film due to poor pipettes which resulted in some lost gels being lost, in the last rows on the platform, particularly for the electrophoresis with circulation (109 ml/min). However, sufficient data was obtained in order to illustrate the distribution across the platform.

5.2.4 Comparison of the electric potential measurements and the tail DNA intensities in the comet assay

There are several critical factors throughout the comet assay procedure which may seriously affect the results. In this study the electrophoresis conditions have been analyzed in some detail, particularly variations in voltage gradient across the platform as a function of different circulation speeds. This approach was mainly caused by the fact that the voltage gradient is a major parameter which determines the migration of DNA. The hypothesis was thus that variations in electric potentials would cause parallel variations in DNA damage measured as relative comet tail DNA intensities.

This study showed that the variations in the electric potentials across the platform were considerably reduced by circulating the electrophoresis solution, as shown in a previous study (Gutzkow et al. 2013). However, the variations in voltages observed from the electric potential measurements during electrophoresis without circulation, were only partly paralleled with the variations in tail DNA intensities from the comet assay performed with or without circulation of different flow rates during electrophoresis. This could indicate that the electrophoresis solution circulation is less important than was initially suggested in the previous study (Gutzkow et al. 2013). Still, a decrease of approximately 1-2 % in the CV of the per cent tail DNA intensity was obtained by circulating the electrophoresis solution at flow rates above 109 ml/min. In addition, a less variating DNA intensity was obtained by circulating the electrophoresis solution. Circulation also contribute to a better temperature stability. Based on these observations, circulation of the electrophoresis solution in the comet assay is thus recommended.

Since the variations in electric potential did not cause parallel variations in tail DNA intensity, questions therefore remain regarding the observed and clearly flow-rate dependent variations in the electric potentials. An electrochemical perspective of the processes occurring during electrophoresis was thus desired. As mentioned in the theory, the electric potential is dependent on the concentration gradients in the solution (Zumdahl & DeCoste 2013). The concentration of reactants and products involved in the redox reaction occurring at each electrode during electric potential measurements will thus affect the measured potential. Small differences in concentrations of these reactants and products between each electrode could thus have caused variation in the measured electric potentials.

Along with two electrochemists at the Department of Materials Science and Engineering at NTNU, it was concluded that a reference electrode must be used in order to determine whether the observed variations in electric potentials occurred due to real potential differences across the platform or only due to minute concentration gradients between the electrodes. The reference electrode must have a well-defined and reproducible potential, i.e. both reactants and products must be present with a kinetics of the reactions sufficiently fast so that the species are

present at their equilibrium concentrations (Newman & Thomas-Alyea 2004). It was considered that a reference electrode as described could not be produced within the scope and short duration of this thesis. Hence, it has not been possible to determine the cause of the electric potential variations which were observed in this study.

Further work

There is a desire to explain the observed variation by a mechanistic approach. Further work regarding the implication of electrophoresis solution circulation in the alkaline comet assay, should thus involve measurements of electric potentials across the platform using a reference electrode suitable for the system. The cause of the electric potential variations can then be determined.

If the electric potential variations across the platform during electrophoresis proves to be real, and not reflecting minute changes in ion concentrations in the close vicinity of the electrodes, further work should involve multiple measurements (more than in this study), both with and without circulation. This statement is based on the obtained results in the measured electric potentials, showing that 7 of 17 measurements performed without circulation resulted in a CV lower than 3 %. There might also be other critical factors throughout the comet assay procedure which have a greater impact on the per cent tail DNA intensity variations compared to the effect of electrophoresis solution circulation.

By assuming real electric potential variations, the impact on reversed circulation in the comet assay should also be investigated. This is due to the larger CVs in the electric potentials observed when performing electrophoresis with reversed circulation compared to the original direction (flow rate of liquid positive from the positive to the negative electrode). The circulation direction could be a critical factor in the comet assay if these electric potential variations seem to be consistent with variations in the tail DNA intensity.

On the other hand, the inconsistent results between electric potential variations and variations in tail DNA intensities obtained in this study could be verified if the variations in the electric potentials are found to reflect minute concentration gradients between the electrodes. Other critical factors throughout the comet assay procedure should thus be examined.

6. Conclusion

The ultimate aim of this study was to reduce variation in the comet assay results within and between laboratories, by developing a more stable and robust comet assay protocol. This aim was pursued, by examining systematically the association between local electric potential variations, and their relations to variations in DNA damage as measured in neighboring cell samples, as a function of circulation speed. No previous studies have investigated in such detail as was done in this thesis regarding the implication of adding circulation of the electrophoresis solution during electrophoresis in the comet assay. The motivation behind this thesis was based on a previous study performed at the Department of Chemicals and Radiation at Norwegian Institute of Public Health, in Oslo, which suggested that circulating the electrophoresis solution lead to more stable local voltages and tail DNA intensities in the comet assay (Gutzkow et al. 2013).

This study showed that the variations in the electric potentials across the platform were considerably reduced by circulating the electrophoresis solution. This was also suggested in a previous publication (Gutzkow et al. 2013), in which such variations were paralleled by variations in DNA damage in neighboring samples. However, it was observed in this thesis that the variations in voltages observed from the electric potential measurements during electrophoresis without circulation, were only partly paralleled with the variations in tail DNA intensities from the comet assay performed with or without circulation of different flow rates during electrophoresis. It should be emphasized that a decrease of approximately 1-2 % in the CV in the per cent tail DNA intensity was obtained by circulating the electrophoresis solution at flow rates above 109 ml/min in this study. In addition, a less variable per cent tail DNA intensity was obtained by circulating the electrophoresis solution. The circulation also contributed to a better temperature stability. Based on these observations, circulation of the electrophoresis solution during electrophoresis in the comet assay is thus recommended.

Along with two electrochemists at the Department of Materials Science and Engineering at NTNU, it was concluded that a reference electrode must be used in order to determine if the observed variations in electric potentials could have occurred due to minute concentration gradients between the electrodes. Due to the limited time available in the thesis this was not accomplished/completed. Further work regarding the implication of electrophoresis solution circulation in the alkaline comet assay, should thus involve measurements of electric potentials across the platform using a reference electrode suitable for the system. The cause of the electric potential variations can then be determined.

7. Bibliography

Alberts, B., Bray, D., Hopkin, K., Johnson, A., Lewis, J., Raff, M., Roberts, K. & Walter, P. (2004), *Essential Cell Biology*, 2nd edn, Garland Science Taylor & Francis Group.

Axis-Shield (2015), *NycoPrep 1.077 Product Specific Document*.

Azqueta, A., Gutzkow, K. B., Brunborg, G. & Collins, A. R. (2011), 'Towards a more reliable comet assay: Optmizing agarose concentration, unwinding time and electrophoresis conditions', *Mutation Research/Genetic Toxicology and Environmental Mutagenesis* **724**, 41–45.

Azqueta, A., Gutzkow, K. B., Priestley, C. C., Meier, S., S-Walker, J., Brunborg, G. & Collins, A. R. (2013), 'A comparative performance test of standard, medium- and high-throughput comet assays', *Toxicology in Vitro* **27**(2), 768–773.

Azqueta, A., Langie, S. & Collins, A. (2015), *30 years of the comet assay: an overview with some new insights*, Frontiers in Genetics.

Azqueta, A., Slyskova, J., Langie, S., Gaivao, I. & Collins, A. R. (2014), 'Comet assay to measure dna repair: approach and applications', *Frontiers in Genetics* **5**, 288.

Brody, J. R. & Kern, S. E. (2004), 'History and principles of conductive media for standard dna electrophoresis', *Analytical Biochemistry* **333**(1), 1–13.

Burtis, C. A. & Ashwood, E. R. (2001), *Tietz Fundamentals of Clinical Chemistry*, 5th edn, W. B. Sanders Company.

Chiarini-Garcia, H. & Melo, R. C. (2011), *Light Microscopy - Methods and Protocols*, Humana Press Springer.

Collins, A. R. & Azqueta, A. (2012), 'Dna repair as a biomarker in human biomonitoring studies; further applications dna repair as a biomarker in human biomonitoring studies; further applications of the comet assay', *Mutation Research/Fundamental and Molecular Mechanisms of Mutagenesis* **736**, 122–129.

Collins, A. R., Oscoz, A. A., Brunborg, G., Gaivao, I., Giovannelli, L., Kruszewski, M., Smith, C. C. & Stetina, R. (2008*a*), 'The comet assay: topical issues', *Mutagenesis* **23**(3), 143–151.

Collins, A. R., Oscoz, A. A., Brunborg, G., Gaivao, I., Giovannelli, L., Kruszewski, M., Smith, C. C. & Stetina, R. (2008*b*), 'Review - the comet assay: topical issues', *Mutagenesis* **23**(3), 143–151.

Collins, A. R., Yamani, N. E., Lorenzo, T., Shaposhnikov, S., Brunborg, G. & Azqueta, A. (2014), 'Controlling variation in the comet assay', *Frontiers in Genetics* **5**(359).

Dahl, H., Gutzkow, K. B., Graupner, A. & Brunborg, G. (2016), *The comet assay - Working protocol*, Department of Chemicals and radiation, National Institute of Public Health.

Elchrom Scientific (2016).
URL: *http://www.thistlescientific.co.uk*

Flower, M. A. . (2012), *Webb's Physics of Medical Imaging*, 2nd edn, Taylor & Francis Group.

GeneralElectric (2014), *Cell Separation Media - Methodology and applications*.

Giordano, N. J. (2013), *College Physics Reasoning and Relationship*, 2nd edn, Brooks/Cole CENGAGE Learning.

Gutzkow, K. B. (2004), cAMP-mediated regulation of G1-S transition in lymphoid cells, PhD thesis, Faculty of Medicine, Univeristy of Oslo.

Gutzkow, K. B., Langleite, T. M., Meier, S., Graupner, A., Collins, A. R. & Brunborg, G. (2013), 'High-throughput comet assay using 96 minigels', *Mutagenesis* **28**(3), 333–340.

Hall, E. J. & Giaccia, A. J. (2012), *Radiobiology for the Radiologist*, 7th edn, Lippincott Williams & Wilkins.

Hansen, E. L. (2014), *Absorbed doses to water for x-ray dosimetry on a PXI X-RAD 225*, Norwegian Radiation Protection Authority.

Hunter, R. J. (1988), *Zeta Potential in Colloid Science: Principles and Applications*, Academic Press.

Israelchvili, J. N. (2011), *Intermolecular and Surface Forces*, 3rd edn, Elsevier.

Keohavong, P. & Grant, S. G. (2005), *Molecular Toxicology Protocols*, Vol. 291, Humana Press.

Kindt, T. J., Goldsby, R. A. & Osborne, B. A. (2007), *Immunology*, 6th edn, W. H. Freeman & Company.

Kirkwood, B. R. & Sterne, J. A. C. (2003), *Medical Statistics*, 2nd edn, Blackwell Science.

Lilley, J. (2001), *Nuclear Physics - Principles and Applications*, John Wiley & Sons, Ltd.

Lilliefors, H. W. (1967), 'On the kolmogorov-smirnov test for normality with mean and variance unknown', *Journal of the American Statistical Association* **62**, 399–402.

Lovell, D. P. & Omori, T. (2008), 'Review - statistical issues in the use of the comet assay', *Mutagenesis* **23**(3), 171–182.

Næss, S. N., Mikkelsen, A. & Elgsæter, A. (2014), *Molecular Biophysics*, Department of Physics, Norwegian University of Science and Technology.

Newman, J. & Thomas-Alyea, K. E. (2004), *Electrochemical Systems*, 3rd edn, Wiley Interscience.

NGU (2015), 'Norges geologiske undersøkelse: Edelmetaller'.
URL: *https://www.ngu.no/fagomrade/edelmetaller*

OECD (2014), *Guidline for the testing of chemicals - in vivo mammalian alkaline comet assay*.

One-Way ANOVA (2016).
URL: *http://se.mathworks.com/help/stats/one-way-anova.html*

Ostling, O. & Johanson, K. J. (1984), 'Microelectrophoretic study of radiation-induced dna damages in individual mammalian cells', *Biochemical and Biophysical Research Communications* **123**(1), 291–298.

RadiometerAnalytical (2005), *4-pole Conductivity Cells - Operating Instructions*.

Sambrook, J. & Russel, D. W. (2001), *Molecular Cloning - A Laboratory manual*, Vol. 1, 3rd edn, Cold Spring Harbor Laboratory Press.

Shaposhnikov, S. A., Salenko, V. B., Brunborg, G., Nygren, J. & Collins, A. R. (2008), 'Research article - single-cell gel electrophoresis (the comet assay): Loops or fragments?', *Electrophoresis* **29**(14), 3005–3012.

Storey, N. (2013), *Electronics - A Systems Approach*, 5th edn, Pearson Education Limited.

Stryer, L. (1988), *Biochemistry*, 3rd edn, W. H. Freeman & Company.

Walker, J. (2013), *DNA Electrophoresis - Methods and Protocols*, Humana Press Springer.

Walpole, R. E., Myers, R. H., Myers, S. L. & Ye, K. E. (2011), *Probability & Statistics for Engineers & Scientists*, 9th edn, Pearson Education.

Westermeier, R. (2005), *Electrophoresis in Practise*, 4th edn, Wiley-VCH Verlag GmbH & Co. KGaA.

Young, H. D., Freedman, R. A. & Ford, A. L. (2011), *University Physics with Modern Physics*, Vol. 2, 13th edn, Pearson Education Limited.

Zumdahl, S. S. & DeCoste, D. J. (2013), *Chemical Principles*, 7th edn, Brooks/Cole Cencage Learning.

Appendices

A. Products

Table A.1: Products and producers

Product	**Producer**	**Country**
34972A LXI Data Acquisition	Keysight Technologies	USA
34901A 20 Channel Multiplexer	Keysight Technologies	USA
BenchLink Data Logger 3 software	Keysight Technologies	USA
CDC566T 4 pole conductivity cell	Meterlab^{TM} Radiometer analytical	France
Centrifuge 5810 R	Thermo Fisher Scientific	USA
Comet Assay Spreadsheet Generator 1.4.1	Perceptives Instruments	United Kingdom
Conductivity standard solution - NaCl 25.0 μS/cm ± 5 (25 °C)	Meterlab^{TM} Radiometer analytical	France
Conductivity Meter CDM 210	Meterlab^{TM} Radiometer analytical	France
Comet assay IV	Perceptive Instruments	United Kingdom
Dimethyl sulphoxide (DMSO)	Merck	Germany
Dri-Block® Heater DB-3	Techne	United Kingdom
Electrode gauge	Locally produced	Norway
Electrophoresis Power Supply EV202	Consort	Belgium
Electrophoresis tank	Locally produced	Norway
Ethanol 96%	Kemetyl	Norway
Ethylenediaminetetraacetic acid disodium salt dihydrate (EDTA-Na_2)	Sigma-Aldrich	USA
EDTA supplemented tubes	Becton Dickinson	USA
Fetal calf serum (FCS)	Gibco	USA
GelBond® Film	Cambrex	USA
Hepes	Sigma-Aldrich	USA
Hydrogen chloride (HCl)	Merck	Germany
Lymphoprep^{TM} tube	Axis-Shield PoC	Norway
Master plastic plate	Locally produced	Norway
Nalgene®Mr. Frosty	Thermo Fischer Scientific	Germany
N-Laurosylsarcosine	Sigma-Aldrich	USA
NuSieve GTG Low Melting Agarose	Cambrex	USA
NycoPrep (1.077 g/ml)	Axis-Shield PoC	Norway
Olympus BX61 microscope	Olympus	Japan
Pathfinder ^{TM} Auto Comet software	IMSTAR	France
Peristaltic pump TBE	Medorex	Germany

Table A.1: Products and producers

Product	**Producer**	**Country**
Phosphate buffered saline (PBS) - Without Ca^{2+} and Mg^{2+}, pH 7.4	Locally produced	Norway
Plastic frames with stainless steel metal feet	Locally produced	Norway
RPMI-1640	Sigma-Aldrich	USA
Sodium chloride (NaCl)	Merck	Germany
Sodium hydroxide (NaOH)	Merck	Germany
Sodium lauryl sarcosinate (SLS)	Sigma-Aldrich	USA
Stainless steel tubing helix	Locally produced	Norway
SYBR® Gold	Invitrogen	USA
Trizma® base	Sigma-Aldrich	USA
Trizma® HCL	Sigma-Aldrich	USA
Triton-X	Sigma-Aldrich	USA
XRAD225 Unit	Precision X-Ray (PXi)	USA

B. Recipes for the stock solutions/buffers

B.1 Lysis stock solution

- 2.5 M NaCl
- 100 mM $Na_2EDTA \times 2H_2O$
- 10 mM Triszma-base
- NaOH (pellets)
- 34 mM N-Lauroylsarcosine sodium salt

Dissolved in distilled water. pH was adjusted to 10 with NaOH pellets. Stirred in the hood overnight. Final concentration of lysis solution was achieved after addition of DMSO and Triton-X.

B.2 Electrophoresis stock solution

- 3 M NaOH
- 0.01 M Na_2EDTA

Dissolved in distilled water.

B.3 PBS/10 mM EDTA

- 10 mM Na_2EDTA

Add 10 mM Na_2EDTA to PBS without Ca^{2+}/Mg^{2+}. pH adjusted to 7.4.

B.4 TE-buffer for SYBR Gold staining

- 1 mM Na_2EDTA
- 10 mM Tris-HCL

Dissolved in distilled water. pH adjusted to 8.0.

C. Tables

Table C.1: Electric potentials at electrode positions as a function of circulation speed. The time integrated corrected electrode voltage per cm and CV averaged for all electrodes during an electrophoresis time of 25 minutes. Data from three experiments with and without circulation at different flow rates.

Circulation speed	Mean voltage [$\frac{V}{cm}$]	CV [%]
0	0.81	8.67
	0.80	1.27
	0.86	14.90
Mean	**0.82**	**8.28**
10	0.88	1.26
	0.81	0.71
	0.85	1.53
Mean	**0.85**	**1.17**
20	0.86	0.73
	0.86	0.27
	0.86	0.58
Mean	**0.86**	**0.53**
30	0.82	0.64
	0.83	0.78
	0.85	0.52
Mean	**0.83**	**0.65**
50	0.82	1.02
	0.83	0.57
	0.86	0.52
Mean	**0.84**	**0.70**
70	0.80	0.34
	0.83	0.87
	0.85	0.28
Mean	**0.83**	**0.50**

Table C.2: Time-integrated corrected electrode voltages without circulation and with nominal circulation speed of 30.

Circulation speed	Mean voltage [$\frac{V}{cm}$]	CV [%]
0	0.81	8.67
	0.80	1.27
	0.86	14.90
	0.84	0.60
	0.84	1.33
	0.89	72.47
	0.74	36.84
	0.82	10.58
	0.85	2.45
	0.83	18.48
	0.86	5.29
	0.90	0.33
	0.90	1.53
	0.89	1.08
	0.90	62.84
	0.81	38.05
	0.87	7.89
Mean	**0.85**	**16.74**
30	0.82	0.64
	0.83	0.78
	0.85	0.52
	0.85	1.78
	0.83	0.66
	0.84	0.73
	0.84	0.43
Mean	**0.84**	**0.79**

D. Figures

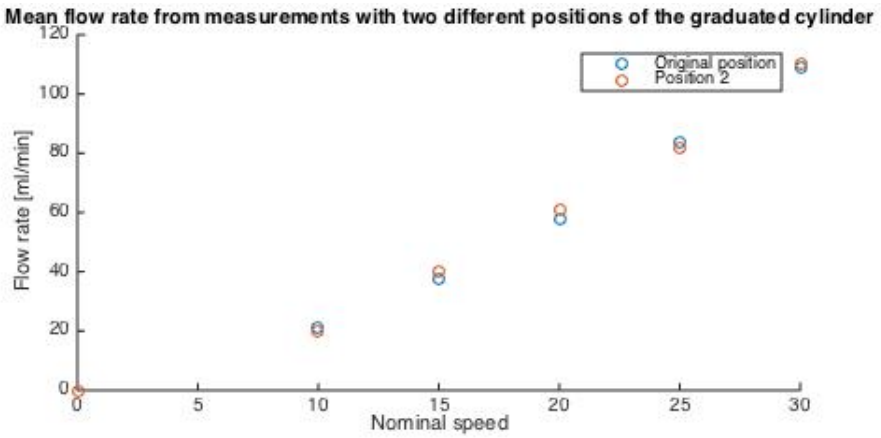

Figure D.1: Mean flow rates [ml/min] from measurements with two different positions of the graduated cylinder. The Original position (blue circles) corresponds to 60 cm below the electrophoresis tank, while Position 2 (red circles) corresponds to 20 cm below the electrophoresis tank.

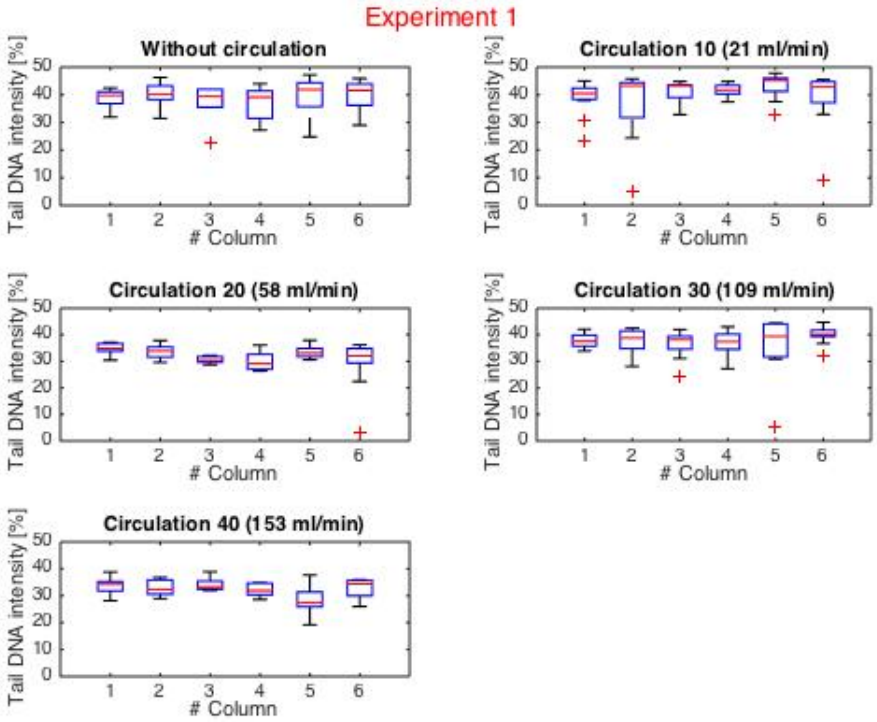

(a)

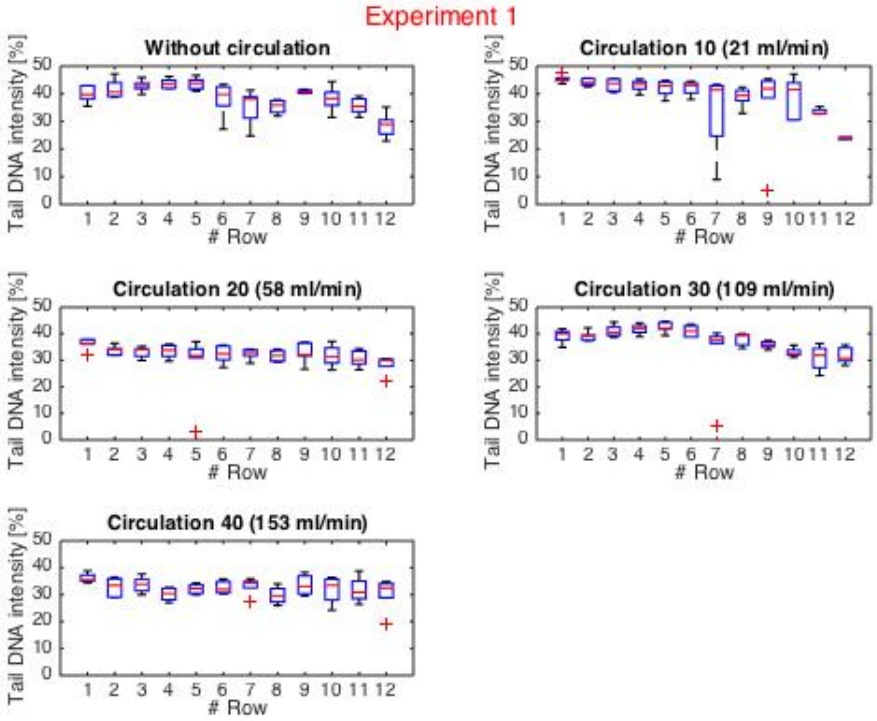

(b)

Figure D.2: Boxplots of the tail DNA intensity [%] along each column (D.2a) and each row (D.2b) of the films in Experiment 1 both without circulation and with circulation of different flow rates during electrophoresis. For each flow rate, the 96 minigels format was used. The lymphocytes were irradiated with X-rays (8 Gy).

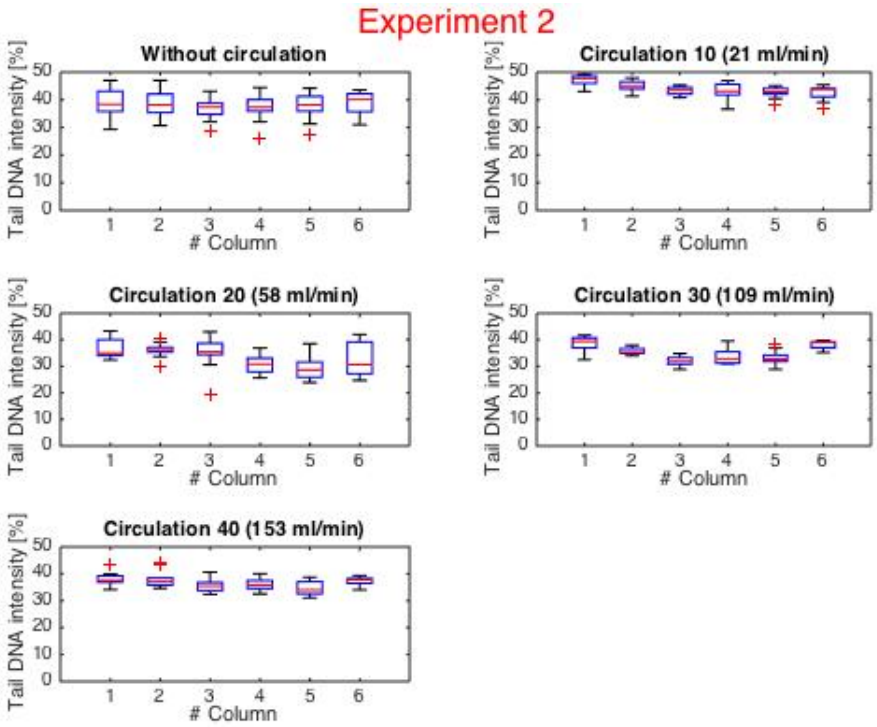

(a)

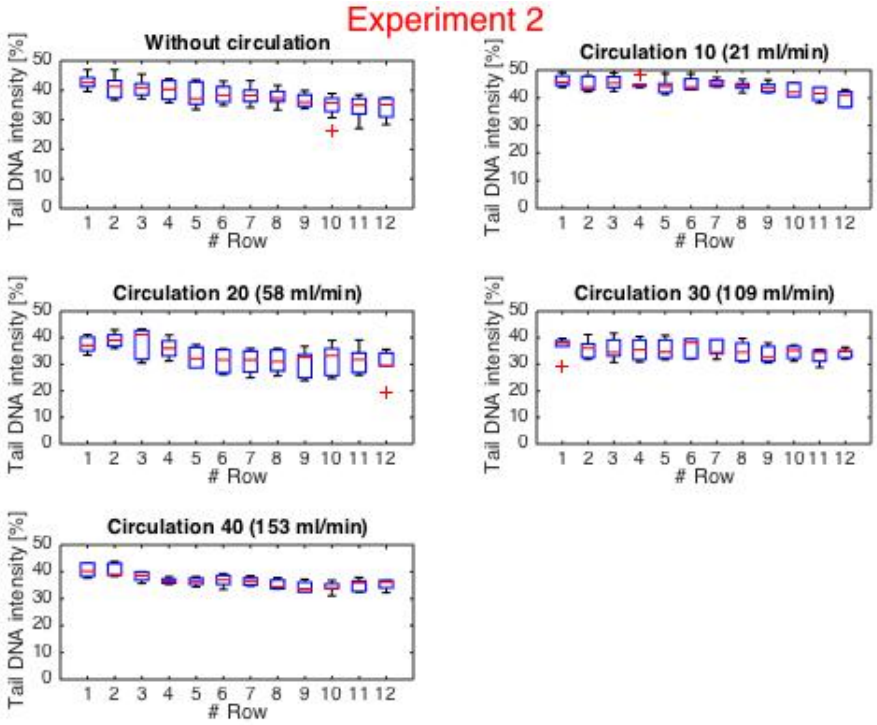

(b)

Figure D.3: Boxplots of the tail DNA intensity [%] along each column (D.3a) and each row (D.3b) of the films in Experiment 2 both without circulation and with circulation of different flow rates during electrophoresis. For each flow rate, the 96 minigels format was used, where electrophoresis without circulation was performed twice. The lymphocytes were irradiated with X-rays (8 Gy).

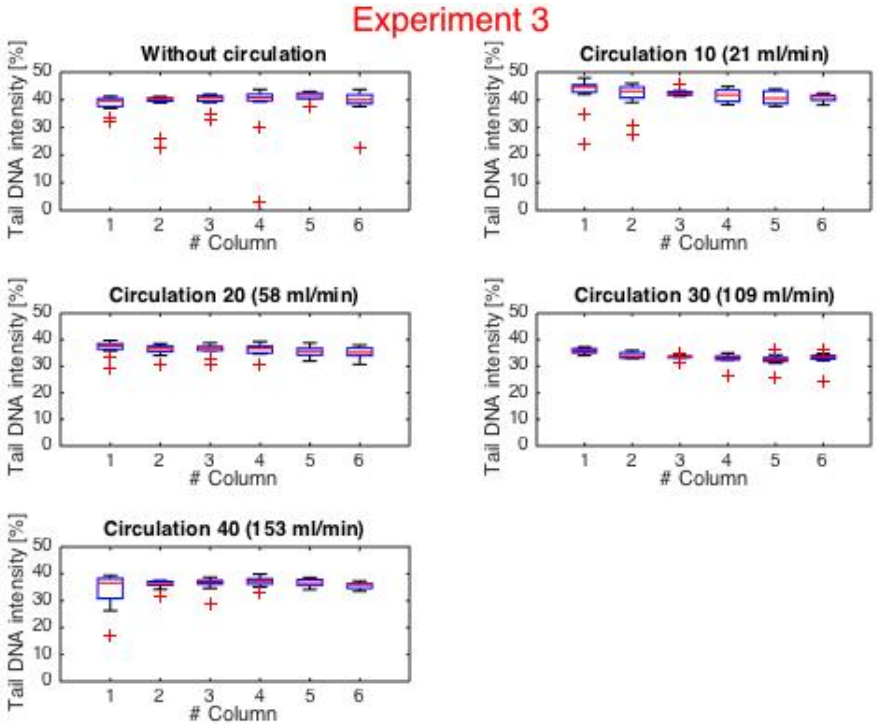

(a)

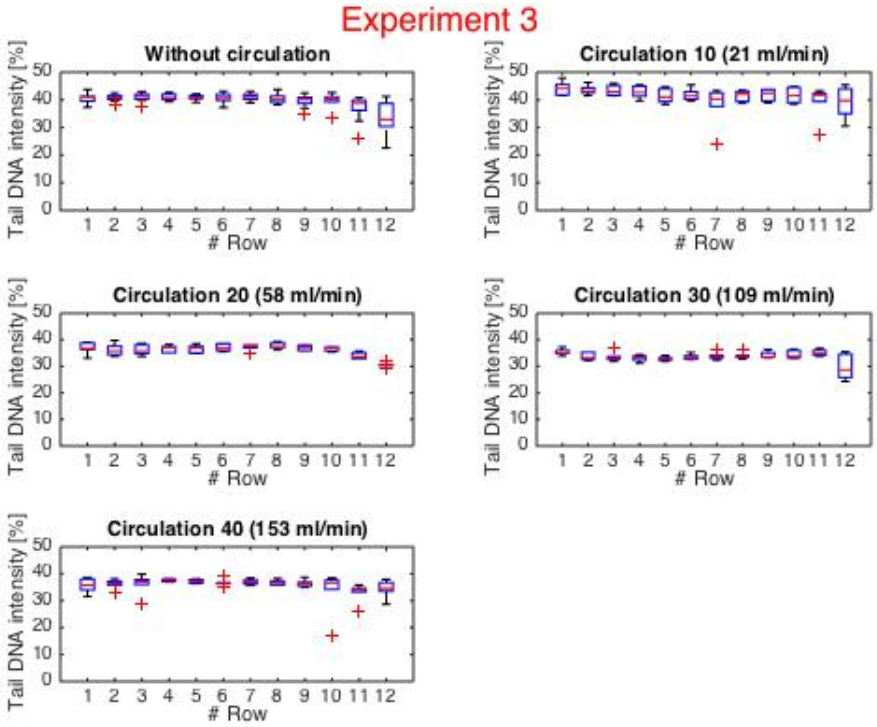

(b)

Figure D.4: Boxplots of the tail DNA intensity [%] along each column (D.4a) and each row (D.4b) of the films in Experiment 3 both without circulation and with circulation of different flow rates during electrophoresis. For each flow rate, the 96 minigels format was used, where electrophoresis without circulation was performed twice. The lymphocytes were irradiated with X-rays (8 Gy).

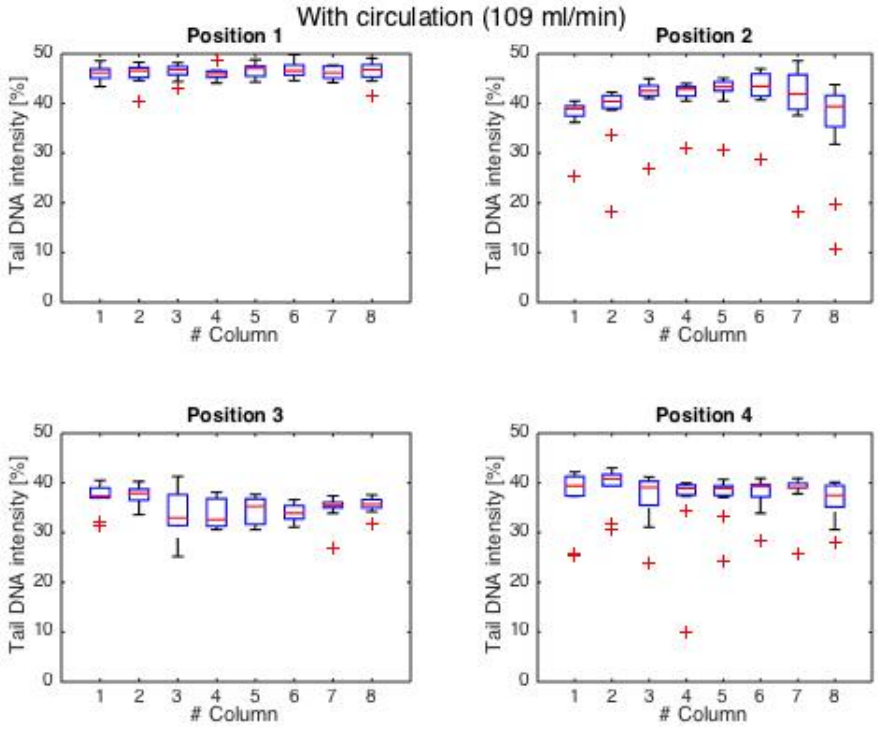

(a)

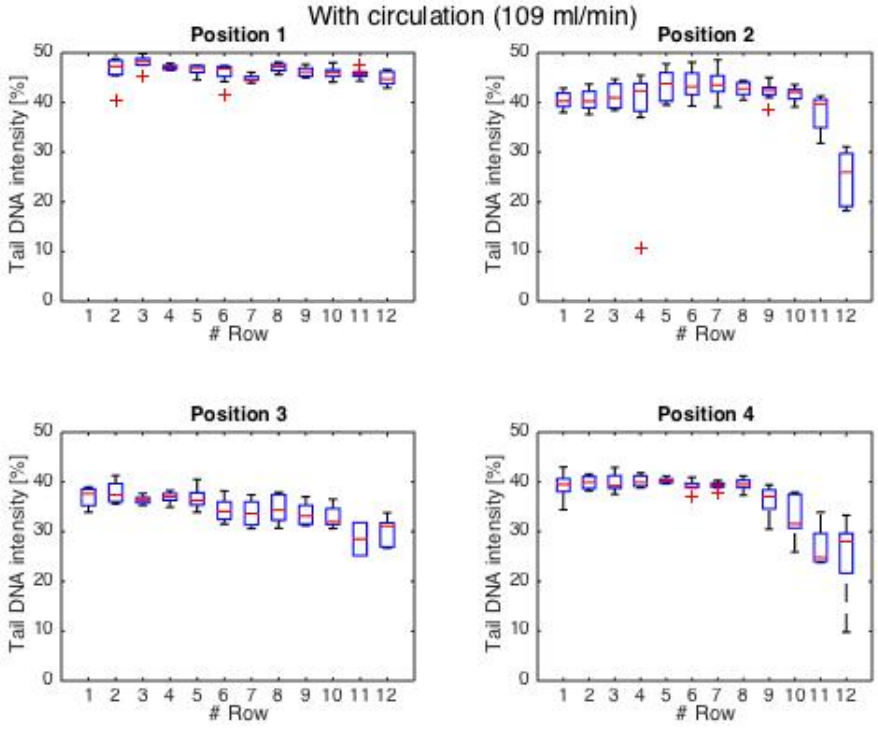

(b)

Figure D.5: Boxplots of the tail DNA intensity [%] along each column (D.5a) and each row (D.5b) of the four positions in Experiment 4 with circulation (109 ml/min) during electrophoresis. For each flow rate, the 96 minigels format was used. The lymphocytes were irradiated with X-rays (8 Gy).

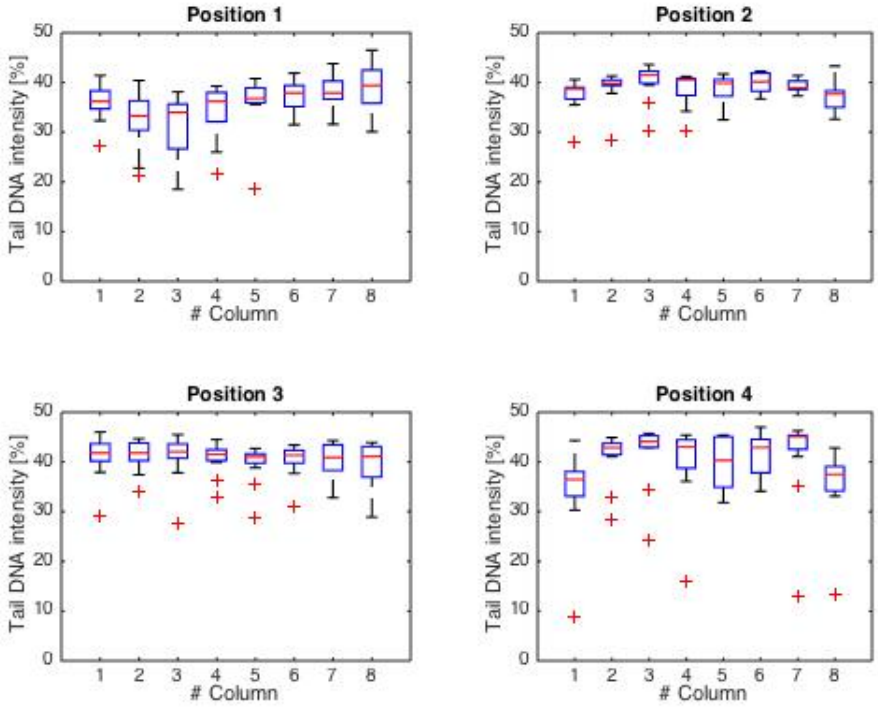

(a)

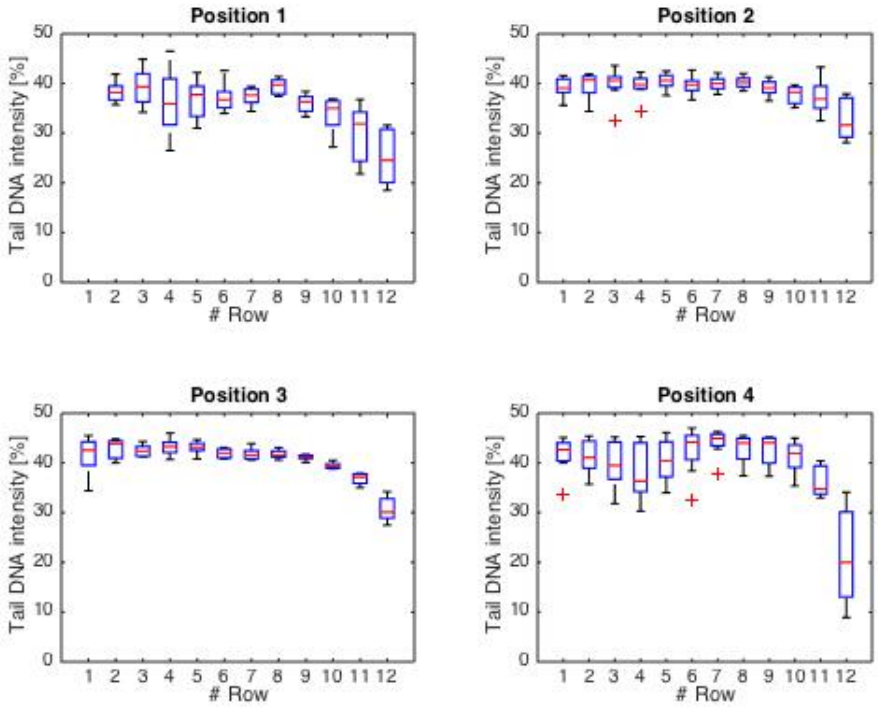

(b)

Figure D.6: Boxplots of the tail DNA intensity [%] along each column (D.6a) and each row (D.6b) of the four positions in Experiment 4 without circulation during electrophoresis. For each flow rate, the 96 minigels format was used. The lymphocytes were irradiated with X-rays (8 Gy).